DISSERTATION THESIS

Protease Inhibitors as a Research Tool:

Design, Synthesis and Evaluation of HIV PR and GCPII Inhibitors

by

Jiří Schimer, MSc.

Scientific Supervisor: Jan Konvalinka, Ph.D.

Department of Biochemistry
Faculty of Science
Charles University

Institute of Organic Chemistry and Biochemistry
Gilead Sciences & IOCB Research Centre
Academy of Sciences of the Czech Republic

Prague 2015

Prohlašuji, že jsem tuto disertační práci vypracoval samostatně pod vedením školitele Doc. RNDr. Jana Konvalinky, Ph.D. a všechny použité prameny jsem řádně citoval.

V Praze dne 30.3. 2015 .....

Acknowledgement

To write a proper acknowledgement, where I thank all the people I would like to, would probably cover more pages than the result section of this dissertation thesis. I will try it nonetheless on the following few lines (I will at least reduce the spacing and make the font smaller to fit it in). Looking back at the last four years, the whole PhD adventure seems almost unreal. It was gone in a blink of an eye and I only hope the rest of my life will not play the same dirty trick on me.

At first and most I would like to thank Jan Konvalinka, who was the best boss I could have ever wished for as well as a great friend to me on personal level. He showed me very often different sides of things which I just did not even realize existed and helped me, at least to a certain level, to be a little bit less black and white in my opinions (which is god damn hard thing to do). He was extremely patient and also gave me as much freedom in my research as I could handle (and sometimes a bit more than that, which was even more fun and I still can`t believe that our lab has still four walls). I only hope we will keep in touch even after I leave his lab, and hopefully we will eventually become (as he would put it): rich and famous! Since that is the sole reason why we are doing science anyways…

Staying on the professional level still, there is Jan Tykvart with whom I spend most of my free time these days, either playing various sports or just discussing science/games/books/movies, you name it. He very often kept me sane, since he is the most phlegmatic guy I know. He always showed me that the things are just not as bad as they seem and no one really cares if I prepare the inhibitor/substrate or not. He was also a great guy to collaborate with and our two joint publications are a proof of that.

Besides Jan I would like to thank Andrej Jancarik, who is way better chemist than I ever will be, for his sometimes somewhat useful advices (more often not) and Jitka Barinkova, who took care of our synthetic lab and helped me whenever she had free time. Also to Pavel Majer for letting me work in his synthetic lab, for his advices, as well as for putting me and Andrej into one room, which was the highest risk anyone ever undertook at this institute up to date. Then there is Pavel Sacha, with whom I cooperated on most of the later projects which will, hopefully, be eventually published. He is great to brainstorm with and has more ideas than he has PhD students and kids combined (again, hard thing to have). I would also like to thank Tomas, Vasek, Bimca, Klara, Milan, Helena, Adriana, and the whole bunch of people from the lab for creating a really nice environment to work in.

Moving to the personal level, hereby I would like to appreciate each of my parents for giving me half of their genetic material. Just kidding. I would like to thank them for helping me during my studies, both financially and personally for teaching me all the things I know outside chemistry field (true, not much) and for supporting me in bad times. My mum for all the love and care she gave me as well as billion other things including correction of my horrible written Czech, whenever I was forced to do that and my father for teaching me how to work also with my hands and not just with my brain as well as for having time for me whenever I needed anything.

I would also like to thank my friends who kept me sane in the hard times and who are fun to talk to, especially Alena Vagnerova, a lawyer who is just way too good-hearted for her job, Eva Hakova who can always offer a valuable opinion about personal matters and sometimes open my eyes a bit (especially during lunches), Helena Maresova whom I`ve known for 20 years and we have been through many things together, and Tereza Nedvedova who is one of the smartest people I know of and is a great sport to have an quasi-scientific argument with whenever there is a chance (and that is one on a daily basis).

Last, but certainly not least I would like to thank Jana Mladkova, for showing me that science, though certainly important, is just not **the** most important thing in the world. It was the best year of my life and even though it ended up pretty badly I would go through the torment again, because it was just worth it.

Table of Contents

1 Abstract

This dissertation thesis focuses on creating tools for the analysis and potential therapeutic intervention in the biological processes regulated by proteolysis. I focus on two important proteolytic enzymes: HIV-1 protease, which is indispensable for the polyprotein processing of the nascent virus and thus for the development of infectious viral particle, and glutamate carboxypeptidase II, a tumor marker and a neuropeptidase from the prostate and central nervous system.

Rational design of inhibitors of these therapeutically relevant enzymes serves two purposes: firstly, protease inhibitors were shown to be powerful drugs (HIV protease is in fact **the** example of successful drug development driven by structural biology). Secondly, and in the context of this thesis perhaps more importantly, inhibitors of medicinally relevant proteases might serve as tools for the elucidation of basic biological questions concerning regulation, timing and spatiotemporal control of such key processes as virus maturation or cancer development. The experimental work described in this thesis summarizes my results in both these areas.

Human Immunodeficiency Virus Protease

Human immunodeficiency virus (HIV), a causative agent of AIDS, has been estimated to kill close to 40 million people during the past four decades with 1.5 million dying the last year only. 35 million more are living with the infection and the disease is spreading with increasing speed in the less developed regions such as sub-Saharan Africa.

Because of its deadliness, during the early 90s of last century, with vaccination nowhere close to completion, scientific community along with pharmaceutical industrial waged unprecedented war against this disease. Their combined effort led to a clinical approval of more than thirty antiretrovirotics and gave rise to a so called highly active antiretroviral therapy (HAART) which dramatically improves the patients` lives as well as their life expectancy.

Among the primary targets chosen for combating HIV is one of the vital enzymes – HIV protease (HIV PR). This small homodimeric aspartyl protease became one of the most studied enzymes in the world. HIV PR plays a crucial role in the viral lifecycle by cleaving the polyproteins into the functional units and its inhibition hinders the viral maturation, making the particles non-infectious. Even thought HIV PR is well understood on the biochemical level – structure and enzymatic activity – its in-depth role in the biological process of viral maturation is not well established. Our knowledge suggests that the cleavage must be strictly

regulated, both in time and place, however how this is done, is not fully determined. Ever emerging resistances of HIV PR to the clinical drugs as well as not fully understood nature of the polyprotein processing makes it even now, more than 25 years after its discovery, an attractive target for many studies.

Glutamate carboxypeptidase II

Unlike AIDS a prostate carcinoma (PCa) causes more havoc in the developed world than in the third world countries. This pathological condition is the leading cause of deaths among all cancerous diseases in men with over 300,000 deaths reported annually. The most common treatment for PCa is a combination of tumor resection with chemotherapy. Systemic chemotherapy is by nature highly non-specific, targeting all dividing cells, and as such causes number of side effects and is very often carcinogenic itself. To circumvent these issues scientists have been trying for more than quarter of a century to develop therapeutics that would be specifically directed to the uncontrollably proliferating cells. The most intensively pursued approach for a development of such a therapeutic is targeted drug delivery, i.e. attempt to find a difference between the malignant and normal cells on a protein level and exploit it.

Glutamate carboxypeptidase II (GCPII) could serve as such a potential target, since it is heavily overexpressed in PCa cells as well as on some solid tumor neovasculature. In addition GCPII is a membrane bound protease which internalizes upon ligand binding, making it an ideal candidate for targeted therapy. Strategies using both small agents, such as inhibitors, and monoclonal antibodies have been tested in the past with some of them entering late stages of clinical trials. However, the potential for further improvement is limitless and novel inhibitors with even stronger binding affinities are still needed.

2 List of Abbreviations

HIV PR	Human immunodeficiency virus protease
ESCRT	endosomal sorting complexes required for transport
CD4	cluster of differentiation 4, cell receptor
CXCR4	chemokine receptore type 4
CCR5	chemokine receptore type 5
ER	endoplasmic reticulum
RT	reverse transcriptase
IN	integrase
PCa	prostate carcinoma
HIV PR	HIV protease
MA	matrix protein
CA	capsid protein
NC	nucleocapsid
P6	protein p6
PI	HIV protease inhibitor
Gag and Gag-Pol	viral polyprotein chains
Env	envelope proteins of HIV
gp120 and gp41	glycoprotein 120 and 41 respectively, viral envelope proteins
GCPII/III	Glutamate CarboxyPeptidase II/III
NAALADase	*N*-Acetylated Alpha-Linked Acidic Dipeptidase
PSMA	Prostate Specific Membrane Antigen
NAAG	*N*-acetyl-L-aspartyl-L-glutamate
FOLH	FOLate Hydrolase
IUBMB	International Union of Biochemistry and Molecular Biology
EDTA	Ethylenediaminetetraacetic acid
EGTA	ethylene glycol tetraacetic acid
ZBG	zinc binding group
bp	base-pair
PDB	Protein Data Bank
DOTA	1,4,7,10-tetraazacyclododecane-1,4,7,10-tetraacetic acid
2-PMPA	2-(phosphonomethyl)pentanedioic acid
MRI	Magnetic Resonance Imaging
CT	Computed Tomography
PET	Positron Emission Tomography
SPECT	Single-photon Emission Computed Tomography
Cryo-EM	cryo electron microscopy
SAR	Structure activity relationship

3 Introduction

3.1 Human immunodeficiency virus (HIV)

3.1.1 HIV Classification and Protein Equipment

Human immunodeficiency virus belongs to a group of lentiviruses, a subgroup of retroviruses.[1] As such, it carries two positive strands of RNA, which are coding only for fifteen proteins. Most of the proteins are expressed in a form of polyprotein chains and has to be further cleaved to gain their functions.

Four out of the fifteen proteins are structural proteins: matrix, capsid, nucleocapsid and p6 protein. These proteins are result of Gag translation (figure 1A), and form more than 50 % of the virion mass.[2] During maturation of the viral particles, capsid protein forms a hexameric lattice enveloping the viral RNA. The RNA is bound to nucleocapsid, which stabilizes the three dimensional conformation of RNA (figure 1B).[3] The matrix protein mainly mediates the interaction between Env proteins (see further) and the expressed polyprotein Gag[4]. The p6 protein is responsible for interaction with the host complexes of the escort system (ESCRT), which help to shuffle the translated polyprotein chains to the plasma membrane. A second major role of p6 is to help with the viral budding.[5]

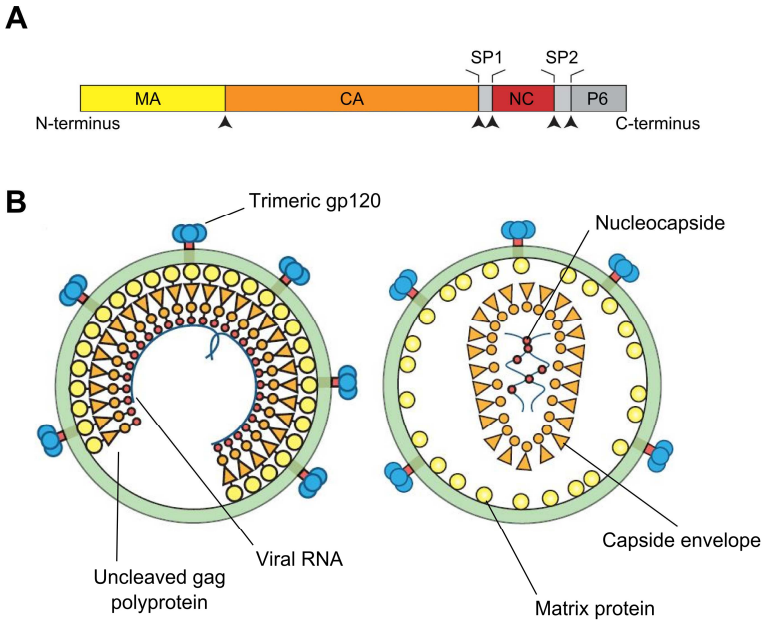

Figure 1: Structural proteins of HIV; **A)** Schematic illustration of Gag polyprotein, arrows indicate the 5 cleavage sites done by the viral protease during viral maturation. MA – matrix, CA – capsid, SP1 – spacer peptide 1, NC – nucleocapsid, SP-2 - spacerpeptide 2, P6-protein p6; **B)** simplified model of virion with processed (right) and unprocessed (left) gag polyprotein. This processing is vital for infectivity and is called maturation. Adapted from [6].

Env is translated into polyprotein gp160 in the endoplasmic reticulum (ER), where it undergoes glycosylation and is cleaved by host protease furin into two functional membrane bound glycoproteins - gp120 and gp41.[7] These glycoproteins form active trimers in the membrane and are responsible for interaction with CD4 receptor (gp120) and co-receptor CXCR4 or CCR5 (gp41). Thanks to this interaction the viral membrane fuses with the host cell membrane (gp41) and subsequently the virus enters into the host cell.[8]

Six proteins of the virus repertoire are accessory proteins (Vif, Vpr, Nef, Tat, Rev, Vpu) responsible for potentiation of the viral infection, by downregulating the immune response and increasing the amount of produced viral particles as well as helping with hijacking of the host proteins. These proteins are not subject of this study and therefore if the reader is interested he is kindly asked to read the following exhaustive review [9].

Finally, the last three proteins possess enzymatic activity. Reverse transcriptase (RT) is an enzyme responsible for translation of the viral RNA into DNA, integrase (IN), is responsible for integration of the viral transcribed genetic information into the host genome and HIV protease (PR), is responsible for dissection of polyprotein chains Gag and Gag-Pol into functional units.[10]

3.1.2 The HIV Life Cycle

HIV life cycle (shown schematically in figure 2, p. 11) begins with interaction between CD4 host cell receptors and the trimeric gp120 envelope protein of the virus. This is followed by recruitment of a co-receptor, either CCR5 or CXCR4, which interacts with smaller envelope protein gp41. The second interaction leads to a dramatic conformation change in the small protein resulting in fusion of the viral membrane with the host cell membrane.[11] The core of the virus then enters the cytoplasm, uncoats and releases two copies of viral positive RNAs along with the roughly 80 molecules of reverse transcriptase (RT). In a series of complicated steps RT transcripts the single stranded RNA into double-helix DNA, degrading the original copy of RNA along the way (RNase H activity).[12] The double stranded DNA is then shuffled into the cell nucleus hijacking number of host cell proteins in the process[13-15], where it is integrated into the genomic DNA by integrase.[16] The incorporated genes are then transcribed back into RNA by host-cell transcription machinery in multiple copies, both for translation purposes and as a genetic material for newly released virions. The RNA is then translated into polyprotein chains which are actively transported to the plasmatic membrane, where they form into spherical lattice by interacting with the envelope proteins (already

present on membrane, translated in ER) and genomic RNA.[6, 17] These events all appear to be simultaneous and are followed by budding of new viral particle out of the cell. The freshly released viral particles, however, are not properly structured and need to be reassembled, forming the conically shaped core (capsid envelope) to become fully infectious (figure 1B, p. 9).[18] Somewhere between the accumulation of the Gag and Gag-Pol polyproteins on the plasma membrane and the final maturation process of the viral particle, HIV PR cleaves the polyprotein chain into the functional counterparts.[17] However, the exact spatiotemporal control of the process is not known.

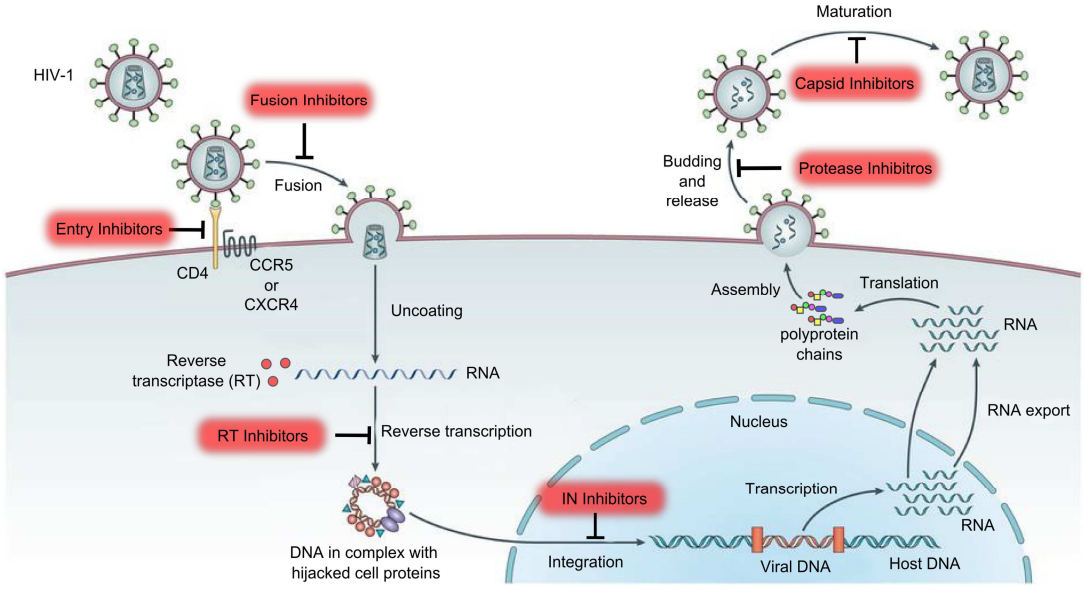

Figure 2: Schematic illustration of life cycle of the HIV; The possible sites for drug targeting are depicted in the red squares. CD4 – host cell receptor; CCR5 and CXCR4 – host cell co-receptors; RT reverse transcriptase; IN integrase. Figure adapted from [19].

3.1.3 Current Treatment of HIV

Nearly all abovementioned proteins have been thoroughly scrutinized as potential targets for therapy of HIV (for potential targeting sites see figure 2). All three enzymes of HIV play indispensable roles in the life cycle of the virus and were the first to be targeted in drug development programs. Inhibition of any single step leads to effective decrease of viral load and increase of CD4 positive cells in the blood of the patients.

Inhibitors of RT were the first to be discovered (zidovudine, 1987) and represent the largest group of medicines against HIV. The inhibitors of RT are divided into two groups classified by either interacting with the allosteric site of the enzyme, or directly inhibiting the polymerase reaction by lacking the 3′ terminal hydroxyl group. Recently, major advances in

development of RNase H inhibitors, subunit responsible for degradation of RNA in DNA-RNA duplex, were announced.[20] For further information regarding all RT inhibitors the reader is recommended to read following reviews [20-22].

Surprisingly enough it took the pharmaceutical industry relatively long time before the first integrase inhibitor was approved in 2007 (raltegravir). This inhibitor remained to be the sole inhibitor for integrase for the following 6 years when two more (elvitegravir and dolutegravir) came into market. For a well written review covering both tedious development and use of integrase inhibitors see [23-25].

The inhibitors of HIV PR will be discussed in the following pages in detail.

Besides the obvious targets – the enzymatic apparatus – scientist came up with various ideas how to prevent the virus to spread by inhibiting various stages of its life cycle.[26] A series of compounds preventing the virus from entry into the host cell – either binding directly to the gp41, thus preventing fusion, or by interaction with host receptor/co-receptor CD4/CCR5 – has been evaluated and resulted in several approved drugs (enfuvirtide or maraviroc, respectively).[27] Another interesting class of potential drugs inhibiting the proper assembly of the capsid core has been explored lately. Ligands binding to either C- or N-terminus of the protein disrupting the proper formation of the capsid lattice have been described and some of them are in preclinical trials and show promise to open a new path for combating the emerging HIV strains which are already resistant to clinically used drugs [28-32].

3.1.4 HIV Protease

HIV protease is the smallest protease known to mankind. To gain the enzymatic activity, this 99 amino acid long aspartyl protease has to form a C-2 symmetric homodimeric structure, with catalytic aspartates in positions 25 and 25`. PR was recognized as a potential target immediately after its discovery, when simple inhibition of this enzyme by non-specific inhibitor pepstatin thwarted the gag processing and led to release of immature non-infectious particles.[33] This has been also confirmed in a similar study when mutating the catalytic aspartates led to identical results.[34]

HIV PR is encoded by the *pol* gene and it is transcribed as part of the Gag-Pol polyprotein by -1 ribosomal frameshifting of the viral mRNA. This process occurs approximately in 5 % of cases compared to the transcription of its structural counterpart *gag*.[35] The mechanism by which the PR is activated during the assembly of the virus is still not fully understood. PR is originally probably inactive within the polyprotein, because it

prevents proper formation of the dimeric structure. However, the huge polyprotein chains form transient dimeric structures with detectable activity that most probably play role in the autocatalytic cleavage of the PR out of the polyprotein.[36] This event, however, must be strictly regulated, because activation of the PR in cytoplasm completely abolishes HIV particle production.[37] Upon activation, PR cleaves the polyprotein chains at 5/9 distinct sites, for Gag and Gag-Pol respectively, giving rise to fully functional proteins.[38]

Surprisingly enough, PR does not show a clear consensus among its naturally occurring cleavage sites in the polyprotein chains. There is a slight preference for aromatic amino acid (Tyr, Phe) occupying the P1´ site and proline residue for P1 site. Both S2 and S2´ are highly hydrophobic, however amino acids such as glutamine are often present in the P2 site of substrates demonstrating further the enzyme promiscuity.[38, 39] The determining factor probably lies more in the structural accessibility of the substrate by the protease rather than in the substrate primary sequence.[40]

3.1.5 Structure of HIV Protease

Structural analysis, especially X-ray crystallography, has become a routine method for evaluation of protease inhibitor binding mode in the past 20 years. The combined effort of scientists resulted in over 500 structures of this enzyme in various states deposited in Protein Databank.[41] The overall structure with bound protease inhibitor ritonavir is shown in figure 3 (p. 14).

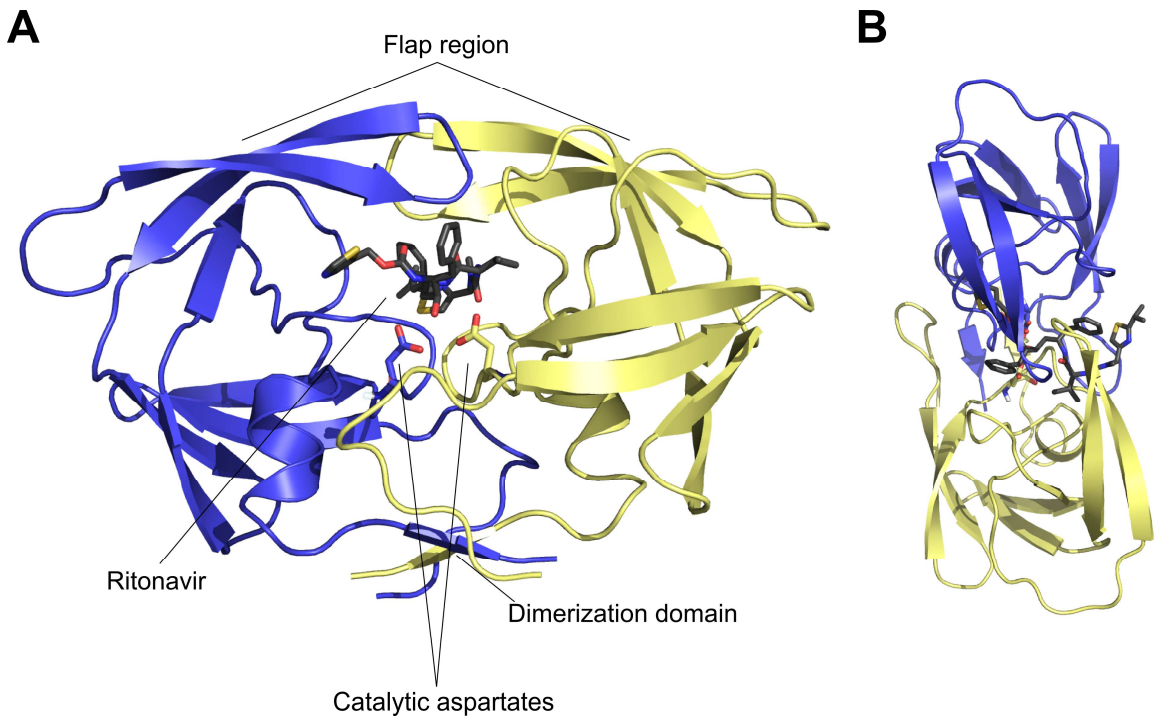

Figure 3: The Overall structure of HIV PR with bound inhibitor ritonavir (RTV); **A)** Front view of the HIV PR with bound protease inhibitor ritonavir. Depicted are the structural features of the protease: flap region closing upon binding substrate/inhibitor, dimerization domain and catalytic aspartates in position 25 and 25´. **B)** The top view at HIV PR showing details of the flap region. The two chains are colored pale yellow and blue and are shown in the cartoon diagram. The bound inhibitor and catalytic aspartates are in the stick representation, colored according to element as follows – dark grey for carbon (inhibitor), blue for nitrogen, red for oxygen and yellow for sulfur. The structure was prepared using available pdb code 1HXW[42] and PyMol software[43].

The HIV PR consists of two identical monomers, with typical catalytic triad Asp-Thr-Gly occupying position 25-27 and 25´-27´, forming a rather rigid structure called "fireman`s grip".[44] The aspartyl residues are in close proximity to each other and are arranged in coplanar fashion to maximize the nucleophilicity of the water molecule cleaving the peptide bond.[45]

Further striking feature of the HIV PR structure is the flap region formed by amino acids 42-58 and 42´-58´. The flaps undergo dramatic structural changes upon substrate binding going from semi-open over open state to a close state, binding the substrate during the process. Reader is kindly asked to see following articles [46, 47] for further information since this fascinating topic does not touch the major aims of this thesis.

The dimerization interface of the functional HIV PR is formed primarily by the interaction between N- and C- termini of both monomeric chains, which are forming anti-parallel β-sheet, and additionally is also stabilized by the interaction between the β-hairpins of each monomer in the flap region and by the interaction of the fireman grip residues in the catalytic

center. The interactions between the termini have been estimated to be responsible for over 75 % of the total binding energy.[48]

3.1.6 HIV Protease as a Therapeutic Target

Immediately after the discovery of HIV PR and its key function in the viral life cycle both academia and pharmaceutical companies put massive endeavor into development of protease inhibitors (PI) as potential therapeutics against HIV. In retrospect this led to a textbook example of structure-guided rational drug design, accompanied by extraordinary development in methodology of medicinal chemistry, especially in methods studying three dimensional structures of proteins. The effort was rewarded by approval of 9 PIs by Food and Drug Administration agency (FDA), helping millions of HIV-positive patients all over the world.

3.1.7 HIV Protease Inhibitors

3.1.7.1 PIs on the Market

As has been mentioned previously, currently there are 9 approved protease inhibitors on the market. All of these inhibitors were designed to mimic the transition state with maximized binding affinity towards the catalytic aspartates and therefore all belong to the competitive class of inhibitors. The development of the first inhibitor – Saquinavir – was a relatively straightforward process of the scissile peptide bond replacement with a hydroxyethylamine moiety, an approach used very commonly in development of protease inhibitors.[49] This peptidomimetic character of the inhibitors prevails all over the scope of the approved inhibitors with the exception of tipranavir which was discovered, unlike all other PIs, initially by a library screening.[50]

The PIs can be divided into two subgroups: the first 5(6) designed inhibitors (saquinavir, ritonavir, indinavir, nelfinavir, amprenavir and fosamprenavir) are often referred to as a first generation of PIs and are rather scarcely used in clinics nowadays (with the exception of ritonavir, which is being used as a pharmaceutical booster). The main reasons for their cutoff in usage are serious side effects, heavy pill burden as well as a fast development of resistances. These common issues led to a development of a second generation of PIs (lopinavir, atazanavir, tipranavir, darunavir) which are better tolerated and have higher genetic barrier for development of resistances. When combined with the pharmaceutic

booster, either ritonavir or recently approved cobicistat, patients do not have to take more than one or two pills a day.[51]

Unfortunately even the second generation of PIs retains some of the side effects, such as gastrointestinal problems, migraines, or liver related issues.[52-55] And even though the genetic barrier for development of resistance is higher toward this new class of PIs, the brute force used by the virus represented by the high replication rate and the error prone nature of the reverse transcriptase combined with the evolutionary bottle neck caused by the PIs led to subsequent development of the resistance to each one of them.[51] These are the main reasons why novel PIs will still be needed in the foreseeable future. This was reflected by several compounds entering the clinical trials in the recent past (*e.g.* brecanavir, PL-100)[56-58], however, all of them failed or were withdrawn at various stages of the trials.

3.1.7.2 Other Non-peptidic Inhibitors of HIV PR

During the three decades of searching for new PIs against HIV PR a surprising wealth of small molecules inhibiting this enzyme has been accumulated. In the following paragraphs a few of the more interesting examples reported in the literature is listed.

An extremely interesting group of compounds inhibiting HIV PR described already in 1993 by Sham *et al* are difluoroketones (figure 4, **1**, p. 17).[59] The most common hydroxyl moiety, which locks the protein in its transition state by interaction with the catalytic aspartates, is substituted by two electron withdrawing fluorine atoms. Even though the K_i values of the resulting inhibitors are relatively low in comparison to other inhibitors (nanomolar range) it shows the outside-box thinking the scientists often did when finding new compounds able to inhibit the HIV PR.

A similar approach of changing the inhibitor mimetic core has been described recently by group of Dr. Vince, who changed the transition mimetic to sulfoximine moiety (figure 4, **2**, p. 17).[60] Sulfoximines can serve both as hydrogen donors and acceptors, a quality which could lead to ideal hydrogen bond formation with the catalytic aspartates. Even though inhibitors with this core show relatively high affinities toward HIV PR their charged core probably prevents the compound to cross the plasma membrane hence rendering the compounds ineffective in cell culture studies.[61]

A large serie of studies describing pyrrolidines as a transition state mimetics was published by prof. Klebe group. The charged amine on pyrrolidine ring forms a strong hydrogen bond network to catalytic aspartates while substituents in position 3 and 4 of the pyrrolidine ring (figure 4, **3**) were designed in analogy to pepstatine to create hydrophobic interactions with

the S2 and S2´ pockets.[62, 63] Even though this certainly presents an interesting idea and rational drug design the obtained inhibitors show rather low affinity toward the enzyme.[64]

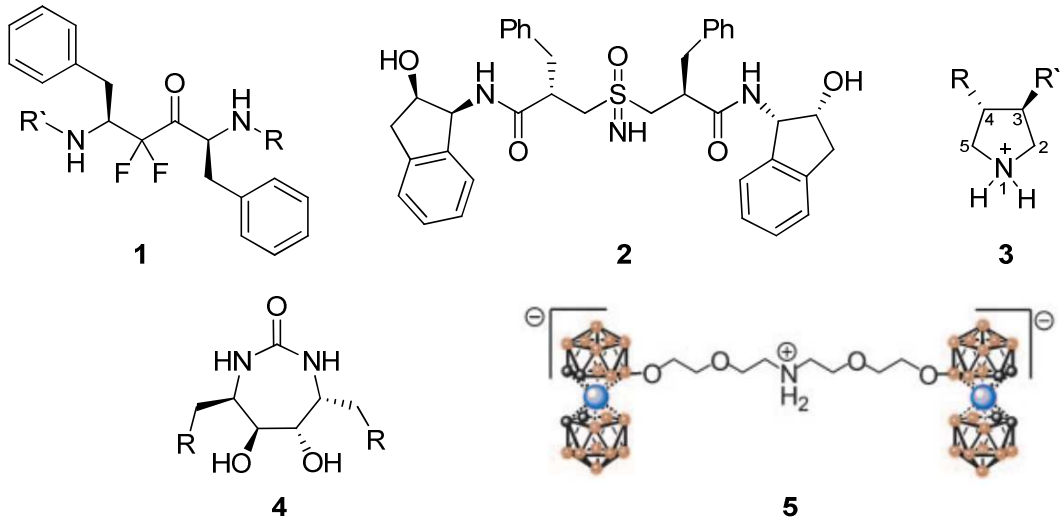

Figure 4: Unorthonox inhibitors of HIV protease; **1**) difluoroketones were designed to form hydrogen bonding to catalytic aspartates with the two electronegative fluorine atoms **2**) sulfoximines were predicted to be able to create perfect hydrogen bond network to catalytic aspartates with their unique donor/acceptor hydrogen bond properties. **3**) pyrrolidines show another example of starting scaffold with their charged amine forming strong hydrogen bonding to the catalytic center. **4**) 7-member ring cyclic ureas, a typical transition mimetic with hydroxyl groups in the catalytic center enhanced by formation of carbonyl oxygen hydrogen bonds with flap region. **5**) boron containing clusters developed by Cigler *et al* interacting with the hydrophobic pockets of the enzyme. Boron atoms are depicted in orange, carbon atoms black and Co^{2+} atoms are shown as blue spheres.

Moving back to hydroxyl groups as the main interacting partner of the inhibitor with the catalytic aspartates, long auspicious 7-member ring cyclic ureas (figure 4, **4**) were in the pipeline and preclinical trials for number of years. [65-67] Besides the double hydroxyl groups forming strong interactions with the catalytic aspartates, the carbonyl group replaces structural water and forms direct hydrogen bonds with the flap region, making it an ideal starting scaffold for further development. However, both solubility issues and resistance profile of the compounds led to a final discontinuation of the studies. The last resurrection of the project came in a substitution of the urea group by sulfamide moiety[68], without changing the susceptibility of the inhibitor to the most common double mutant V82F and I84V, and so this probably also proved to be the final chapter of the studies.[69, 70]

In the search of unorthodox inhibitors, Cigler *et al* discovered boron containing icosahedral carboranes (figure 4, **5**,) to be rather potent inhibitors occupying the hydrophobic pocket of the protease.[71] Subsequent structural analysis showed two molecules of the inhibitor bound to

hydrophobic pockets of the enzyme, namely into the S3 and S3´ sub-sites, and subsequent connection of the two boron containing cages with a flexible linker further improved their binding affinity. The follow up studies showed that these inhibitors preserve their strong affinity even to highly mutated resistant proteases isolated from the patients.[71] However, due to difficulties regarding the solubility the compounds were not further developed.

3.1.7.3 Irreversible Inhibitors of HIV PR

Irreversible inhibitors of HIV PR create a covalent bond to the catalytic aspartates upon binding, thus ultimately preventing the enzyme from ever fulfilling its function. Furthermore the only mutation that leads to complete resistance to the inhibitor would be mutation in the catalytic aspartate, which would, however, be fundamentally detrimental for its activity. It should be stated, however, that even other mutations in the catalytic center can decrease the susceptibility of the protease to such an inhibitor. Driven by these advantages a relatively high number of studies have been published on this topic, however without any clinical result.

The most commonly exploited reactive group proved to be the epoxide moiety (figure 5, **1**), which upon nucleophilic attack by one of the aspartyl dissociated carboxylates opens and stays covalently bound as an ester.[72-74] α,β-unsaturated ketones have been also tested, but were shown to bind to a cysteine present in the dimerization domain rather than to the catalytic aspartates.[74] This inhibition could be easily circumvented by C95F mutation, which has already been reported.[75, 76] Therefore, only studies concerning the epoxide moieties were continued, but even these did not at the end give rise to any clinical candidates, most commonly because of their lack of specificity and short half-life in solutions.

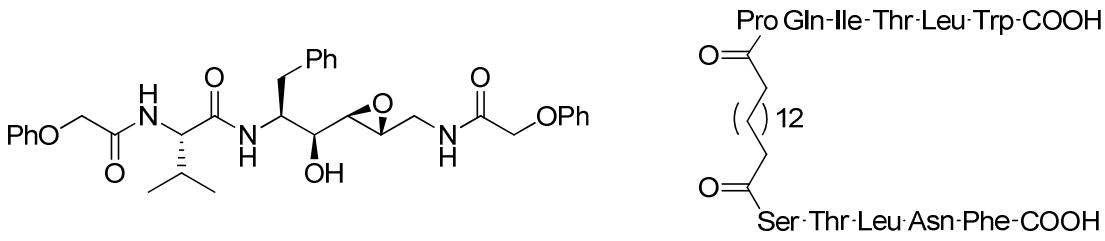

1 **2**

Figure 5: Irreversible and dimerization inhibitors of HIV PR; **1**) most potent irreversible inhibitor of HIV PR identified up to date containing the *cis*-epoxy moiety as a war head. **2**) dimerization inhibitor designed by connecting the two peptides disrupting the dimerization profile identified during library screening.

3.1.7.4 Inhibitors Targeting Domains Outside the Active Site

HIV PR is a homodimeric protein, which is completely inactive in its monomeric form Any compound disrupting the dimerization would be therefore potent inhibitor.[77] Targeting the dimerization domain would also circumvent the multidrug-resistant variants of HIV PR which have emerged upon treatment with the approved PIs. As has been already mentioned in the general introduction, 75 % of the dimerization energy of HIV PR comes from the formation of four stranded β-sheet antiparallel structure between the four N- and C-termini.[48] This is the reason why the domain was also targeted by various groups in development of dimerization inhibitor with various results. First, small peptides mimicking both N- and C-termini were subjected to study resulting in several micromolar inhibitors.[78, 79] Subsequent connections of these small peptides with either rigid[80] or flexible[81, 82] linkers (figure 5, **2**, p. 18) produced low nanomolar inhibitors. Unfortunately, particular issues with this set of compounds were originating in their peptide character. The inhibitors proved not to be able to penetrate the membrane into the cell which led to an end of their development.

HIV PR is a surprisingly flexible enzyme, which undergoes a dramatic conformational change upon binding the substrate. The most pronounced changes are in the flap region, which directly binds the substrate.[46, 47] Of particular interest are the cavities opening in the region directly below the flap elbows and on the top of the flap region upon binding the substrate (figure 6, p. 20).[83] Both library screenings and small fragment base rational drug design were used to target this region, identifying several small compounds, which are able to lock the enzyme in the closed state, preventing from release of the cleaved substrate. The binding affinities of these small molecules were in micromolar range. A number of crystal structures were solved in the following studies, proving the binding mode of these compounds into the allosteric sites. Small compound such as 2-methylcyclohexanol or indole-6-carboxylic acid prove to be excellent starting scaffold for further development of the exo-site targeting inhibitors.[84] These studies came too late to join main research effort in the development of PIs and were probably never followed up any further. Nonetheless, they show an excellent example of modern rational drug design.

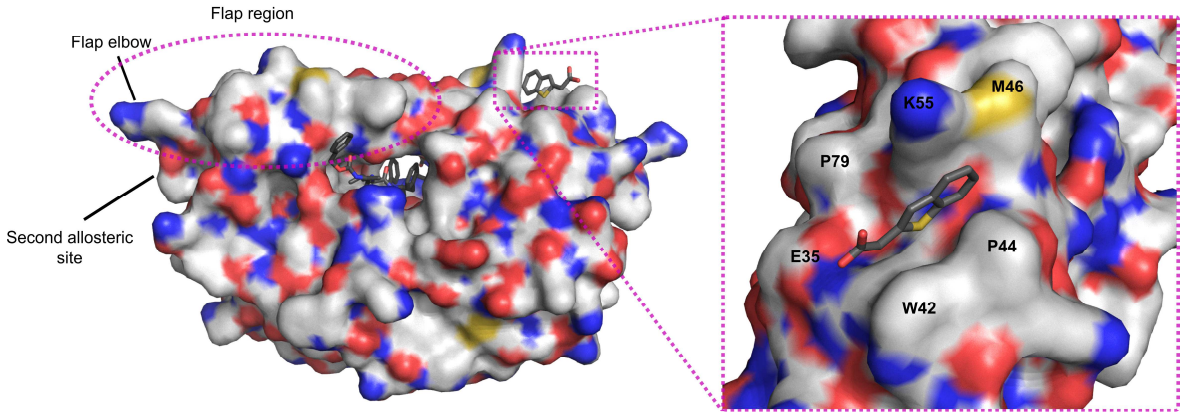

Figure 6: Allosteric sites of HIV protease. HIV PR goes through a dramatic conformational change upon binding either substrate or inhibitor. This change opens two small cavities which can be targeted by small molecules and thus lock the HIV PR in the closed state, inhibiting the protease activity. A binding mode of one identified inhibitor, indole-6-carboxylic acid, is displayed in both front and top view. HIV PR show in water-exposed model, coloring is as follows: nitrogen blue, oxygen red, sulfur yellow, carbon off-white. The inhibitors are shown in stick representation. The structure was prepared using available pdb code 3KFS[84] and PyMol software[43].

3.1.8 Drug Resistance of HIV PR

Reverse transcriptase, lacking the proofreading activity, is one of the most erroneous enzymes discovered up to date, having an average error rate of 1/1700 per nucleotide incorporated.[85] Taken into account that the viral genome of HIV is close to 10 000 nucleotides, there is no surprise that almost each budding virus has, to some degree, altered genetic information. Combined with the high replication rate of the virus this gives rise to a numerous newly emerging genetically distinct variants of HIV on daily basis. In each untreated patient there can be as many as 10^9 of mutated variants of HIV, often referred to as quasispecies.[86] Evolution of the virus is thus extremely fast, and when one adds selection pressure in form of an inhibitor, mutated viral strains resistant to the inhibitor emerge rapidly.

The development of HIV PR drug resistance is believed to be a stepwise processs.[87-89] At first mutations close to the active site are developed directly decreasing the affinity of the PIs to the HIV PR, and are referred to as major, or primary, mutations. They are commonly very similar for various PIs and therefore the emerging strains are cross-resistant to treatment with different PIs.[69] However, the altered structure of the catalytic site causes the HIV PR to be less able to cleave its natural substrate, resulting in a reduced capacity of the virus, decreasing its viral fitness.[90] The viral fitness is very often then restored by successive secondary mutations, also known as minor mutations, which can occur relatively far away from the

active site. While these residues are not directly responsible for interactions with the substrate, they re-shape the active site slightly by changing the overall conformation fold, increasing the affinity of the protease to the natural substrate.[91] Other compensatory changes, restoring the viral fitness, have been even described to crop up at the cleavage site of the Gag and Gag-Pol polyprotein chains, remodeling its overall structure to fit better into the mutated protease.[92-94] Besides the direct mutations, insertions of amino acids, ranging in length from 1-6, reducing the susceptibility to PIs or restoring viral fitness have been also reported.[95, 96]

Out of the 99 amino acids of HIV PR more than 50 have been reported to be prone to mutation and a single isolate can harbor as many as 21 mutations. Naturally, such a dramatic change in the primary sequence leads to a massive decrease in activity (~5 % k_{cat} of wild type), however the virus is still able to replicate.[97]

A set of mutations leading to resistance have been described to the every single approved PI on the market (for complete list see [98]) and this is the main reason for ongoing research efforts in the field of PIs. Development of yet novel PI with completely different binding mode could potentially circumvent the evolved resistant strains of the virus.

3.2 GCP II

3.2.1 Discovery of GCPII

The discovery of GCPII dates back to late 80s of the past century, when Robinson *et al* identified novel dipeptidase activity in the rat brain, specifically cleaving of the most abundant peptide neurotransmitter N-acetyl-L-aspartyl-L-glutamate (NAAG). The NAAG is processed to its corresponding amino acids, N-acetyl-L-aspartate and L-glutamate, and the enzyme was denominated N-acetylated-α-linked acidic dipeptides (NAALADase).[99]

In less than a month apart a seemingly unrelated study describing monoclonal antibodies against cancer LNCaP cells, isolated from prostate cancer, was published. They termed the monoclonal antibody 7E11-C5 and showed its almost exclusive organ specificity to prostate, with only slight recognition of kidney samples. Because of this, the unknown antigen was called prostate specific membrane glycoprotein, later renamed to prostate specific membrane antigen (PSMA).[100]

To add salt into injury of the scientists, an enzyme responsible for cleavage of L-glutamates from the poly–γ–L–glutamyl folate, helping resorption of the vitamin B_9 from the small intestine was found in the upper gastrointestinal tract. Naturally because of its activity it was labeled folate hydrolase (FOLH).[101]

In 1996, almost ten years after these discoveries, a study showing that PSMA posses peptidase activity, and is readily able to cleave the NAAG dipeptide, was printed out.[102]The striking high sequence identity between PSMA and NAALADase was also pointed out. Moreover, during the same year it was also established by Pinto *et al* that the enzyme possesses folate hydrolase activity[103] and a link between PSMA and FOLH was established.

At this time the International Union of Biochemistry and Molecular Biology (IUBMB) stepped into this complex nomenclature and proposed a unifying name to be glutamate carboxypeptidase II (GCPII; EC 3.4.17.21). Unfortunately this was not fully reflected by number of scientists in the specialized fields who very often still refer to the enzyme according to their specialization. Throughout this thesis I will strictly stick to the internationally approved term GCPII.

3.2.2 General Information about GCPII

The human GCPII gene is mapped on the chromosome 11p11.2 and can be found in the database under *FOLH1* name. It contains 19 exons and 18 introns spanning over 60 kbp genomic DNA.[104] Expression of the GCPII is regulated by an enhance present in the third intron of FOLH1 gene, and is responsible for the overexpression during the prostate carcinoma.[105] There are number of possible splice variants of GCPII, for more information, see [106, 107] reviewed in [108].

The full length transcript of *FOLH1* gene codes for 750 amino acids long class II transmembrane protein. The protein forms a dimer under native conditions and only as such possesses the hydrolase activity.[109] GCPII is heavily N-glycosylated and these post-translational modifications have been shown to be vital for its enzymatic activity.[110-112] The properly post-translationally modified protein weights approximately 100 kDa.

According to MEROPS database, GCPII belongs to the superfamily of metallopeptidases (clan MH), specifically to metallopeptidase family M28.[113] The enzymes of this superfamily contains two catalytic zinc atoms bound in the active center, which are responsible for the peptidase activity.[114] The protein is mostly extracellular, with over 700 amino acids protruding into the extracellular space (amino acids 44-750). 23 amino acids are predicted to form a non-polar α-helical structure inside the membrane (amino acids 19-43), and the remaining 18 intracellular amino acids on the N- terminus (amino acids 1-18) are containing the MXXXL internalization motif.[115]

The closest known homolog of GCPII is GCPIII, having 68% sequence identity and 81% similarity compared to GCPII. It is also a type II transmembrane protein and was shown to embody a highly similar overall structure as GCPII including the posttranslational modifications.[116] Unlike GCPII it is more evenly distributed over the body tissues (found mainly in prostate, heart, placenta, intestine, pancreas, liver, kidney, and brain), however its expression levels are relatively lower (determined on the mRNA level by qPCR).[117] As opposed to GCPII, it is highly expressed in testis and uterus. Its physiological function in these tissues is unknown - however, GCPIII has been found to cleave beta-citrylglutamate, which is also abundantly expressed in testis.[118] GCPIII is able to cleave the natural substrate NAAG (see next chapter) albeit with slightly lower specific activity.[119]

3.2.3 Enzymatic Activity of GCPII

As mentioned in the broad introduction of this chapter, GCPII enzymatic activity was found both in the small intestine and in the brain, where it fulfills completely different physiological roles. The catalytic activity, however, remains the same: the cleavage of terminal glutamate by hydrolysis of a peptide bond (figure 7, p. 25). The role of GCPII in the prostate is currently unknown and it not clear if it is actually related to its enzymatic activity.

In the brain GCPII cleaves the most abundant dipeptide neurotransmitter [120], N-acetyl-L-aspartyl-L-glutamate (NAAG) into N-acetyl-L-aspartate and L-glutamate (figure 7A, p. 25). This process is vital for proper function of signal transduction by this neurotransmitter, since no reuptake of the dipeptide is known. The glutamate, however, is by itself a neurotransmitter, and has to be then reabsorbed by astrocytes.[99] Furthermore, NAAG was shown to be neuroprotective in the brain.[121]

In the small intestine GCPII cleaves of the glutamic acid from the poly–γ–L–glutamyl folate (figure 7B, p. 25). Since poly–γ–L–glutamyl folate, a dietary precursor of vitamin B_9, is strongly charged and relatively large, it cannot be resorbed through the intestinal brush border membrane. GCPII cleaves off the redundant glutamic acids, thus reducing the overall negative charge of the folate and facilitating its resorption.[103, 122]

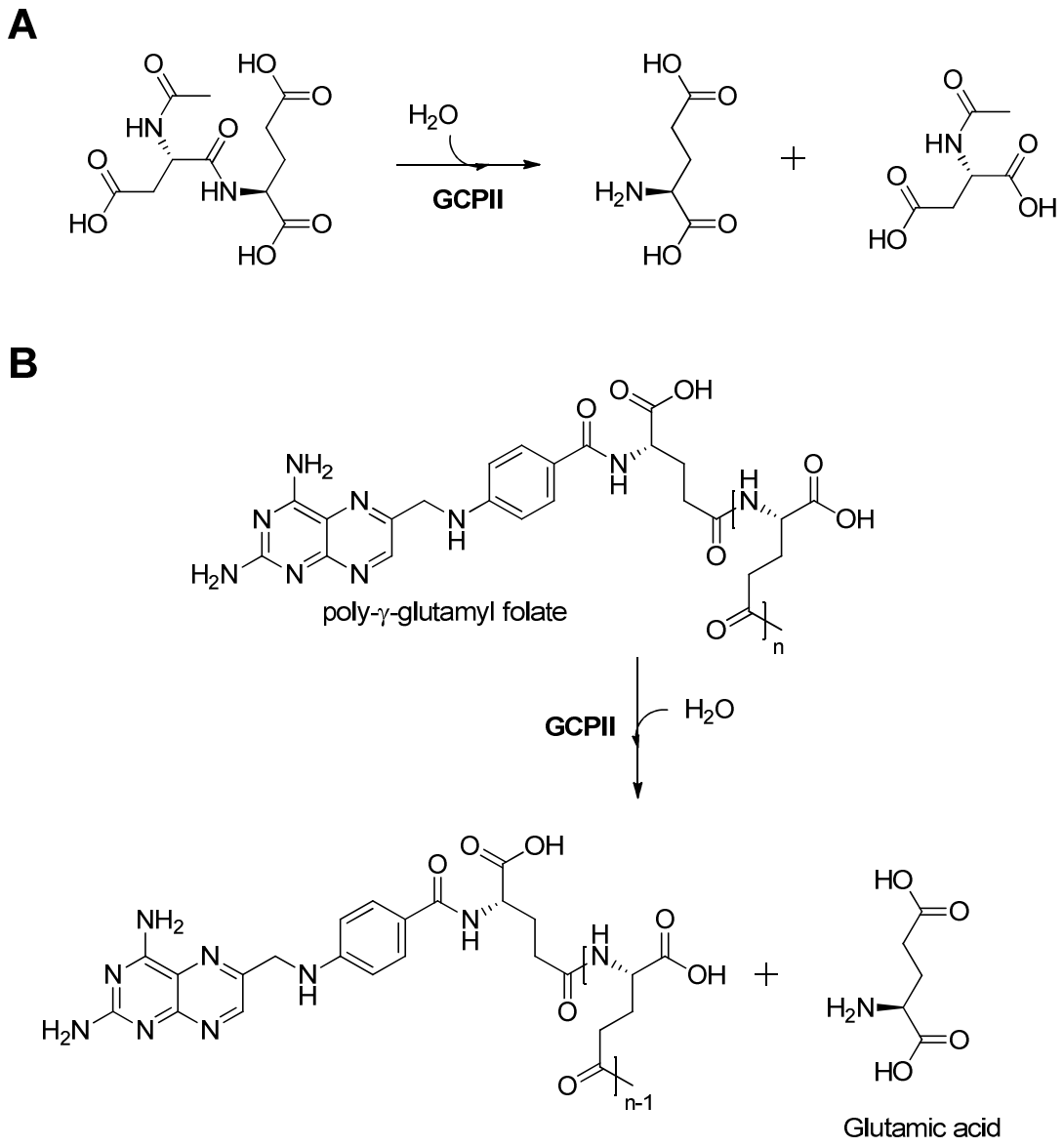

Figure 7: Enzymatic activity of GCPII. **A**) cleavage of neurotransmiter NAAG; **B**) cleavage of glutamic acid from poly-γ–glutamyl folate.

3.2.4 Structure of GCP II

Even before the experimental x-ray structure of the protein was obtained in 2005, predictions based on similarity of GCPII overall structure with transferrin receptor and also with other M28 metallopeptidase family members were made. It was suggested that His377, Asp387, Glu425, Asp453, and His553 directly coordinate the two zinc atoms bound in the active site[113] and that Glu424 serves as a proton shuffle in the catalytic site (see further).[123]

Two separate groups reported the x-ray structure of GCPII ectodomain in 2005.[124, 125] The experimental data confirmed the similarity to transferrin receptor, defined three domains of GCPII and identified the dimerization interface of the protein. The overall structure of

homodimeric GCPII with bound inhibitor is shown in figure 8 (p. 27). The extracellular part of the domain consists of protease domain (amino acids 57-116 and 352-590), the apical domain (amino acids 117-351) and the C-terminal domain (amino acids 591-750). All these domains participate in the formation of enzyme active site. The most dominant structural feature of the protease domain is a mixed β-sheet conformation in close juxtaposition to 10 α-helices. Between the first and second strand of the beta sheet the apical domain is inserted, covering the active site and thus forming a deep tunnel between the two domains. The C terminal domain is formed mainly by four interacting helices which play major role in formation of the homodimer, forming several salt bridges and multiple hydrophobic interactions between the monomers.[125]

The way to the active site is formed by irregularly shaped funnel which ends with a pharmacophore cavity. The cavity is dominated mainly by the two firmly bound Zn^{2+} atoms, which are the main players in the cleavage of the peptide bond. The two zinc atoms are strongly coordinated by the following amino acid residues: His377, Asp453 for zinc I and His553 and Glu425 for zinc II. The two metal ions are further bridged by bidentally coordinated Asp 387 and with hydroxyl anion, the nucleophile attacking the peptide bond. Glu424 works as a proton shuttle abstracting the hydrogen from the water molecule coordinated to the zinc core, thus forming the nucleophile which readily attacks the peptide bond. Concomitantly Glu424 gives the second proton to the leaving amino group of the glutamate, finishing so the peptide bond cleavage.[125, 126].

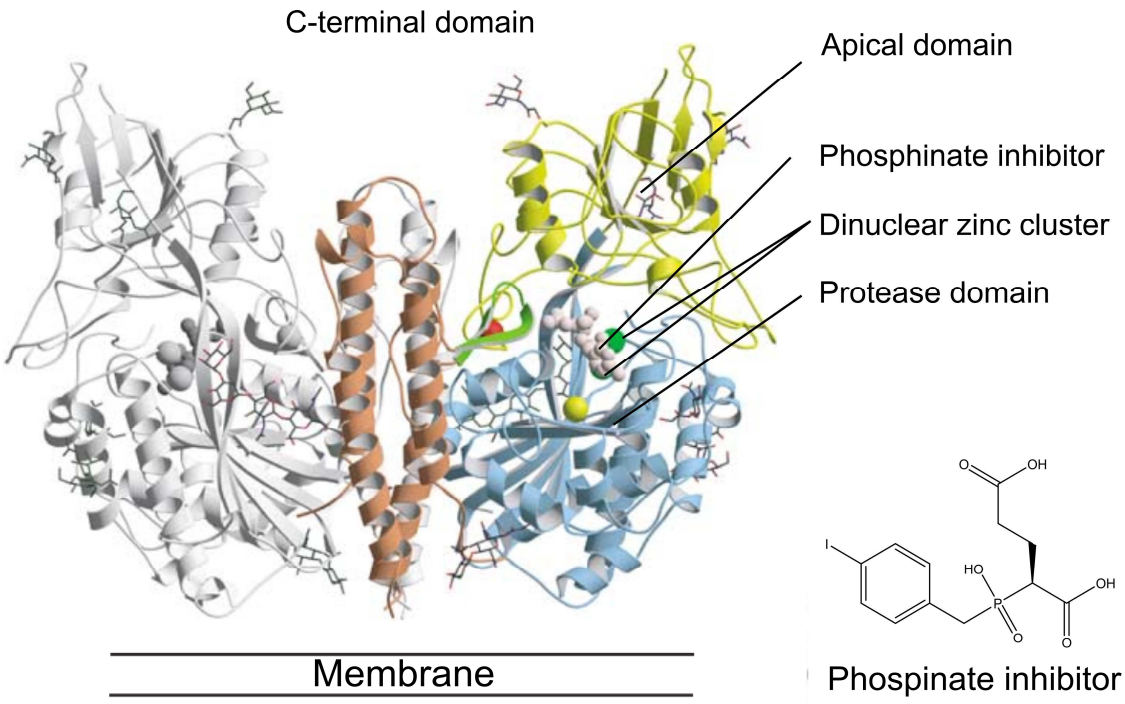

Figure 8: The overall structure of GCPII with bound phosphinate inhibitor. One of the subunit is shown in grey, the other is colored according to the domain organization: light blue for protease domain, yellow for apical domain and brown for C-terminal domain. The two zinc atoms are shown as green spheres, the calcium cation is shown as a red sphere and the chloride ion is shown as a yellow sphere. The figure was adapted from [125].

3.2.5 Substrate specificity and mechanism of action

Glutamic acid is the only naturally occurring amino acid in the substrates P1´ position. The recognition of this residue in the S1´ pocket is provided by several strong interactions (figure 9**E**, p. 28). The main interactions responsible for recognition of the γ-carboxylate are the salt bridge between the dissociated carboxylic acid and Lys699 as well as strong hydrogen bond between Asn257 amide and the γ-carbonyl oxygen. The α-carboxylic acid is bound by several hydrogen bonds to Tyr700, Tyr552 and Arg210. Interestingly, the binding of glutamate into the active center dramatically changes the overall structure of the active site, by displacing a relatively loose loop formed by residues Lys699 and Tyr700, by almost 5 Å. This is a typical textbook example of an induced fit mechanism of substrate binding (figure 9**A**, p. 28). The loop was thus labeled "glutarate sensor". [125]

Moving to the surface of the enzyme from the active site one encounters several interesting structural features, which can be exploited during design of inhibitors (often referred to as exosites, summarized in figure 9, p. 28). The whole active site is shielded from the external space by a flexible loop (amino acids Trp541-Gly548) also known as the entrance lid. It has been found either in closed or opened state, depending on the bulkiness of the bound ligand.

Interestingly, when the entrance lid is in its opened state, a cavity directly below it is exposed (figure 9**B**). This site has been targeted with aromatic moieties during design of ultra-high affinity inhibitors, which led to a 60 fold increase in inhibitor potency.[127]

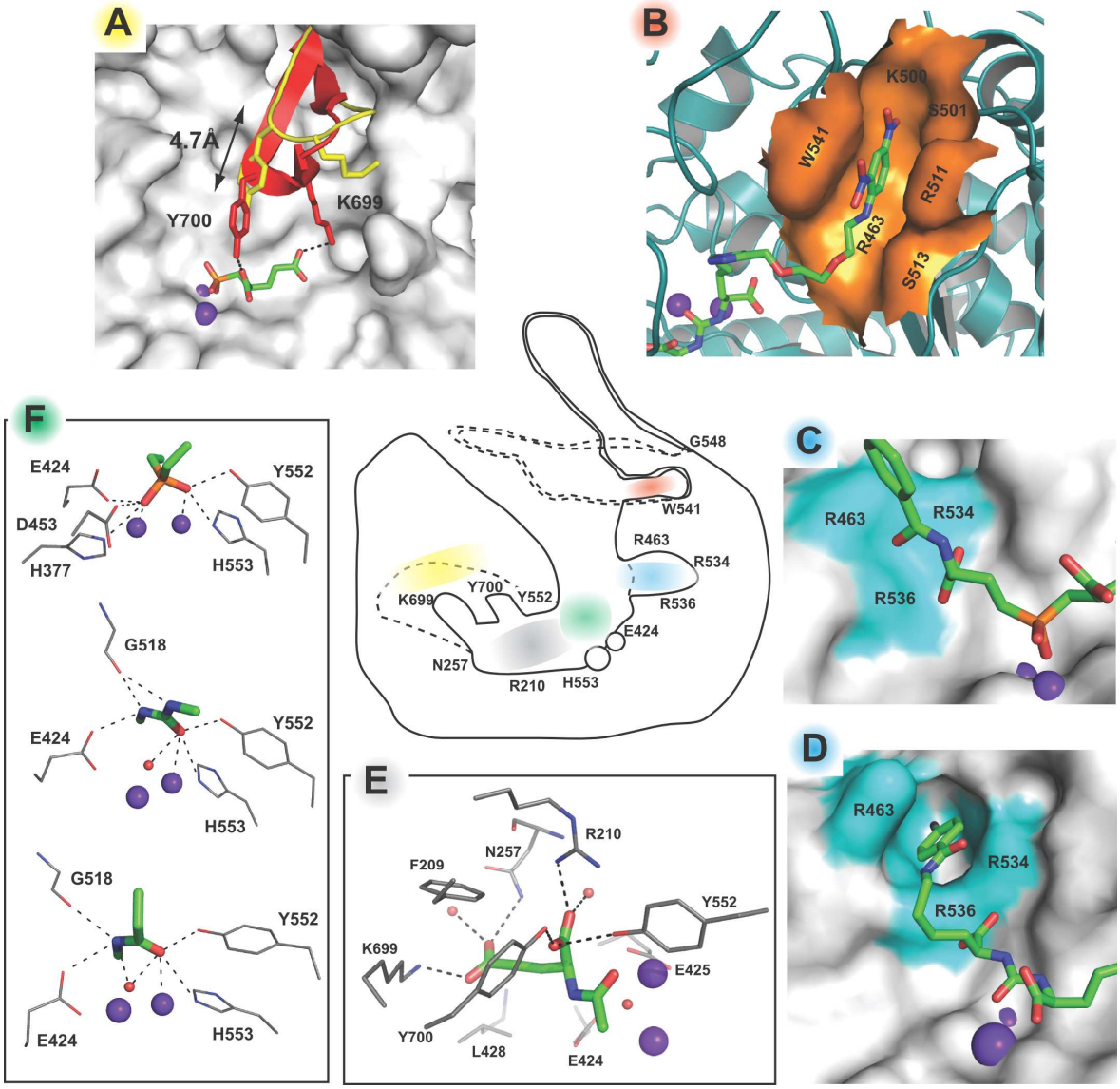

Figure 9: The internal cavity of GCPII; The schematic illustration of the GCPII is shown in the center of the figure. The flexible regions of GCPII are shown in both possible conformations, with dashed and full lines. Selected residues are shown in one letter coding with appropriate number in sequence. The zinc atoms are shown invariably as violet spheres throughout the figure, the rest of the figure is colored according to the center scheme. **A**) The S1´ site - the glutarate sensor. **B**) The details of arene binding site. **C)** and **D** the arginine patch showed in surface representation. **E**) The S1´ site – specificity. **F**) hydrogen bonding in the immediate vicinity of the zinc atoms. Inhibitors with different zinc binding groups and their interactions with the zinc atoms are shown for phosphinate (top) and urea based inhibitor (middle). For comparison a structure with the natural substrate NAAG is also shown (bottom); The substrates/inhibitors are shown in stick representation with color coding as follows: carbon-green, nitrogen-blue, oxygen-red. Hydrogen bonds are shown as dashed lines. Taken from [128].

Another apparent feature of the tunnel is a positively charged region formed by three stacked arginine residues (Arg463, Arg534 and Arg536; figure 9**C** and 9**D**, p. 28). The heavily charged side chains are stabilized through the interactions with a chloride ion. This region is often referred to as arginine patch and is probably responsible for preferential binding of negatively charged residues at the end of the S1 pocket.[129, 130] The Arg463 can change conformation upon ligand binding opening so a pocket big enough to accommodate aromatic residues, which are stabilized with π-stacking interactions. The site was successfully targeted by moieties as large as 4-iodobenzyl, which tightly fits in the cavity, increasing the inhibitor potency significantly. [131]

3.2.6 Inhibitors of GCPII

The inhibitors of GCPII have been thoroughly studied during the past two decades for their potential neuroprotective function as well as a potential use in targeting of prostate carcinoma (see chapter 3.2.6).

GCPII is a metallopeptidase and therefore it came as a no surprise that small chelator molecules (such as EDTA, EGTA) were found out to inhibit its enzymatic activity at millimolar concentrations. Glutamate, as a resulting cleavage product of the naturally abundant substrate, is also a weak inhibitor of GCPII (IC_{50} = 31 μM).[99]

Nearly all specific inhibitors of GCPII are originally based on the structure of NAAG (Fig 7A). The defining region of the inhibitor is the part interacting with the catalytic zinc atoms, often referred to as zinc binding group (ZBG). With respect to the zinc coordinating moiety the inhibitors are divided into three major groups: the phosphonates/phosphinates based, urea based and thiol based inhibitors.[132] It should be also noted that other moieties such as sulfonamides and hydroxamic acids have been tested, however, they display relatively low potencies in comparison with the previously mentioned groups.[133, 134]

3.2.6.1 Phosphorus Based Inhibitors

The tetrahedral structure of phosphorus based inhibitors, mimicking the transition state, has been utilized in development of various protease inhibitors since the beginning of modern medicinal chemistry.[135] The landmark of discovery in phosphorous based inhibitors of GCPII dates back to 1996 when 2-(phosphonomethyl)pentanedioic acid (2-PMPA, figure 10, p. 30) was synthesized and displayed subnanomolar potency.[122] The follow-up studies showed that the *S* enantiomer binds approximately 300 times stronger than the *R* enantiomer, which was

expected since that is the respective enantiomer of the naturally occurring amino acid in the substrate.[136] Subsequent studies tried to derivatize the P1´ of the inhibitor, however this proved to be a dead end (for chemical formulas and enzymatic activities see figure 10, **1**-**3**), since S1´ site of the enzyme is very finely tuned to precisely accommodate the glutamic acid,[137] as has been later shown in the x-ray structures of GCPII with bound inhibitor (described in detail in chapter 3.2.5, p 27).[138] 2-PMPA does not target the S1 site of the enzyme and therefore a small library of phosphinates has been synthesized to evaluate their potential to bind to this site (figure 10, **4**-**6**). This derivatization was also explored to improve the horrible pharmacokinetic properties of 2-PMPA, which is heavily charged with logP value of -3.23.[139] The substitution of the free hydroxyl, however, proved to be decreasing the activity in vast majority of the cases, probably because of loss of hydrogen bonding between the zinc atoms and the free hydroxyl group.

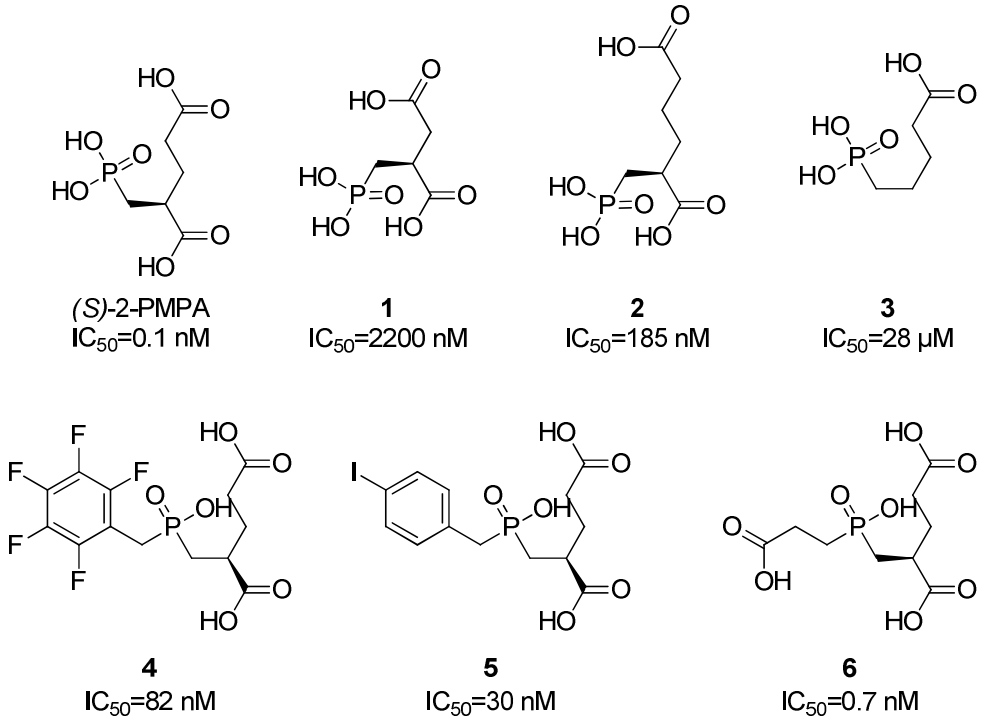

Figure 10: Phosphonate and phosphinate based inhibitors of GCPII

3.2.6.2 Urea Based Inhibitor

The urea and carbamate moieties have been heavily used in development of peptidomimetic inhibitors,[140] but are not so commonly utilized to target the metallopeptidases. The urea based inhibitors were discovered as a possible replacement for the highly charged phosphonate/phosphinate moieties. The symmetrical inhibitor arising from connection of the two *S*-glutamic acids by urea linker (figure 11, **1**), proves to be a strong inhibitor with IC_{50} value of 49 nM.[141] Unlike the phosphonate and phosphinate inhibitors of GCPII the urea based inhibitors are rather easily accessible, and are already intrinsically chiral if chiral amino acids are used at the beginning. This led to a fast development of small libraries of these compounds (exemplified by **2** in figure 11) aiming to optimize the binding ligand into the S1 pocket. The effort was rewarded by several compounds displaying sub-nanomolar potencies (figure 11, **3**).

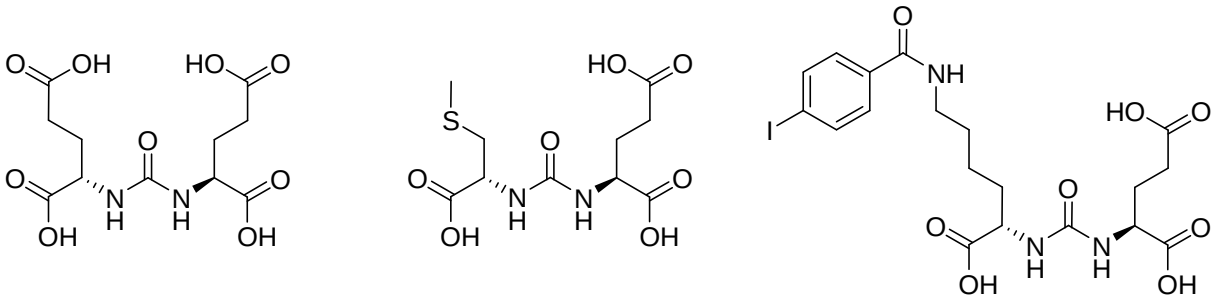

1 IC_{50}=49 nM

2 IC_{50}=17 nM

3 IC_{50}=0.06 nM

Figure 11: Inhibitors based on urea scaffold

3.2.6.3 Thiol Based Inhibitors

In search of orally available inhibitors of GCPII a series of thioalkyl derivatives of pentanedioic acid have been explored (figure 12, **1-6**, p. 32). The optimal length between the thiol moiety coordinating the zinc atoms and the pentandioic acid was surprisingly established to be three-carbon-long linker.[142] Even though these inhibitors have higher K_i values compared to the inhibitors of the two previous groups, they still exhibit low nanomolar potencies towards GCPII and unlike phosphonate and urea based inhibitors actually display its effectiveness even in mouse models and were shown to exhibit efficacy in various models of neurological disorders.[143-145] The group of Barbara Slusher at Guilford Pharmaceuticals, working on the thiol based inhibitors, was not discouraged by the negative results of their predecessors who tried to further optimize the P1´ part of the inhibitor. They did manage to

find a suitable candidate in compound **7** (figure 12), which displays slightly increased activity while gaining a bit of so much needed hydrophobicity.[146] Up to date, this is the only modification of the P1´ which led to an increase in inhibitor's activity. Surprisingly enough this substitution is not transferable to other classes of inhibitors with different ZBG (*e.g.* the substitution of thiol group for phosphate leads to a loss of activity, figure 12, **8**).[146]

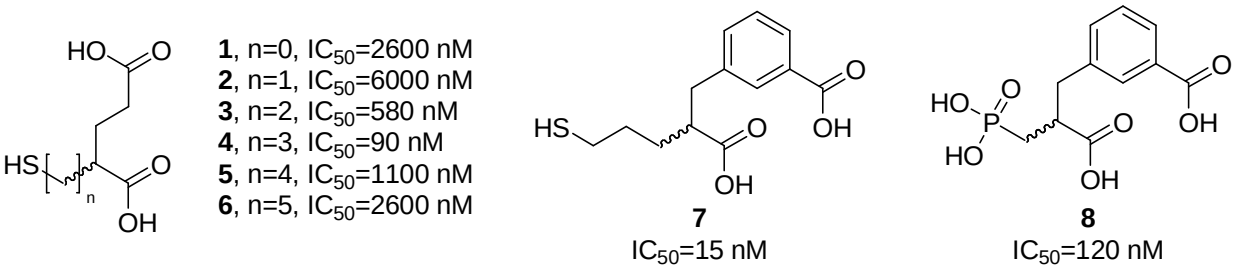

Figure 12: Thiol based inhibitors of GCPII

3.2.7 GCPII and Cancer

Both normal and malignant prostate cells were found to express high amount of GCPII, even though the function of it in this organ is not known. The expression of GCPII in the prostate carcinoma cells exceeds the expression in the non-malignant cells by the factor of ten.[147] Some studies hypothesize that this expression could serve as a form of glutamate source for the cells, others claim it has to do with possible folate transport, however neither have been proven up to date.[148, 149] Another possibility is that GCPII serves as a partner for yet unknown protein, referring to its structural homology and function of transferrin, but no such partner has been identified yet.

Even though the function of GCPII in the cancer growth is still unknown, GCPII obviously plays an important role in this pathophysiological condition, since almost all metastatic tumors originating from prostate cancer found in bone marrow and in lymph nodes were shown to retain the GCPII overexpression levels.[150, 151]

Besides the prostate carcinoma, GCPII has been also linked with solid tumors, specifically with the blood vessel endothelial cells associated with most solid tumors. These cells are responsible for nutrition of the tumor cells. Here it was suggested, that GCPII plays a role in angiogenesis and in formation of neovasculature.[152]

3.2.8 Role of GCPII in Cancer Imaging

Imaging has become one of the first choices for diagnosis of prostate cancer, mainly because of its noninvasiveness in comparison to biopsies. The field covers number of imaging techniques including positron emission tomography (PET), single-photon emission computed tomography (SPECT), magnetic resonance imaging (MRI), x-ray computed tomography (CT), ultrasound and other less frequent techniques.[153] As such, all of these methods are non-specific and can often lead to falsely negative results. By targeting the biological difference unique for prostate carcinoma cells the imaging has an upper hand in earlier diagnosis, carcinoma recurrence diagnosis as well as early detection of potential metastatic bodies.

3.2.8.1 Imaging of Prostate Carcinoma Using GCPII Monoclonal Antibodies

Radiolabelled monoclonal antibodies have been a research interest of many scientific and pharmaceutical companies for over 50 years, as potentially both diagnostic and therapeutic tools.[154] In diagnostics the radiolabeled antibodies are detected by either (PET) or by (SPECT), depending on the type of radioactive decay. Up to date the only FDA approved monoclonal antibody for prostate carcinoma imaging is radioactive conjugate of monoclonal antibody 7E11/Cyt-356 with ^{111}In, commercially known as ProstatScint™. The preparate recognizes the intracellular part of the GCPII, limiting it to binding only the necrotic and apoptotic cells of the prostate carcinoma,[155] which results in rather poor ability to detect prostate cancer.[156] Unfortunately, ProstaScint™ is very often accumulated nonspecifically in the kidneys, liver and other non-prostate sites, resulting in high background, often preventing from making a proper diagnosis.[157] Even though ProstaScint™ is of a great help in identification of the prostate carcinoma, the space for improvement in this diagnostic field is great.

Mainly because of the above mentioned downsides of ProstaScint™ a number of other monoclonal antibodies conjugates cropped up in the past two decades. The antibody probably most worth mentioning is deimmunized monoclonal antibody J591. Its radiolabeled conjugates have been heavily investigated as both diagnostic and therapeutic tool for prostate carcinoma.[158-162] For diagnosis its conjugate with chelated ^{111}In and ^{99m}Tc have been tested and are currently in clinical trials.[163]

3.2.8.2 Imaging of Prostate Carcinoma Using Low Molecular Weight Agents

Even though the monoclonal antibodies represent an excellent tool for imaging the prostate carcinoma, they posses several major disadvantages. The major setback is in form of pharmacokinetics. Antibodies have usually long clearance from the organism which can be disadvantageous, for prolonged exposure of the organism towards the radiation.[153] Another hindrance might be the relatively low shelf-life and high costs of manufacturing.

Since GCPII is an enzyme towards which number of sub-nanomolar inhibitors has been identified, many small molecule agents carrying either radionuclides or flurophores have been examined. There are basically two strategies which can be employed when attaching a radionuclide to the small inhibitor. Either one can use elements which are commonly used in the organic synthesis, but is limited to rather small set (^{11}C, ^{18}F, $^{123;124;125;131}$I). It should be also noted that these radionuclides have relatively short half-lifes which can be both advantageous and disadvantageous.[164, 165] The other option is to broaden the scope with radionuclides of metals (*e.g.* ^{99m}Tc, ^{137}Cs, ^{192}Ir, ^{67}Ga, ^{64}Cu, ^{111}In), which show superior imaging properties, however one has to think how to incorporate them into the scaffold of the inhibitor. The heavy metals are also commonly extremely toxic to the organism and therefore have to be strongly bound to the inhibitor. Since a direct covalent linkage of the metals is synthetically not possible, chelators are the most common choice. Luckily GCPII has a relatively big entrance tunnel through which such chelators can be brought out to surface of the protein.

Number of inhibitors utilizing either of the two strategies has been synthesized and tested, with various results. The most commonly exploited scaffold for development of such imaging agents was incorporating the urea based core into the inhibitors (figure 13, p. 35). Utilizing the common synthesis, inhibitors containing ^{18}F, ^{125}I were subsequently prepared (figure 13, **1** and **2**, p. 35) each exhibiting low nanomolar K_i values. They are selectively binding to the GCPII positive cells and show specific uptake in the GCPII -positive xenografts.[166-168] They were also shown to be able to detect metastatic lesions.[169] Further clinical trials will be needed to fully evaluated their potential.[153] The most commonly used chelators are derivatives of cyclene, with three attached methylenecarboxylic acids to the core nitrogens (DOTA), both enhancing the chelating effect by providing further coordination electron pairs and by compensating the chelated charged metal. The chelating group is usually attached to the core of inhibitor by flexible linker (figure 13, **3**, p. 35). These compounds show comparable inhibitory properties with the inhibitors discussed above.[170, 171]

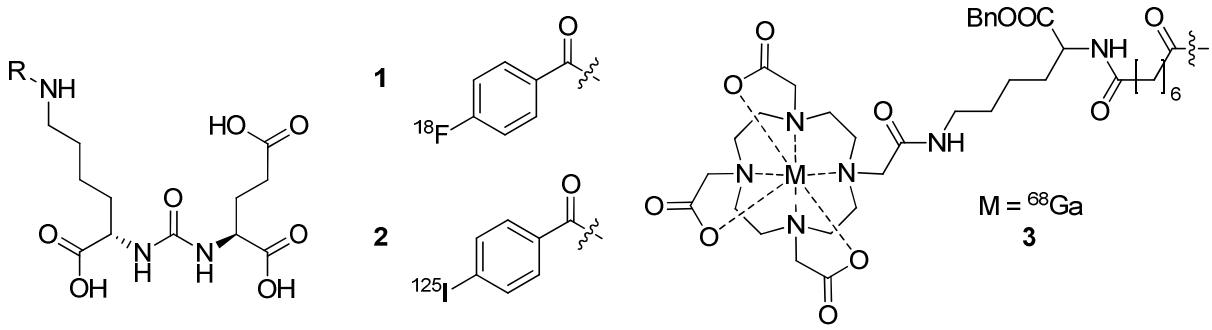

Figure 13: Radiolabeled urea based inhibitors of GCPII as potential diagnostics of prostate carcinoma

3.2.9 GCPII and Prostate Cancer Therapy

Overexpressed GCPII is an excellent target for prostate carcinoma treatment not only because of its organ specificity but also because of its ability to be internalized upon substrate/antibody binding. This clathrin mediated process greatly enhances the possibilities that can be utilized in killing the malignant cells.[115, 172]

The prevalent agents in treatment of the prostate carcinoma are monoclonal antibodies conjugated with either radionuclides, or with other highly toxic agents. As has been already mentioned conjugate of monoclonal antibody J591with number of isotopes has been heavily investigated.[161, 162, 173, 174] Its conjugate with ^{213}Bi, undergoing α-decay, which is not commonly used in cancer therapy for the close range of α particles, has been tested for killing off micrometastatic tumors in bones.[173,175] Furthermore the radionconjugate with ^{111}In is currently under second stage of clinical trials and the conjugate with ^{177}Lu has finished the second clinical trial and is scheduled for stage III.[174]

The second strategy, which is exploiting highly toxic compounds as the killing agents conjugated to the GCPII recognizing carrier (antibodies[176], aptamers[177, 178] and scFV fragments[179, 180]), has been also in the spotlight of the scientists across the field. The most commonly used toxins are compounds targeting the cytoskeleton stability of the cell[176] or disruptors of proteosynthesis at various stages.[179, 180] The toxic compounds (*e.g.* paclitaxel, monomethyl auristatin E) are usually attached to the carriers by disulfide bonds or hydrazone bonds, which are upon internalization in the endosome broken, thus leading to their release into cytoplasm.[176]

The role of small molecules in prostate cancer therapy is rather negligible, due the rapid clearance of these agents from the body.

4 Research Aims

- To design novel HIV PR inhibitors with improved properties by structure-aided drug design based on lead compounds from library screening

- To design, prepare and evaluate a photolabile inhibitor of HIV protease and use it in the cell culture to synchronize the maturation of viral particles and analyze the dynamics of the polyprotein cleavage by reactivating the protease by inhibitor degradation by light

- To design, synthesize and assess potent inhibitors of GCPII, targeting the active site of the enzyme, derivatized with linkers enabling to attach the compound to appropriate nanoparticle for imaging, isolation and targeting of GCPII-expresing cells.

5 Publications

Publications included in the dissertation thesis

I. Schimer, J., Cigler, P., Vesely, J., Grantz Saskova, K., Lepsik, M., Brynda, J., Rezacova, P.,Kozisek, M., Cisarova, I., Oberwinkler, H., Kraeusslich, H.G., and Konvalinka, J., **Structure-aided design of novel inhibitors of HIV protease based on a benzodiazepine scaffold.** J Med Chem, 2012. **55**(22): p. 10130-10135.

II. Tykvart, J., Schimer, J., Barinkova, J., Pachl, P., Postova-Slavetinska, L., Majer, P., Konvalinka, J., and Sacha, P., **Rational design of urea-based glutamate carboxypeptidase II (GCPII) inhibitors as versatile tools for specific drug targeting and delivery**. Bioorg Med Chem, 2014. **22**(15): p. 4099-4108.

III. Schimer, J., Pavova, M., Anders, M., Pachl, P., Sacha, P., Cigler, P., Weber, J., Majer, P., Rezacova, P., Krausslich, H.G., Muller, B., and Konvalinka, J**., Triggering HIV polyprotein processing by light using rapid photodegradation of a tight-binding protease inhibitor**. Nat Commun, 2015. **6**: 6461.

Publications not included in the dissertation thesis

I. Valero, G., Schimer, J., Cisarova, I., Vesely, J., Moyano, A., and Rios, R., **Highly enantioselective organocatalitic synthesis of piperidines**. Formal synthesis of (-)-Paroxitene. Tetrahedron Letters, 2009. **50**: p. 1943-1946.

II. Číhalová, S., Valero, G., Schimer, J., Humpl, M., Dračínský, M., Moyano, A., Rios, R., and Vesely, J., **Highly enantioselective organocatalytic cascade reaction for the synthesis of piperidines and oxazolidines**. Tetrahedron, 2011. **67**: p. 8942-8950.

III. Schimer, J. and Konvalinka, J., **Unorthodox inhibitors of HIV protease: looking beyond active-site directed peptidomimetics**. Curr Pharm Des, 2014. **20**(21): p. 3389-3397.

IV. Neirynck, P., Schimer, J., Jonkheijm, P., Milroy, L.-G., Cigler, P., and Brunsveld, L., **Carborane–b cyclodextrin complexes as a supramolecular connector for bioactive surfaces**. Journal of Materials Chemistry B, 2015. **3**: p. 539-545.

5.1 Structure-aided design of novel inhibitors of HIV protease based on a benzodiazepine scaffold

Background:

HIV protease (HIV PR) is one of the primary targets for virostatics during the treatment of the infection. There are currently nine approved inhibitors in the clinics, however, due to the high error prone nature of the reverse transcriptase and the fast replication rate of the virus, resistances to each one of them has been already described.[98] There are several ways to circumvent the drug resistance of HIV PR. One of the possibilities is finding an inhibitor which binds outside the active site, either into allosteric site of the HIV PR, or into its dimerization domain (chapter 3.1.8.4). However, probably the easier approach is to identify a novel competitive inhibitor with different binding mode inside the active center and design it to combat the resistant strains that have already been identified.

Summary:

In the search for novel capsid assembly inhibitors by large library screenings we discovered also several weak inhibitors of HIV PR. While going through the structures of these small entities we could not overlook one of the candidates – a benzodiazepine based compound. Benzodiazepines have a long history in the clinical care ranging over more than 60 years, mostly because of their non-toxicity and great pharmacokinetical properties. We therefore decided to pursue this lead and evaluate it further.

The inhibitor (figure 14, **1**, p. 39) proved to be a low micromolar inhibitor (IC_{50} (**1**) = 5 µM) in our hands. A subsequent crystallographic analysis showed surprisingly two inhibitors bound in the active center. We decided to utilize this observation by the connection of the two molecules by a short linker (figure 14, **2**, p. 39). This connection led to a powerful increase in activity of the inhibitors by two orders of magnitude (IC_{50} (**2**) = 60 nM). Unfortunately, there were four stereogenic centers on the molecule, making it rather difficult to work with. We further decreased the number of stereogenic centers to 2 with slight increase in the activity (IC_{50} (**3**)= 30 nM). Despite extensive efforts invested into obtaining structure of complex of HIV PR with inhibitor **3** we were not successful, and, therefore, we decided to tackle the problem using molecular dynamics. The molecular dynamics model identified a strong hydrogen bonding formed between the catalytic asparates and the carbonyl atoms of the oxalyl linker, which is probably the main reason for the increased activity of the dimeric inhibitors.

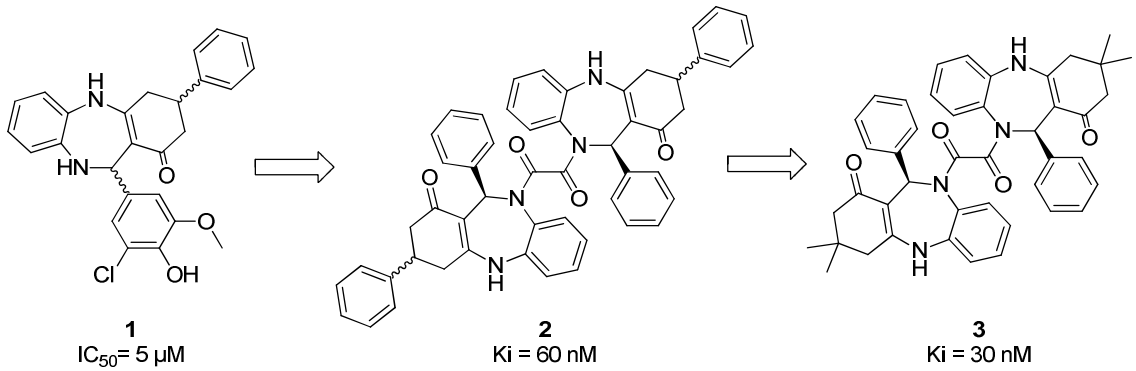

Figure 14: Novel class of inhibitors of HIV PR based on dibenzodiazepine scaffold. Synthetizing the dimeric structure increased the activity of the inhibitor by two orders of magnitude. We further decreased the number of stereogenic centers to two (**3**). It has been suggested from the docking model of the dimeric inhibitors that the oxalyl oxygens form strong hydrogen bonds to the catalytic aspartates, which is probably the main contribution for the increase in activity.

My contribution:

I prepared all the dimeric inhibitors, separated them to diastereomerically pure products, and evaluated their enzymatic constants against both mutated and wild type forms of HIV PR. I further conducted all the crystallization experiments and wrote the draft of the manuscript.

Schimer, J., Cigler, P., Vesely, J., Grantz Saskova, K., Lepsik, M., Brynda, J., Rezacova, P.,Kozisek, M., Cisarova, I., Oberwinkler, H., Kraeusslich, H.G., and Konvalinka, J., **Structure-aided design of novel inhibitors of HIV protease based on a benzodiazepine scaffold**. J Med Chem, 2012. **55**(22): p. 10130-10135.

Journal of Medicinal Chemistry

Article

pubs.acs.org/jmc

Structure-Aided Design of Novel Inhibitors of HIV Protease Based on a Benzodiazepine Scaffold

Jiří Schimer,[†,‡] Petr Cígler,[†] Jan Veselý,[§] Klára Grantz Šašková,[†] Martin Lepšík,[†] Jiří Brynda,[†,∥] Pavlína Řezáčová,[†,∥] Milan Kožíšek,[†] Ivana Císařová,[¶] Heike Oberwinkler,[⊥] Hans-Georg Kraeusslich,[⊥] and Jan Konvalinka*[,†,‡]

[†]Institute of Organic Chemistry and Biochemistry, Gilead Sciences and IOCB Research Center, Academy of Sciences of the Czech Republic, Flemingovo n. 2, 166 10, Prague 6, Czech Republic

[‡]Department of Biochemistry, [§]Department of Organic Chemistry, and [¶]Department of Inorganic Chemistry, Faculty of Science, Charles University, Hlavova 8, 128 43, Prague 2, Czech Republic

[∥]Institute of Molecular Genetics, Academy of Sciences of the Czech Republic, Vídeňská 1083, Prague 4, Czech Republic

[⊥]Department of Infectious Diseases, Virology, Heidelberg University, Im Neuenheimer Feld 324, 69120 Heidelberg, Germany

Supporting Information

ABSTRACT: HIV protease is a primary target for the design of virostatics. Screening of libraries of non-peptide low molecular weight compounds led to the identification of several new compounds that inhibit HIV PR in the low micromolar range. X-ray structure of the complex of one of them, a dibenzo[*b*,*e*][1,4]-diazepinone derivative, showed that two molecules of the inhibitor bind to the PR active site. Covalent linkage of two molecules of such a compound by a two-carbon linker led to a decrease of the inhibition constant of the resulting compound by 3 orders of magnitude. Molecular modeling shows that these dimeric inhibitors form two crucial hydrogen bonds to the catalytic aspartates that are responsible for their improved activity compared to the monomeric parental building blocks. Dibenzo[*b*,*e*][1,4]diazepinone analogues might represent a potential new class of HIV PIs.

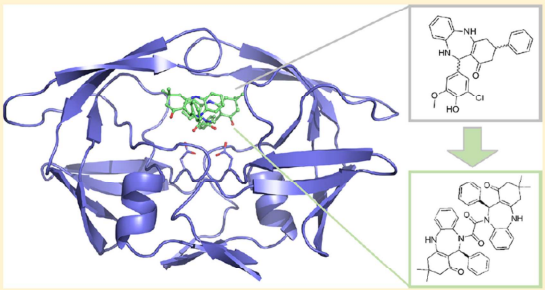

INTRODUCTION

More than 25 years after its discovery, HIV protease (HIV PR) remains one of the primary targets for development of novel HIV treatments. Because HIV PR plays a key role in the life cycle of the virus, its inhibition prevents maturation of the viral particles and renders them noninfectious.[1] Protease inhibitors (PIs), combined with other antiretroviral drugs in "highly active antiretroviral therapy" (HAART), can decrease viral load below measurable levels and greatly increase the life expectancy and quality of life of HIV patients. However, the high cost of HAART, the occurrence of various side effects, and the emergence of highly mutated viral strains cross-resistant to antivirotics have motivated both academic researchers and the pharmaceutical industry to develop novel PIs. These second generation PIs exhibit improved pharmacokinetic properties, fewer side effects, and a more favorable activity profile against highly resistant viral species than their predecessors.[2] Development of HIV PIs remains one of the most remarkable examples of structure-aided drug design and a test case for novel approaches in medicinal chemistry (for review see refs 3 and 4).

In the past decade, the U.S. Food and Drug Administration (FDA) has approved several highly effective second generation PIs, including darunavir, that exhibit a low picomolar K_i and favorable resistance profile.[5] A number of other PIs have been recently reported. We searched for novel structures that might adopt an alternative binding mode to HIV PR and thus possibly exhibit a different resistance profile than current PIs. As a result, we and others identified several unexpected chemical structures that have been reported to inhibit HIV PR. These compounds include fullerenes, niobium-based polyoxometalates, and icosahedral carboranes (for a recent review of new PIs, see ref 6). The need for new structural types that open alternative pathways for rational drug design, however, remains urgent.

Recently, our laboratory screened a variety of chemical structures for inhibition of HIV replication. This led to the identification of several new compounds that inhibit HIV PR in the low micromolar range. One of these compounds is a dibenzo[*b*,*e*][1,4]diazepinone derivative (compound **1**, Table 1). 1,4-Benzodiazepines have been widely used as psychoactive compounds since the mid-1960s. In the past two decades, benzodiazepines experienced a renaissance period during which high throughput screening panels containing various diazepine analogues were applied to various enzymatic targets. These

Received: August 29, 2012
Published: October 11, 2012

Table 1. Diazepine-Based Inhibitors of HIV-1 PR and Their in Vitro Inhibitory Activity toward HIV-1 PR

Compound No.	Structure	Molecular weight	IC_{50} [μM]
1	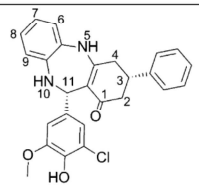	446.14	4.3 [a]
2	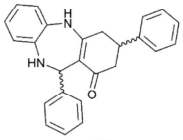	366.17	20 [a]
3	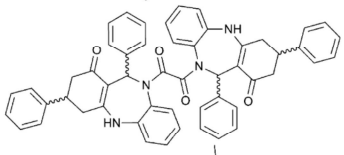	786.32	0.06 [b]
4	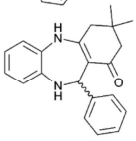	318.17	110 [a]
5	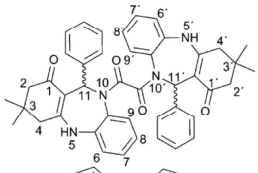	690.32	0.03 [b]
6	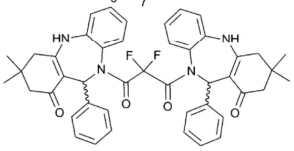	740.31	0.3 [a]

[a] IC_{50} of diastereomeric mixture was determined. [b] IC_{50} of more active diastereomer (11*R*,11′*R* and 11*S*,11′*S*) was determined.

screens led to identification of several potential drugs, some of which were recently approved for clinical use (for a review of diazepines, see ref 7). Because benzodiazepines are considered an excellent pharmacophore owing to their nontoxicity and good pharmacokinetic properties, **1** was selected for further development by structure-aided drug design.

RESULTS

Compound **1** (Table 1) is a low micromolar (IC_{50} of 4.3 μM) inhibitor of HIV PR. Kinetic analysis showed that **1** is not purely competitive (Supporting Information). Nevertheless, X-ray crystallography of the corresponding complex with HIV PR showed that the inhibitor does bind to the PR active site. Interestingly, two molecules of **1** were found in the PR binding cleft (Figure 1).

The two molecules of **1** bind symmetrically into the C2 symmetric protease dimer with semiopen flaps covering the active site. The inhibitor molecules occupy the active site of the enzyme but do not directly interact with the catalytic aspartates. They make numerous van der Waals interactions with flap residues Ile47, Gly48, and Leu50 and residues 80−84, which

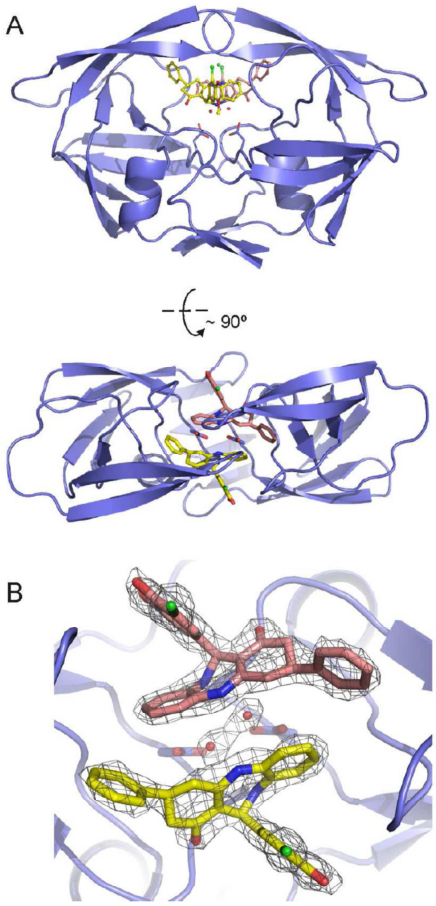

Figure 1. Crystal structure of wild-type HIV PR in complex with compound **1**. (A) Two views of the overall structure. The protein is shown in cartoon representation with the catalytic aspartates shown in stick representation. Two copies of **1** bound to the active site are shown in stick representation. Carbon atoms are shown in pink and yellow to distinguish the two molecules. Oxygen, nitrogen, and chlorine atoms are colored red, blue, and green, respectively. Structural water molecules and chloride ion are shown as red and green spheres, respectively. (B) Detailed top view of the enzyme active site. The electron density map ($2F_o - F_c$ map contoured at 1.5σ level) for the two molecules of **1** and water molecules W1 and W2 is shown in gray. Flap residues covering the active site are omitted for clarity. Stereoview version of Figure 1 is shown in Supporting Information.

belong to the S3 and S3′ substrate binding pockets (Figure 2A). The only polar interaction between inhibitor and enzyme is between imino group N21 of **1** and the main-chain carbonyl oxygen of Gly 27. Additional interactions are mediated through water molecules located at the bottom of the active site and through a chloride anion located under the tips of the flaps. Water molecules (designated W1 and W2 in the crystal structure) make hydrogen bonds with the side chains of the catalytic aspartates and are within hydrogen-bonding distance of N21 of compound **1**. A chloride ion located between the inhibitor and enzyme flaps bridges the imino groups of Ile50 in both chains and N14 of compound **1** through four acceptor hydrogen bonds. This interaction is analogous to that of the so-called flap water molecule present in crystal structures of HIV PR in complex with peptidomimetic inhibitors.[4] The

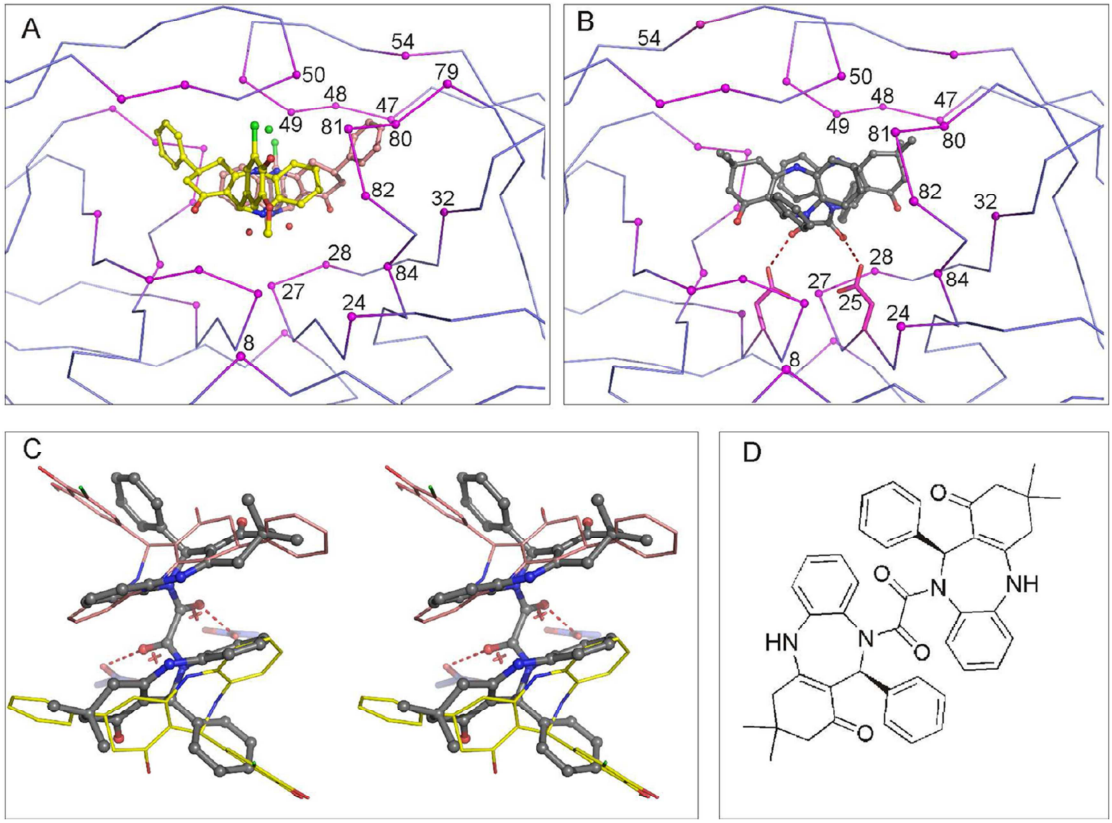

Figure 2. (A) Interaction of compound **1** in the active site of HIV PR in the crystal structure. Cα atoms of residues in contact with the inhibitor are depicted as spheres and colored magenta (residue numbering is indicated only for one protein chain). A detailed list of interactions is summarized in Supporting Information Table S2. (B) Interaction of compound **5a** (11*S*,11′*S* configuration) in the active site of HIV PR in the model. Residues in contact with inhibitor are highlighted by their Cα atoms and colored magenta. Polar contacts with catalytic aspartates are shown as red dashed lines (the hydrogen-bonding distances between protein and inhibitor oxygens are 2.6 Å). (C) Superposition of the binding modes of compounds **1** and **5**. Stereoview of the active site corresponds to bottom panel of Figure 1. For clarity, the protein chain is not shown and catalytic aspartates are represented by sticks. Two structural water molecules present in the crystal structure are represented by red crosses. (D) Structural formula of the single enantiomer of compound **5a** (11*S*,11′*S*) which fitted into the active site cavity based on docking (cf. Figure 3).

replacement of the flap water by a properly positioned oxygen atom from an inhibitor molecule has often been used to improve the binding of non-peptide inhibitors of HIV PR (for recent examples, see refs 25 and 26)

Binding of two molecules of **1** to the active site suggests that linking the molecules might lead to more favorable binding to the PR binding cleft. There are examples of this in the literature, observed with both HIV PR and other proteins, as well as a theoretical explanation of this phenomenon.[27] Two molecules of a derivative of **1** (**2**, Table 1) were connected by a two-carbon linker (oxalyl), mainly for synthetic simplicity. The resulting inhibitor (**3**, Table 1) showed an inhibition constant lower than that of the monomeric **2** by more than 2 orders of magnitude.

Compounds lacking the phenyl moieties attached to carbons 11 and 11′ (**7** and **8**) showed moderate decreases in inhibitory activity and decreased solubility.

The most potent inhibitor (**5a**) is selective for HIV PR. It inhibits neither the related aspartic protease human cathepsin D nor papain, a prototype cysteine protease (see Supporting Information for details).

Molecular docking suggested that only one enantiomer of **5** would fit into the active site of HIV PR for steric reasons (Figure 2D). The docked conformation of **5a** showed an occupation of the active site similar to the two molecules of **1**. Notably, the positions of the two carbonyl oxygens of the linker nearly coincided with the positions of the two water molecules found in the X-ray structure of the HIV PR−**1** complex (cf. Figure 2A,B). Thus, the carbonyl oxygens of **5a** were positioned appropriately to form two hydrogen bonds with the enzyme's catalytic aspartates (Figure 2B).

A comparison of the docked structure of **5a** in HIV PR with the X-ray structure of the HIV PR−**1** complex shows that the two dibenzodiazepine cores occupy similar positions in the enzyme binding pocket, but because of the short oxalyl linker, those of **5** are closer to each other and adopt an almost parallel mutual orientation (Figure 2C). While the two cores occupy the S3−S2′ enzyme subsites in a unique arrangement, their substituents (the phenyl moieties attached to C3 in **1**) point to previously unexplored parts of the binding site. Interestingly, the two structural water molecules, W1 and W2, which are within hydrogen-bonding distances of the outer Oδ atoms of Asp25 and Asp25′ (2.82 and 2.59 Å, respectively), nearly

perfectly coincide with the two oxalyl oxygens of **5a** (Figure 2C).

DISCUSSION

Here, we report the identification of dibenzo[*b*,*e*][1,4]-diazepinones as a new class of HIV PIs. As shown by the X-ray structure, two molecules of the parental compound (**1**) bind to the PR active cleft in a unique mode. By joining two molecules of the weakly inhibiting **1**, we obtained dimeric compounds that bind over 2 orders of magnitude more favorably, thus confirming general theoretical predictions.[28]

Despite extensive efforts, our attempts to obtain the crystal structure of **5a** in complex with HIV PR were not successful. We therefore employed molecular modeling to suggest a possible structure (Figure 2B). The greatly enhanced inhibitory ability of dimeric inhibitor **5a** compared to monomeric inhibitor **4** may be explained in part by thermodynamics. The entropic contribution of only a single molecule in the active center of HIV PR is lower than that of two molecules (as in the case of the monomeric inhibitor). Furthermore, two key hydrogen bonds that are formed between the catalytic aspartates and two oxygens from the oxalyl group of **5a** (Figure 2) contribute to the improved binding. The lack of these crucial hydrogen bonds might explain the decreased activity of **6** (Table 1) compared to **5a**. In the case of **6**, a diastereomeric mixture was tested for inhibition of HIV PR (the ratio of diastereomers was 2.5:1). However, even if the less abundant diastereomer was the only active one, the inhibitory activity of **6** is still lower than that of **5a**.

The only structural difference between **5a** and **5b** (Table 2) is the relative configuration of phenyl groups connected to carbons 11 and 11′. Multidimensional NMR analyses combined with molecular modeling suggested that the absolute configuration of **5a** is 11*R*,11′*R*, and 11*S*,11′*S* (i.e., **5a** is a mixture of two enantiomers) while **5b** is the 11*S*,11′*R* enantiomer. These configurations were confirmed by X-ray analysis. This finding is similar to the results of the crystallographic analysis conducted on **2** (the crystal was grown from a diasteromeric mixture, and both active diastereomers were present in the crystal). The isolated diastereomers of **2** differ only in the configuration of phenyl groups connected to carbon 3, and the phenyl groups at carbon 11 are in the same configuration as in **5a**. A significant drop in inhibitory activity is observed when the phenyl groups are removed (compare the IC_{50} values for **7** and **8** with that for **5a**). Thus, we can conclude that the phenyl groups and their relative configurations play a crucial role in the activity of this novel class of inhibitors.

The docking of the substituted dimeric variants allowed us to identify the enantiomers that could favorably fit into the binding pocket (see Figure 3). Thus, for example, the 3-order-

Table 2. Relationship between Relative Configuration and Inhibitor Activity for Dimers of 1

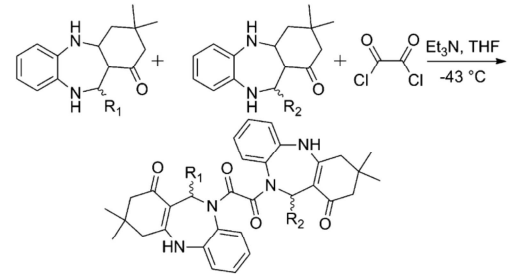

Compound No.	R_1=R_2	Absolute configuration	IC_{50}
5a		11R, 11′R; 11S, 11′S	30 nM[a]
5b		11R, 11′S	> 1 μM
7		—	200 nM
	R_1	R_2	
8			11R; 11S 100 nM[a]

[a] IC_{50} of enantiomeric mixture was determined.

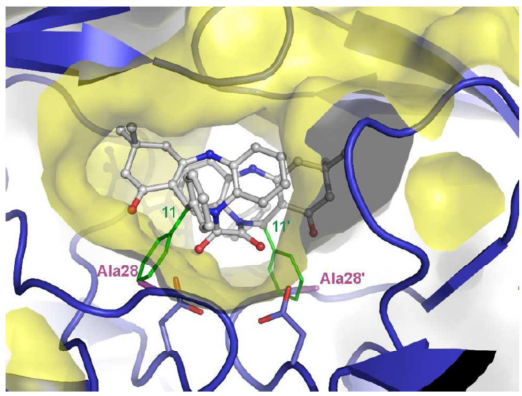

Figure 3. Compound **5** (in sticks) docked into the active site of HIV-1 PR (blue protein with yellow surface). A single enantioner of compound **5a** (the two phenyls in the 11*S*,11′*S* configuration) fitted into the cavity, while the second enantiomer (with 11*R*,11′*R* configuration) depicted in green sticks showed serious steric clashes with the area of the active site around Ala28/28′ (side chain depicted in magenta).

of-magnitude difference in affinity between **5a** and **5b** (Table 2) may be due (Figure 3) to steric clashes of 11/11′ phenyls with PR residues (mostly Ala28/28′).

In summary, we have shown that dibenzo[*b*,*e*][1,4]-diazepinone analogues are a potential new class of HIV PIs, with apparent K_i values as low as 12 nM. We used X-ray structure analysis combined with molecular modeling to show that dimeric inhibitors form two crucial hydrogen bonds to catalytic aspartates. This is likely the most important feature of their improved activity compared to the monomeric parental building blocks.

EXPERIMENTAL SECTION

Compound libraries and screening will be described elsewhere.

Chemical Synthesis. *Instrument Techniques.* ^1H, ^{13}C, and ^{19}F NMR spectroscopy was performed with three different instruments: Varian $_{UNITY}$Inova 300 MHz, Bruker Avance 600 MHz, and Bruker Avance 500 MHz. Chemical shifts are shown in ppm, and coupling constants are shown in Hz. To fully verify the structure of inhibitors,

two-dimensional NMR spectroscopy was employed, including HSQC, HMBC, COSY, and ROESY (measured with the Bruker Avance 600 MHz instrument). High resolution mass spectrometry measurements were performed on LTQ Orbitrap XL instrument (Thermo Fisher Scientific) using electrospray ionization. Positive ions were detected. Solvents and reagents were used as purchased from Sigma Aldrich (U.S.) with the exception of dry THF, which was purchased from Acros Chemicals (Belgium). Crystallographic data were collected on three different instruments (for details, see Supporting Information). The purity of all compounds was determined by elemental analysis and met the criteria for ≥95% purity (except for compounds **6** and **7**; for details see Supporting Information). An automated CHN analyzer (PE 2400 series II CHNS/O analyzer) was used for determination of C, H, N elemental composition. For determination of Cl, the X-ray fluorescence method (SPECTRO iQII spectrometer) was employed.

*General Procedure for Preparation of Dimeric Inhibitors (Example of Synthesis and Spectral Data Shown for Compound **5**).* In a round-bottom flask compound **4** (1.500 g, 4.71 mmol) and Et_3N (1.017 g, 10.8 mmol) were dissolved in dry THF (30 mL) under argon atmosphere and cooled to −43 °C. Oxalyl chloride (0.299 g, 2.36 mmol) was slowly added dropwise (0.299 g added in 1.5 h) to the stirring solution under argon atmosphere. The rate at which the oxalyl chloride is added determines which diastereomer is formed (faster rate results in formation of enantiomer with 11*R*,11′*S* configuration only). After 10 min, the mixture was left to warm up to room temperature and stirred for further 1h. The reaction was then quenched by addition of 30 mL of EtOAc. The organic phase was washed with 0.1 M HCl (25 mL) and twice with water (2 × 25 mL). White precipitate in the organic phase was then filtered yielding a mixture of diastereomers **5a** and **5b** in moderate yield (600 mg, 37%). The two diastereomers were separated using preparative TLC (Merck, TLC silica gel 60 F_{254}, 2 mm); the mobile phase was DCM/MeOH (19:1).

Bis(3,3-dimethyl-11-phenyl-2,3,4,5,10,11-hexahydro-1*H*-dibenzo-[*b*,*e*][1,4]diazepin-1-one-10-yl) oxalate (compound **5a**, mixture of enantiomers 11*R*,11′*R* and 11*S*,11′*S*) was prepared as described in the general procedure (600 mg, 37% for mixture of diastereomers). ^{1}H NMR (500 MHz, DMSO): δ 8.23 (bs, 2H), 7.13−7.10 (m, 2H), 7.10 (s, 2H), 7.09−7.05 (m, 4H), 7.02−6.98 (m, 4H), 6.80−6.77 (m, 4H), 6.67 (bt, 2H, J = 7.3 Hz), 6.67−6.65 (m, 2H), 2.35 (d, 2H, J = 16.8 Hz), 2.19 (d, 2H, J = 16.8 Hz), 2.04 (d, 2H, J = 15.6 Hz), 2.02 (d, 2H, J = 15.6 Hz), 1.03 (s, 6H), 0.99 (s, 6H). ^{13}C NMR (125 MHz, DMSO): δ 192.41, 162.77, 153.09, 139.20, 137.09, 129.32, 127.83 (overlap), 127.28, 126.80, 126.72, 121.96, 120.45, 106.34, 53.72, 49.36, 43.81, 31.32, 29.32, 26.70. Calculated monoisotopic mass: 691.3279. HRMS ESI$^+$ found: 691.3280. Calculated elemental composition (%): C 76.50, H 6.13, N 8.11. Found: C 74.04, H 6.06, N 7.81.

Enzymes. The expression, refolding, and purification of HIV PR were performed as previously described.[8] Human cathepsin D, kindly provided by Michael Mares (Institute of Organic Chemistry and Biochemistry, Academy of Sciences of the Czech Republic), was isolated from human placenta as previously described.[9] Papain was purchased from Sigma (St. Louis, MO, U.S.).

Inhibition Assays. For inhibition of HIV PR, both IC_{50} and K_i values were determined by spectrophotometric assay using the chromogenic substrate KARVNleNphEANle-NH_2, as previously described.[10] The mechanisms of inhibition were determined using Lineweaver−Burk plots.

For inhibition of cathepsin D and papain, a spectrofluorometry assay in a microplate setup was used to determine the possible inhibitory activity of compound **5a**. The enzymes (0.7 nM) were preincubated with various concentrations of **5a** in 0.1 M sodium acetate, pH 4.8, containing up to 2.5% DMSO, for 1 min at 37 °C. The reaction was started by adding substrate (Abz-KPAEFF*AL, 6.3 mM; Abz represents chromogenic *o*-aminobenzoic acid, and the asterisk indicates the cleavage site) prepared by Fmoc solid phase peptide synthesis. The product release was continuously monitored using excitation and emission wavelengths of 330 and 410 nm, respectively, with a GENios Plus instrument (Tecan Group Ltd., Switzerland).[9]

Crystallization, Data Collection, and Structure Solution. The HIV PR−**1** complex was prepared by mixing the enzyme with a 5-fold molar excess of the inhibitor dissolved in DMSO, followed by concentration to 5 mg/mL by ultrafiltration using Microcon-10 filters (Millipore, Billerica, MA, U.S.). Crystals were grown by the hanging drop vapor diffusion technique at 19 °C. The crystallization drops contained 2 μL of protein−inhibitor complex and 1 μL of reservoir solution (0.7 M NaCl and 0.1 M MES, pH 6.5). For diffraction measurements, crystals were soaked in reservoir solution supplemented with 25% (v/v) glycerol and cryocooled in liquid nitrogen.

X-ray diffraction data were collected at 120 K on a Mar345 image plate system using a Nonius FR591 rotating anode generator. Diffraction data were integrated and reduced using MOSFLM[11] and scaled using SCALA[12] from the CCP4 suite.[13] Crystal parameters and data collection statistics are given in Table S1.

The crystal structure was determined by molecular replacement using the program Molrep[14] with the structure of HIV PR (PDB code 1U8G,[15]) as a template. Model refinement was carried out using the program REFMAC 5.5.0109[16] from the CCP4 package,[13] interspersed with manual adjustments using Coot.[17] The final steps included TLS refinement.[18] The quality of the final models was validated with Molprobity.[19] All figures showing structural representations were prepared with the program PyMOL.[20]The electron density used for modeling of **1** into the enzyme active site was of excellent quality. Considering the abundance of chloride ion in crystallization buffer as well as the chemical environment in the structure (namely, the presence of four hydrogen bond donor groups in the vicinity), the spherical electron density map observed under the tip of flaps was explained by the presence of a chloride anion.

Final refinement statistics are given in Table S1. Atomic coordinates and experimental structure factors have been deposited in the Protein Data Bank with the code 3T11 (http://www.pdb.org).

Molecular Modeling. Docking of all the enantiomers of compound **5** into HIV PR was performed using DOCK 6.2.[21] The crystal structure of HIV PR in complex with **1** (PDB code 3T11, this work) was used as a starting structure. The protein was prepared by removing the ligands, waters, and ions and by adding hydrogens. All the enantiomers of **5** were constructed starting from the X-ray structure of **5a** (Figure S2, this work). Hydrogens were added, and GAFF parameters[22] and AM1-BCC charges[23] were assigned using Chimera 1.5.3.[24] The chiral center inversion was done in PyMOL.[19] The binding site was defined by spheres extending to 2 Å from **1** in the HIV PR complex X-ray structure. A grid across the binding site was generated with default parameters except that an all-atom model was used. Rigid docking was thereafter performed with default settings except that the maximum number of ligand orientations was increased to 1500 and the maximum number of minimization iterations was set to 2500.

■ ASSOCIATED CONTENT

Supporting Information

Synthesis of remaining inhibitors, further characterization of all compounds (^{1}H and ^{13}C NMR, high resolution mass spectrometry), X-ray characterization of individual inhibitors and HIV PR complex with compound **1** (list of all contacts between HIV PR and compound **1**), kinetic analysis of HIV PR inhibition by compound **1**, and inhibition study of cathepsin and papain with compound **5a**; a separate file containing stereoview of Figure 1. This material is available free of charge via the Internet at http://pubs.acs.org.

■ AUTHOR INFORMATION

Corresponding Author

*Phone: +420-220183218. Fax: +420-220183578. E-mail: konval@uochb.cas.cz.

Notes

The authors declare no competing financial interest.

■ ACKNOWLEDGMENTS

The authors thank Hillary Hoffman for critical proofreading of the manuscript and the Grant Agency of the Czech Republic (Program P208/12/G016 and Grant P/207/11/1798) for funding. This work was also in part supported by research projects AV0Z40550506, and AV0Z50520514 awarded by the Academy of Sciences of the Czech Republic.

■ ABBREVIATIONS USED

HIV PR, human immunodeficiency virus protease; PI, protease inhibitor; HAART, highly active antiretroviral therapy; FDA, Food and Drug Administration

■ REFERENCES

(1) Kohl, N. E.; Emini, E. A.; Schleif, W. A.; Davis, L. J.; Heimbach, J. C.; Dixon, R. A.; Scolnick, E. M.; Sigal, I. S. Active human immunodeficiency virus protease is required for viral infectivity. *Proc. Natl. Acad. Sci. U.S.A.* **1988**, *85* (13), 4686−4690.

(2) Wensing, A. M.; van Maarseveen, N. M.; Nijhuis, M. Fifteen years of HIV protease inhibitors: raising the barrier to resistance. *Antiviral Res.* **2010**, *85* (1), 59−74.

(3) Menendez-Arias, L. Molecular basis of human immunodeficiency virus drug resistance: an update. *Antiviral Res.* **2010**, *85* (1), 210−231.

(4) Wlodawer, A.; Vondrasek, J. Inhibitors of HIV-1 protease: a major success of structure-assisted drug design. *Annu. Rev. Biophys. Biomol. Struct.* **1998**, *27*, 249−284.

(5) Koh, Y.; Nakata, H.; Maeda, K.; Ogata, H.; Bilcer, G.; Devasamudram, T.; Kincaid, J. F.; Boross, P.; Wang, Y. F.; Tie, Y.; Volarath, P.; Gaddis, L.; Harrison, R. W.; Weber, I. T.; Ghosh, A. K.; Mitsuya, H. Novel bis-tetrahydrofuranylurethane-containing nonpeptidic protease inhibitor (PI) UIC-94017 (TMC114) with potent activity against multi-PI-resistant human immunodeficiency virus in vitro. *Antimicrob. Agents Chemother.* **2003**, *47* (10), 3123−3129.

(6) Pokorna, J.; Machala, L.; Rezacova, P.; Konvalinka, J. Current and novel inhibitors of HIV protease. *Viruses* **2009**, *1* (3), 1209−1239.

(7) Ramajayam, R.; Giridhar, R.; Yadav, M. R. Current scenario of 1,4-diazepines as potent biomolecules—a mini review. *Mini-Rev. Med. Chem.* **2007**, *7* (8), 793−812.

(8) Saskova, K. G.; Kozisek, M.; Lepsik, M.; Brynda, J.; Rezacova, P.; Vaclavikova, J.; Kagan, R. M.; Machala, L.; Konvalinka, J. Enzymatic and structural analysis of the I47A mutation contributing to the reduced susceptibility to HIV protease inhibitor lopinavir. *Protein Sci.* **2008**, *17* (9), 1555−1564.

(9) Masa, M.; Maresova, L.; Vondrasek, J.; Horn, M.; Jezek, J.; Mares, M. Cathepsin D propeptide: mechanism and regulation of its interaction with the catalytic core. *Biochemistry* **2006**, *45* (51), 15474−15482.

(10) Richards, A. D.; Phylip, L. H.; Farmerie, W. G.; Scarborough, P. E.; Alvarez, A.; Dunn, B. M.; Hirel, P. H.; Konvalinka, J.; Strop, P.; Pavlickova, L.; et al. Sensitive, soluble chromogenic substrates for HIV-1 proteinase. *J. Biol. Chem.* **1990**, *265* (14), 7733−7736.

(11) Leslie, A. G. Integration of macromolecular diffraction data. *Acta Crystallogr., Sect. D: Biol. Crystallogr.* **1999**, *55* (Part 10), 1696−1702.

(12) Evans, P. R. Data Reduction. In *Proceedings of CCP4 Study Weekend on Data Collection and Processing*; Daresbury Laboratory: Warrington, U.K., 1993; pp 114−122.

(13) The CCP4 suite: programs for protein crystallography. *Acta Crystallogr., Sect. D: Biol Crystallogr* **1994**, *50* (Part 5), 760−763.

(14) Vagin, A.; Teplyakov, A. An approach to multi-copy search in molecular replacement. *Acta Crystallogr., Sect. D: Biol. Crystallogr.* **2000**, *56* (Part 12), 1622−1624.

(15) Brynda, J.; Rezacova, P.; Fabry, M.; Horejsi, M.; Stouracova, R.; Soucek, M.; Hradilek, M.; Konvalinka, J.; Sedlacek, J. Inhibitor binding at the protein interface in crystals of a HIV-1 protease complex. *Acta Crystallogr., Sect. D: Biol. Crystallogr.* **2004**, *60* (Part 11), 1943−1948.

(16) Murshudov, G. N.; Vagin, A. A.; Dodson, E. J. Refinement of macromolecular structures by the maximum-likelihood method. *Acta Crystallogr., Sect. D: Biol. Crystallogr.* **1997**, *53* (Part 3), 240−255.

(17) Emsley, P.; Cowtan, K. Coot: model-building tools for molecular graphics. *Acta Crystallogr., Sect. D: Biol. Crystallogr.* **2004**, *60* (Part12, Part 1), 2126−2132.

(18) Winn, M. D.; Isupov, M. N.; Murshudov, G. N. Use of TLS parameters to model anisotropic displacements in macromolecular refinement. *Acta Crystallogr., Sect. D: Biol. Crystallogr.* **2001**, *57* (Part 1), 122−133.

(19) Lovell, S. C.; Davis, I. W.; Arendall, W. B., 3rd; de Bakker, P. I.; Word, J. M.; Prisant, M. G.; Richardson, J. S.; Richardson, D. C. Structure validation by Calpha geometry: phi,psi and Cbeta deviation. *Proteins* **2003**, *50* (3), 437−450.

(20) DeLano, W. L. *The PyMOL Molecular Graphics System*; DeLano Scientific LLC: San Carlos, CA; http://www.pymol.org.

(21) Lang, P. T.; Brozell, S. R.; Mukherjee, S.; Pettersen, E. F.; Meng, E. C.; Thomas, V.; Rizzo, R. C.; Case, D. A.; James, T. L.; Kuntz, I. D. DOCK 6: combining techniques to model RNA-small molecule complexes. *RNA* **2009**, *15* (6), 1219−1230.

(22) Wang, J.; Wolf, R. M.; Caldwell, J. W.; Kollman, P. A.; Case, D. A. Development and testing of a general Amber force field. *J. Comput. Chem.* **2004**, *25* (9), 1157−1174.

(23) Jakalian, A.; Jack, D. B.; Bayly, C. I. Fast, efficient generation of high-quality atomic charges. AM1-BCC model: II. Parameterization and validation. *J. Comput. Chem.* **2002**, *23* (16), 1623−1641.

(24) Pettersen, E. F.; Goddard, T. D.; Huang, C. C.; Couch, G. S.; Greenblatt, D. M.; Meng, E. C.; Ferrin, T. E. UCSF Chimera—a visualization system for exploratory research and analysis. *J. Comput. Chem.* **2004**, *25* (13), 1605−1612.

(25) Hodge, C. N.; Aldrich, P. E.; Bacheler, L. T.; Chang, C. H.; Eyermann, C. J.; Garber, S.; Grubb, M.; Jackson, D. A.; Jadhav, P. K.; Korant, B.; Lam, P. Y.; Maurin, M. B.; Meek, J. L.; Otto, M. J.; Rayner, M. M.; Reid, C.; Sharpe, T. R.; Shum, L.; Winslow, D. L.; Erickson-Viitanen, S. Improved cyclic urea inhibitors of the HIV-1 protease: synthesis, potency, resistance profile, human pharmacokinetics and X-ray crystal structure of DMP 450. *Chem. Biol.* **1996**, *3* (4), 301−314.

(26) Muzammil, S.; Armstrong, A. A.; Kang, L. W.; Jakalian, A.; Bonneau, P. R.; Schmelmer, V.; Amzel, L. M.; Freire, E. Unique thermodynamic response of tipranavir to human immunodeficiency virus type 1 protease drug resistance mutations. *J. Virol.* **2007**, *81* (10), 5144−5154.

(27) Specker, E.; Bottcher, J.; Lilie, H.; Heine, A.; Schoop, A.; Muller, G.; Griebenow, N.; Klebe, G. An old target revisited: two new privileged skeletons and an unexpected binding mode for HIV-protease inhibitors. *Angew. Chem., Int. Ed.* **2005**, *44* (20), 3140−3144.

(28) Zhou, H. X.; Gilson, M. K. Theory of free energy and entropy in noncovalent binding. *Chem. Rev.* **2009**, *109* (9), 4092−4107.

5.2 Triggering HIV polyprotein processing by light using rapid photodegradation of a tight-binding protease inhibitor

Background:

The majority of the HIV virus proteins is expressed in a form of a polyprotein chain (Gag and Gag-Pol) which have to be cleaved into functional units to fulfill their function. HIV protease (HIV PR) plays this key role, which is vital for the virus to gain infectivity. Inhibition of HIV PR prevents viral particles maturation, rendering them non-infectious. The process of maturation can be observed under electron microscope. The immature virion particles are of a spherical character, unlike the mature ones which form a cone shaped core (formed by hexameric lattice of capsid protein (figure 1**B**, p. 9).

The cleavage of the polyprotein chain must be strictly time-regulated, because premature activation of HIV PR prevents particle formation at the first place. Even though HIV PR is probably the most studied enzyme in the world, this is where our knowledge about the timing ends. The biggest problem while studying the dynamics of polyprotein cleavage lies in the proper synchronization of the maturation process. The viral particles are budding from the plasma membrane randomly, and the diversity between the cells is even greater, creating thus diverse pool of virions in different stages of development at every given time point. Therefore to answer any of the basic questions, such as when does the polyprotein cleavage start, one needs a tool to synchronize the virus-producing cell culture.

Summary:

We designed, synthesized and evaluated a sub-nanomolar tight binding inhibitor of HIV PR which upon irradiation dramatically loses its potency (by four orders of magnitude) and therefore works as a switch-on for the enzyme (figure 15, p. 47). We co-crystallized both the inhibitor and the photodegradation product in complex with HIV PR to explain the unprecedented loss of inhibitory activity. We further showed that the reactivation works in principle in the test tube with purified HIV PR, and that the irradiation and photodegradation of the inhibitor does not ruin the protease activity by damaging the protein itself.

Moving further into cell culture studies we showed that using our system we are able to reactivate the HIV PR even in the isolated virions. The reactivated HIV PR is readily able to cleave the polyprotein chains into the functional proteins in the preformed immature virions. By observing the time dependence of the concentration of the final product of the

cleavage, we were able to analyze the dynamics of the polyprotein processing and establish a half-life of the polyprotein chain in the virion.

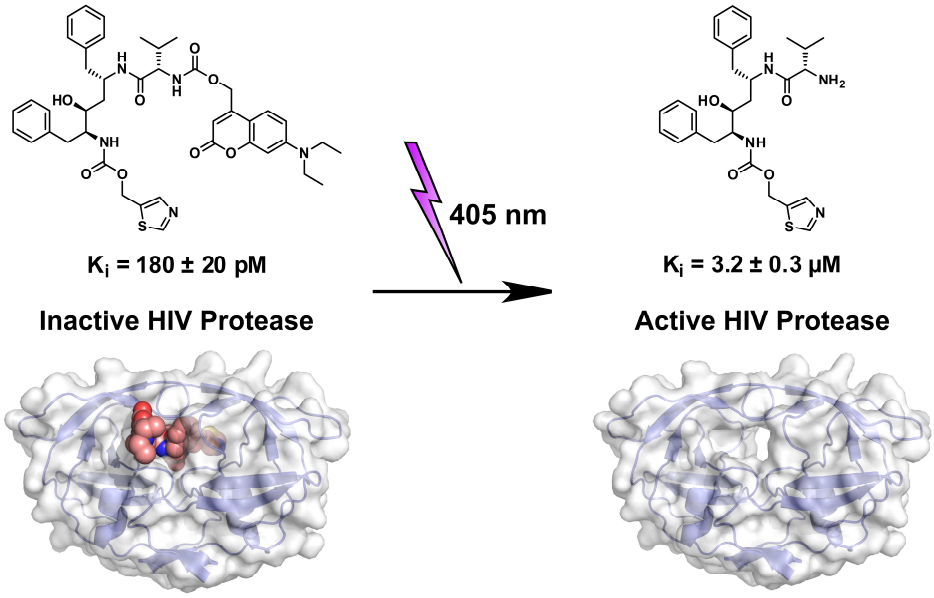

Figure 15: Tight binding photodegradable inhibitor of HIV PR. Irradiation of the tight binding inhibitor by 405 nm light leads to a bond cleavage which results in dramatic loss in activity and therefore works as a switch on for the enzyme.

My contribution:

I designed, synthesized and evaluated the inhibitor of HIV PR. I conducted all the crystallization experiments, and optimized the irradiation setup for the PI degradation. With help of one lab technician I also did all the cell culture experiments and determined the kinetics of polyprotein degradation inside the virions. I wrote draft for the manuscript.

Schimer, J., Pavova, M., Anders, M., Pachl, P., Sacha, P., Cigler, P., Weber, J., Majer, P., Rezacova, P., Krausslich, H.G., Muller, B., and Konvalinka, J., **Triggering HIV polyprotein processing by light using rapid photodegradation of a tight-binding protease inhibitor**. Nat Commun, 2015. **6**: p. 6461.

ARTICLE

Received 5 Sep 2014 | Accepted 29 Jan 2015 | Published 9 Mar 2015

DOI: 10.1038/ncomms7461 OPEN

Triggering HIV polyprotein processing by light using rapid photodegradation of a tight-binding protease inhibitor

Jiří Schimer[1,2], Marcela Pávová[1], Maria Anders[3], Petr Pachl[1], Pavel Šácha[1,2], Petr Cígler[1], Jan Weber[1], Pavel Majer[1], Pavlína Řezáčová[1], Hans-Georg Kräusslich[3,4], Barbara Müller[3,4] & Jan Konvalinka[1,2]

HIV protease (PR) is required for proteolytic maturation in the late phase of HIV replication and represents a prime therapeutic target. The regulation and kinetics of viral polyprotein processing and maturation are currently not understood in detail. Here we design, synthesize, validate and apply a potent, photodegradable HIV PR inhibitor to achieve synchronized induction of proteolysis. The compound exhibits subnanomolar inhibition *in vitro*. Its photolabile moiety is released on light irradiation, reducing the inhibitory potential by 4 orders of magnitude. We determine the structure of the PR-inhibitor complex, analyze its photolytic products, and show that the enzymatic activity of inhibited PR can be fully restored on inhibitor photolysis. We also demonstrate that proteolysis of immature HIV particles produced in the presence of the inhibitor can be rapidly triggered by light enabling thus to analyze the timing, regulation and spatial requirements of viral processing in real time.

[1] Institute of Organic Chemistry and Biochemistry, Academy of Sciences of the Czech Republic, Gilead Sciences and IOCB Research Center, Flemingovo n.2, 166 10, Prague 6, Czech Republic. [2] Department of Biochemistry, Faculty of Science, Charles University in Prague, Hlavova 8, 128 43, Prague 2, Czech Republic. [3] Department of Infectious Diseases, Virology, University Hospital Heidelberg, Im Neuenheimer Feld 324, 69120 Heidelberg, Germany. [4] Molecular Medicine Partnership Unit, Heidelberg, Germany. Correspondence and requests for materials should be addressed to J.K. (email: konval@uochb.cas.cz) or to B.M. (email: Barbara_Mueller@med.uni-heidelberg.de).

HIV-1 protease (HIV-1 PR) is among the best-studied enzymes in biochemistry. This 99 amino acid long homodimeric aspartic PR plays a pivotal role in the viral replication cycle[1]. PR is synthesized as part of the viral Gag-Pol polyprotein. Approximately 125 molecules of Gag-Pol co-assemble at the plasma membrane with ~2,500 molecules of the main structural polyprotein Gag to create an immature virion. In the assembled immature particle, the PR domain of Gag-Pol cleaves Gag and Gag-Pol at nine distinct sites to create the mature, functional subunits. Proteolytic processing results in a dramatic rearrangement of the particle core termed maturation, which is a prerequisite for HIV-1 infectivity. Consequently, inhibitors of HIV-1 PR are powerful virostatics. Due to major efforts from both academia and industry 10 specific HIV-1 PR inhibitors are currently available for antiretroviral therapy (for review, see ref. 2).

While the structure and the enzymatic properties of HIV-1 PR *in vitro* are well characterized, key questions concerning proteolytic maturation remain unanswered. Virological studies from many groups indicate that the maturation process needs to be tightly controlled. Not only inhibition, but also premature activation of PR is detrimental for virus replication[3], and blocking or even partially inhibiting processing at one of the cleavage sites strongly reduces HIV-1 infectivity[4]. According to current understanding, Gag proteolysis occurs when the polyprotein has already assembled into a tight hexameric lattice, but it is unclear what prevents premature proteolysis and how PR is activated once the immature virion has been assembled[5]. Furthermore, the sequence, timing, and topology of cleavage events during particle maturation remain largely unclear. The key obstacle in dissecting this complex process is the asynchronous formation of mature HIV-1 particles in tissue culture, since any virus population harvested from culture media constitutes an ensemble of particles in different stages of polyprotein processing and maturation. Overcoming this fundamental obstacle requires an experimental tool for triggering HIV-1 PR activity at a defined moment, thus inducing and synchronizing the viral maturation process.

Several approaches can in principle be used to achieve synchronization. Temperature-sensitive PR mutants have been developed to analyze individual steps of the replication cycle of picorna and other viruses[6]. However, attempts to prepare temperature-dependent mutants of HIV-1 PR have met with limited success. Although several HIV-1 PR mutants with temperature-dependent differences in proteolytic activity have been reported, none of these allowed switching from a non-active to an active enzymatic state, which would be required to trigger HIV-1 maturation[7,8].

Alternatively, one may induce proteolysis by wash-out of a specific PR inhibitor from immature particles produced in the presence of the inhibitor. We have recently explored this strategy by systematic testing of a panel of available and experimental PR inhibitors and found that PR activation can indeed be accomplished by inhibitor wash-out, provided that inhibitors with a high off-rate are used[9]. With a half-time of 4-5 h, the kinetics of proteolysis were slow, however, and morphologically mature virus particles and virus infectivity were not recovered[9]. Accordingly, inhibitor wash-out does not appear to trigger functional maturation and more efficient and faster induction of proteolysis inside the immature virion may be needed.

A possible way to overcome this limitation is the use of caged compounds that are released on irradiation with light of a specific wavelength. The release of effector molecules by light-induced cleavage of inactive precursors is well-established in chemical biology. Following pioneering studies describing photocaged cAMP and ATP[10,11], photocaged small molecules acting as secondary messengers, for example, calcium[12] and nitric oxide[13], as well as caged hormones[14,15], neurotransmitters[16,17], nucleic acids[18,19] and diacylglycerols[20] were developed. Whole proteins have also been caged to analyze signalling and other regulatory events in the cell (for example, refs 21,22; for recent reviews covering caged small molecules, see refs 23–25).

To trigger the activity of an enzyme in the absence of a specific small molecule activator would require a caged version of the enzyme of interest. However, caging of a large biomolecule presents a major technical challenge. Furthermore, the caged protein must be delivered into the cell (for example, by microinjection), and would compete with the endogenously expressed protein[26]. In the specific case of HIV-1 PR, the enzyme is part of a polyprotein which needs to be incorporated into the nascent virus particle, rendering this strategy not feasible.

An alternative to protein caging is the use of a photolabile enzyme inhibitor that could be inactivated by light, to trigger enzyme activity. An effective photodegradable enzyme inhibitor is characterized by a substantial decrease in inhibitory activity on photolysis, and a few examples for this strategy have been published. Li *et al.*[26] connected two peptidic inhibitors of two distinct domains of Src kinase via a photodegradable linker. Separation of the bivalent inhibitor into two compounds, each binding the target with lower affinity, reduced inhibitory potency by ~50-fold. Porter *et al.*[27] developed a mechanism-based approach to analyze activation of a serine PR. Photolysis of a covalent adduct in the active site of the PR led to PR activation.

The wealth of structure-activity data accumulated on purified HIV-1 PR and its inhibitors renders HIV-1 polyprotein processing and maturation an excellent target for the development of a specific photoinactivatable inhibitor. We thus set out to develop a method to activate HIV-1 maturation by photodegradation of a specific and potent PR inhibitor. Here we describe the design, synthesis, validation and application of a subnanomolar HIV-1 PR inhibitor that is cleaved on irradiation by 405-nm light. After irradiation, the inhibitor's potency decreases by 4 orders of magnitude, leading to nearly full restoration of enzyme activity and to rapid induction of polyprotein processing in assembled HIV-1 particles in tissue culture.

Results

Kinetic analysis of inhibitor and its photodegradation product. The design of a photoinactivable inhibitor of HIV-1 PR (**1**) was based on the structure of the PR inhibitor ritonavir (RTV; Fig. 1a)[28]. Compound **1** contains a photolabile 7-diethylamino-4-(hydroxymethyl)coumarin group connected via a carbamate linker to a RTV fragment (Fig. 1b), and is a tight-binding inhibitor of HIV-1 PR, displaying subnanomolar inhibition potency ($K_i = 170 \pm 20$ pM, for detailed synthesis see Supplementary Fig. 1). The degradation fragment **2** displayed only weak inhibitory activity, with a K_i value of 3.2 ± 0.3 μM (Fig. 1b). The other product of photolysis, the coumarin group, did not show any inhibitory activity at a concentration of 10 μM. The identities of the photodegradation fragments of compound **1** were confirmed by independent measurement using analytical high-performance liquid chromatography (HPLC; Supplementary Fig. 2).

Determination of binding mode into HIV-1 PR. To investigate the binding modes of compounds **1** and **2**, we co-crystallized both with HIV-1 PR and determined the corresponding structures at resolutions of 1.6 Å and 1.4 Å, respectively. Both crystals were of identical space group ($P6_1$), and contained one PR dimer in the asymmetric unit. The structures were refined with two inhibitor molecules bound in alternative orientations related by 180° rotation with 50% relative occupancy. The quality of the electron

density map for residues 35–60 for 35–45 for HIV-1 PR-**1** and HIV-1 PR-**2** complex, respectively, was limited, suggesting that these regions of flaps are partially disordered. The electron density for the remaining part of the protein as well as compounds bound to the active site were of good quality enabling unambiguous modelling (Supplementary Fig. 3).

The crystal structures revealed that compounds **1** and **2** both occupy enzyme subsites S2, S1, S1′ and S2′. In addition, compound **1** interacted with the S3 enzyme subsite through the coumarin moiety. The extent of interactions with S3 residues was rather limited, however, and the coumarin moiety protruded from the enzyme active site cavity (Fig. 2a). The suboptimal interaction in the S3 pocket, compared with the interaction of the P3 moiety of RTV, is likely to contribute to the 10-fold difference in K_i values for RTV and compound **1**. Binding of the P2′, P1′ and P2 substituents of compound **1** was similar to that of RTV (Fig. 2b), whereas differences were observed for interactions in the S1 and S2 pockets. In the HIV-1 PR-compound **1** complex, the carbamate between the coumarin moiety and the inhibitor formed a hydrogen bond with the Asp29A side chain, similar to the interaction of the corresponding group of RTV.

Interestingly, the positions and conformations of moieties common to compound **1** and **2** as well as their interactions within the S2 to S2′ subsites were quite different (Fig. 2c). The largest difference was observed in the P1 and P2′ moieties, where the extent of interactions was much lower for compound **2** compared with compound **1**. This might provide a structural explanation for the observation that compound **2** displayed a low inhibitory activity against HIV-1 PR, considering that it occupies the S2 to S2′ enzyme binding subsites. In addition, compound **2** differs from compound **1** in that it has a free terminal amine group, which is charged at lower pH and likely repulsed from the enzyme cavity. In support of this hypothesis, acetylation of the free amine of compound **2** led to a major increase in inhibitory activity.

Reactivation of HIV-1 PR by photolysis of compound 1. To evaluate the efficacy of photodegradation, we analyzed the restoration of HIV-1 PR activity that had been inhibited by compound **1** (Fig. 3a) on irradiation at 405 nm. For irradiation, two lasers with outputs of 130 mW and 170 mW, respectively, were used in parallel. First, we tested a standard cuvette set up, in which 8 nM purified recombinant HIV-1 PR (final concentration of compound **1**: 10 or 100 nM; Fig. 3b) in 1 ml cleavage buffer was irradiated. At the lower concentration, irradiation led to a significant restoration of enzyme activity (65% compared with the uninhibited enzyme reaction). At the higher concentration of compound **1**, however, PR reactivation was limited even after prolonged irradiation (only 35% activity after 5 min of irradiation). We reason that the product of photodegradation (compound **2**) interferes with degradation of compound **1** in this set up, because the absorption spectrum of compound **2** is almost identical to that of compound **1**. Therefore, we investigated a number of alternative irradiation set ups, and obtained optimal results when the inhibitor solution was irradiated while being pumped through a thin glass capillary at which the two lasers were focused (Fig. 3c). This set up ensured homogeneous irradiation throughout the sample and prevented absorption of light by the released coumarin product. At a flow rate of 15 µl min^{-1}, up to 75% of original PR activity was recovered, despite an inhibitor concentration 4 orders of magnitude above its K_i value ($K_i = 170$ pM, inhibitor concentration 100 nM). Considering that compound **1** is a tight-binding inhibitor (see Fig. 3a) and 75% of the PR activity was restored, we estimate that up to 98% of compound **1** was degraded.

Reactivation of HIV-1 PR inside immature virions. Based on these results, we analyzed whether photodegradation of compound **1** can be used to trigger HIV-1 PR activity inside intact immature HIV-1 particles produced in tissue culture in the presence of the inhibitor. PR-mediated cleavage of the Gag polyprotein yields the mature structural proteins and two small spacer peptides (Fig. 4a), and different rates of cleavage at individual sites result in the generation of characteristic processing intermediates[29]. First, we assessed the inhibitory potency of compound **1** on HIV-1 Gag polyprotein processing in virus producing cells. For this, particles were purified from the supernatant of HEK293T cells transfected with an HIV-1 proviral plasmid and incubated in the presence of various concentrations of compound **1**. Gag processing was efficiently inhibited with ~50% reduction in Gag cleavage at ~500 nM compound **1** (Fig. 4b). Previous studies had indicated that infectivity is severely impaired at concentrations where polyprotein processing is only inhibited to a minor extent[30,31]. Accordingly, compound **1** inhibited HIV-1 replication in the MT-4T-cell line with an EC_{50} of 8.1 nM, although almost no effect on Gag processing could be seen at this concentration (Supplementary Fig. 5). Compound **1** was soluble and noncytotoxic at a concentration of 2 µM in 0.5% DMSO ($CC_{50} = 7.3$ µM for MT4, $CC_{50} > 50$ µM for HEK293T cells; for more detailed information see Supplementary Chapter 5).

Having established conditions for the inhibition of HIV-1 polyprotein processing by compound **1**, we proceeded to prepare immature particles for *in situ* activation of PR. For this, virus particles were produced in transfected HEK293T cells grown in the presence of 2 µM inhibitor. The experimental set up is schematically illustrated in Fig. 5a. Particles collected from inhibitor-treated cells were either subjected to inhibitor wash-out

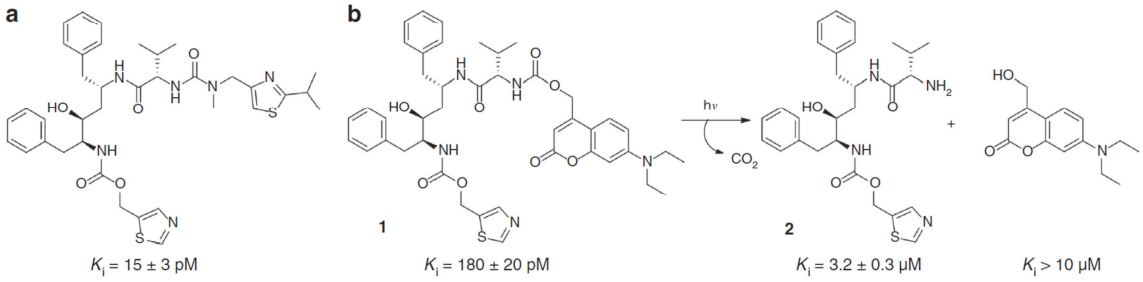

Figure 1 | A photolabile inhibitor of HIV-1 PR and its degradation triggered by light. (**a**) HIV-1 protease inhibitor Ritonavir; (**b**) Photodegradable inhibitor of HIV-1 PR (compound **1**) and products resulting from photolysis (compound **2** and coumarin derivative). Inhibition constants determined as in Fig. 3a are shown for each compound.

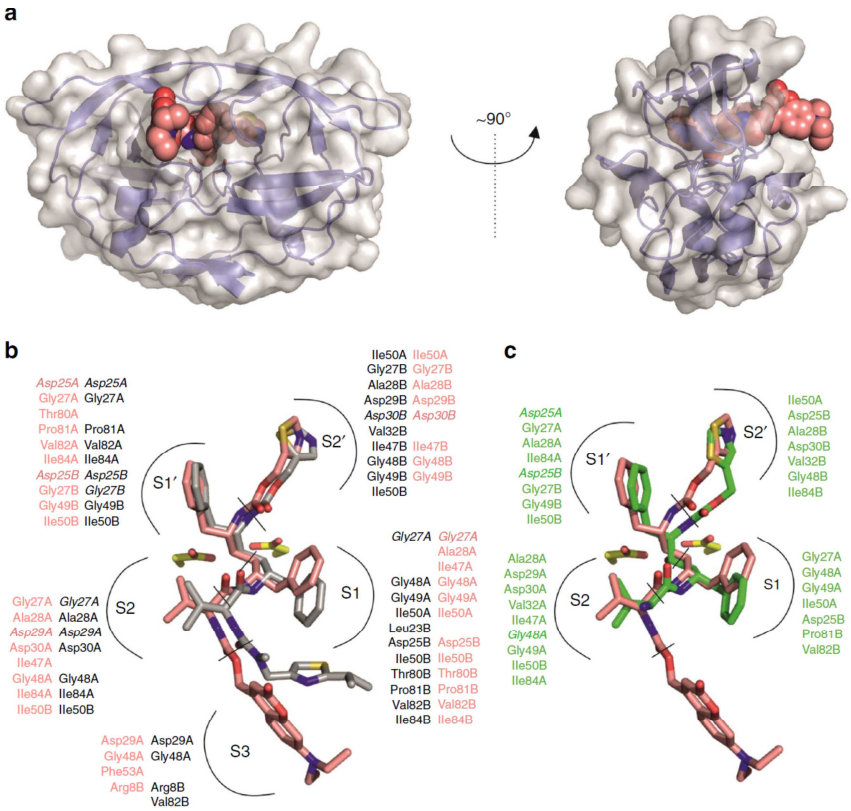

Figure 2 | Comparison of binding mode of compounds 1 and 2 to HIV-1 PR. (**a**) Two views of the HIV-1 PR-**1** complex (PDB code 4U7Q). The protein is shown in cartoon representation with a transparent surface, while the inhibitor atoms are represented by spheres. The coumarin moiety protrudes from the enzyme active site cavity. (**b**) Superposition of **1** (pink carbon atoms) and RTV (ritonavir; grey carbon atoms) bound in the HIV-1 PR active site. (**c**) Superposition of **1** with **2** (in green, PDB code 4U7V) bound to HIV-1 PR (PDB code 1HXW (ref. 28)). (**b**,**c**) Residues interacting with **1**, **2** and RTV are indicated in the corresponding colours for individual enzyme subsites. Residues forming polar interactions are highlighted in bold italics. To identify non-polar interactions, the cut-off for distance between any atom of residue and any atom of inhibitor was 4 Å. For polar interaction, the cut-off for distance between hydrogen bond donor and acceptor was 3.5 Å. Active site aspartates are shown in stick representation.

by two subsequent ultracentrifugation steps (Fig. 5b), or only filtered to remove cell debris (Fig. 5c). In both cases, samples were then either irradiated (405 nm) in a glass capillary (Fig. 5b,c, bottom panels) or passed through the capillary in the absence of irradiation (Fig. 5b,c, top panels).

Wash-out of compound **1** in the absence of irradiation resulted in slow PR activation and Gag processing (Fig. 5b, top), with kinetics closely resembling those observed in our previous study (Fig. 5d)[9]. In contrast, mature CA was produced much more rapidly in the irradiated sample (Fig. 5b, bottom), yielding ~30% mature CA within 15 min (Fig. 5d). Gag processing remained incomplete, however, with ~50% unprocessed or partially processed products remaining at 6 h of incubation. Direct irradiation of particle-containing culture medium without prior ultracentrifugation allowed us to process samples much more rapidly, thereby protecting sample integrity and PR activity. In this set up, no induction of proteolysis was observed in the absence of irradiation even after prolonged incubation (Fig. 5c, top). In contrast, irradiation of culture medium without any inhibitor removal resulted in rapid PR activation and virtually complete Gag processing (Fig. 5c, bottom). The irradiated sample exhibited a level of Gag processing comparable to that observed for an uninhibited control virus after ~2 h of incubation, yielding an apparent half-time of ~20 min for Gag processing (Fig. 5e).

Discussion

This report demonstrates that a photodestructible inhibitor can be used to trigger HIV-1 PR activation and polyprotein processing *in situ* inside the assembled immature virus. This was accomplished by design, synthesis and validation of a photolabile tight-binding inhibitor of HIV-1 PR ($K_i = 170 \pm 20$ pM) that demonstrates a 4-order-of-magnitude loss of potency on irradiation with a 405 nm laser. The inhibitor thus served as a photocage for HIV-1 PR activity and allowed initiating HIV-1 polyprotein processing within the assembled virion in a controlled manner. Analysis of Gag processing kinetics under these conditions revealed that the mature CA subunit was released with a half-time of ~20–30 min, which is substantially faster than the half-time of 4–5 h observed using an optimized inhibitor wash-out strategy[9]. The direct comparison between wash-out and photodestruction of the newly described inhibitor (Fig. 5) clearly showed that much more rapid activation is accomplished by photodestruction. Furthermore, processing rates were not enhanced by including a wash-out step prior to irradiation, demonstrating the effectiveness of photodestruction.

At first glance, the half-time of 20–30 min measured in the experiments shown in Fig. 5 appears rather slow. It needs to be considered, however, that the experiments with immature virus do not directly measure the kinetics of PR activation by

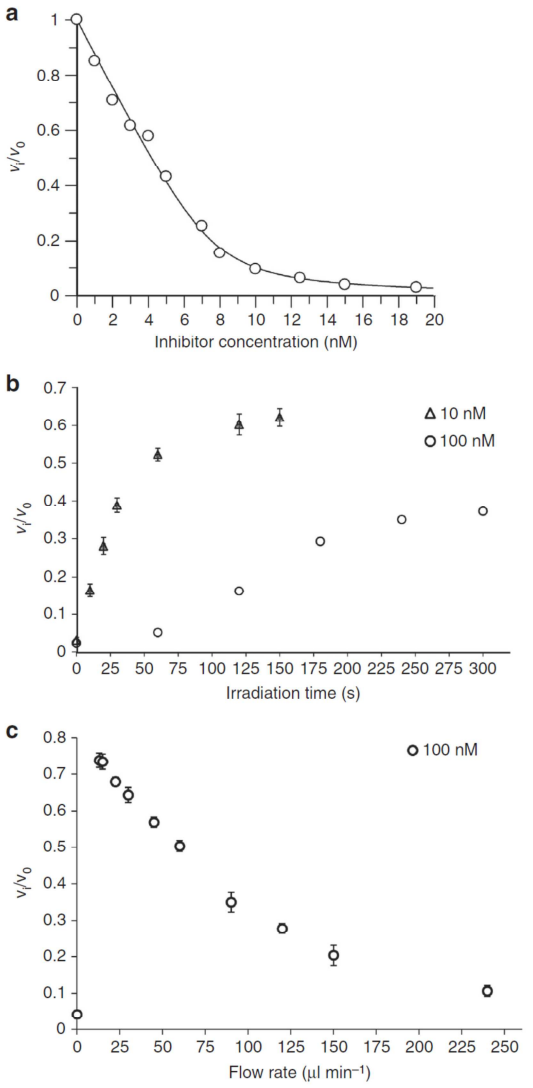

Figure 3 | Kinetic analysis of HIV-1 PR reactivation by inhibitor photodegradation. (**a**) A non-linear fit of Morrison equation of inhibition of HIV-1 PR by compound **1**. The activity of purified recombinant HIV-1 PR was determined *in vitro* as described in the experimental section in the presence of the indicated inhibitor concentrations. Two independent experiments yielded very similar results; (**b**,**c**) Reactivation of purified recombinant HIV-1 PR in buffer (100 mM sodium acetate, 300 mM NaCl, 4 mM EDTA, pH 4.7) by photodegradation of **1** using either the cuvette set up (**b**) or the capillary set up (**c**): (**b**) Purified recombinant HIV-1 PR (8 nM) incubated with compound **1** at the indicated concentrations was irradiated with two 405 nm lasers (combined output of 300 mW) for various time intervals. The PR activity was then measured using a chromogenic substrate. The plot shows relative PR activity as a function of time. (**c**) Purified recombinant HIV-1 PR (160 nM) incubated with 2 µM compound **1** was pumped at different flow rates through a thin glass capillary onto which two 405 nm lasers (combined output of 300 mW) were focused (for set up see Supplementary Fig. 4). Relative PR activity was determined as in **b** after 20-fold dilution into cleavage buffer using the same chromogenic substrate (for details, see Experimental section) and plotted against the flow rate of the sample through the capillary. Flow rate 0 represents a non-irradiated sample. The graph shows mean values and s.d. from three independent experiments.

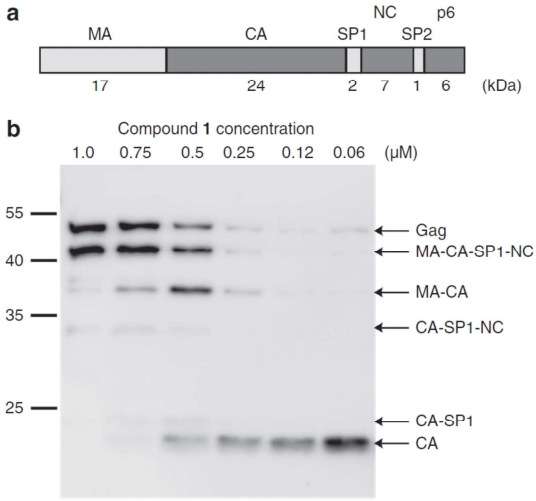

Figure 4 | Inhibition of HIV-1 Gag processing by compound 1. (**a**) Schematic representation of the 55 kDa HIV-1 Gag polyprotein and its cleavage products. (**b**) Inhibition of HIV-1 Gag processing by compound **1.** HIV-1 particles were produced in HEK293T cells in the presence of the indicated inhibitor concentrations. The experiment was performed in duplicate and a representative result is shown. Molecular mass standards are shown on the left; Gag and its respective cleavage products are identified on the right. CA, capsid; MA, matrix; NC, nucleocapsid; p6, p6 protein; SP1, spacer peptide 1; SP2, spacer peptide 2.

photodestruction, as the biochemical experiments shown in Fig. 3, but rather reflect the production of mature CA by processing of the Gag polyprotein assembled in a tight hexagonal lattice. Although HIV-1 proteolytic maturation presumably involves only the viral PR and its substrates Gag and Gag-Pol in the relatively defined environment of the virus particle, the reaction entails at least 66 distinct substrates, intermediates or products, and numerous competing intermolecular interactions occurring simultaneously[32]. Arrangement of the substrate in a multimeric lattice presents further constraints that likely reduce processing rates. The time course of this complex reaction in the virus is currently unknown, and our current study provides an upper time limit for HIV-1 polyprotein processing. Estimates for the period required for polyprotein processing in retroviruses in the literature are based almost exclusively on indirect and very limited evidence and range from a few minutes up to several hours[33] for completion of proteolytic maturation. Modelling based on simplified assumptions from *in vitro* data yielded an estimate of 30 min for completion of HIV proteolysis[32], which would be in good agreement with our results. We want to emphasize, however, that our results provide an upper limit for the half-time of Gag proteolysis, assuming instantaneous and complete photodestruction and concomitant PR activation inside the immature particle. Conceivably, authentic polyprotein processing may be even faster, while the slower rates of Gag proteolysis reported in a previous study[33] are clearly inconsistent with our results.

The possibility to trigger HIV-1 PR activity by light in precisely defined time and space enabled us to induce HIV-1 polyprotein processing inside the native immature virion, and to analyze the timing, regulation, spatial requirements and kinetics of Gag proteolysis in real time. This system now provides the opportunity for a targeted analysis of HIV-1 maturation, which should eventually lead to an understanding of the dynamics of

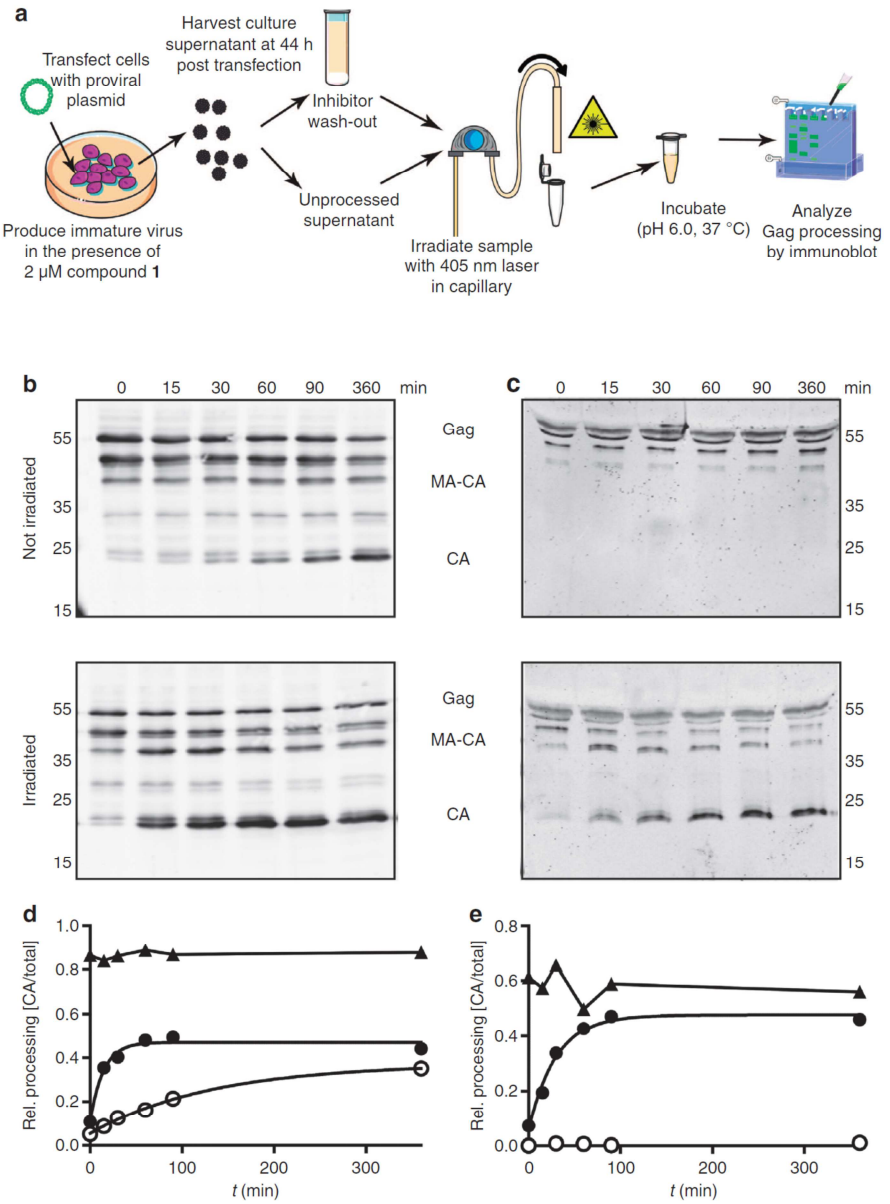

Figure 5 | Photoinduced Gag processing in the context of the assembled virion. (**a**) Schematic illustration of the irradiation experiment to trigger HIV-1 maturation using photoinactivation of compound **1**. HEK293T cells were transfected with a proviral HIV-1 plasmid and particles were produced in the presence of 2 µM compound **1**. At 44 h post transfection, tissue culture supernatant was harvested and either subjected to ultracentrifugation (**b**,**d**) or used directly (**c**,**e**). In both cases, samples were then pumped through the capillary set up shown in Supplementary Fig. 4 either with or without ultraviolet irradiation. Subsequently, samples were incubated for various lengths of time. (**b**,**c**) Immunoblot analysis of Gag processing products. Samples were separated by SDS–PAGE, and products of Gag processing were detected by quantitative immunoblot (LiCor) using antiserum raised against recombinant HIV-1 CA. The figures show samples incubated for the indicated times without prior irradiation or following irradiation, respectively. Positions of Gag-derived proteins are indicated. (**d**,**e**) Quantitative analysis of the experiments shown in **b** or **c**, respectively. Anti-CA reactive bands from the immunoblots shown and from corresponding blots from irradiated mature control virus produced in the absence of inhibitor (not shown here) were quantified using Image Studio Light. The graphs show the proportion of mature CA relative to the sum of all anti-CA reactive bands in the respective lane. Filled triangles, irradiated control virus; open circles, inhibitor-treated virus, not irradiated; filled circles, inhibitor-treated virus, irradiated. Curves through data from inhibitor-treated samples represent fits to a single exponential equation. The results are representative of several independent experiments with a slight variation in the half-time of Gag polyprotein processing between 20 and 30 min. CA, capsid; MA, matrix.

this crucial step in the HIV-1 life cycle. We suggest that a similar approach, that is, design of specific photolabile inhibitors that can be photolysed to inactive products, thus triggering enzymatic activity, can be used for photocaging of other regulatory PRs to analyze their roles *in situ*.

Methods

Chemical synthesis. The synthesis of all intermediates and their full chemical analyses are described in the Supplementary Information. All compounds tested in biochemical assays were of at least 99% purity. All peaks in NMR spectra for all compounds were assigned using standard 2D NMR techniques (COSY, HMBC, HSQC).

Compound **1**: Compound **2** (20 mg, 31.3 µmol, 1.0 equiv.) was dissolved in 0.5 ml tetrahydrofurane along with 16 µl + N,N-Diisopropylethylamine (93.9 µmol, 3.0 equiv.). (7-(Diethylamino)-2-oxo-2H-chromen-4-yl)methyl(2,5-dioxopyrrolidin-1-yl) carbonate (13.5 mg, 34.4 µmol, 1.1 equiv. (for preparation, see Supplementary Information) was added in one portion, and the reaction was stirred overnight. The crude product obtained after removal of all volatiles was purified on preparative scale HPLC (gradient 50–100% acetonitrile in 30 min. R_t = 16 min). Yellow powder was obtained on lyophilization (10 mg, isolated yield = 35%). Analytical HPLC (gradient 2–100% in 30 min, flow rate 1 ml min^{-1}; R_t = 25.5 min). ^{1}H NMR (500 MHz, DMSO-*d6*):*δ* 9.05 (d, *J* = 0.8, 1H, N-*CH*-S), 7.86 (q, *J* = 0.8, 1H, S-C-*CH*-N), 7.79 (d, *J* = 8.7, 1H, CH-*NH*-Val), 7.45 (d, *J* = 9.7, 1H, Val-*NH*-COO), 7.45 (d, *J* = 9.1, 1H, C-*CH*-CH-C-N-Et$_2$), 7.23-7.07 (m, 10H, 2 × *Ph*), 6.91 (d, *J* = 9.4, 1H, *NH*-CH-CH-OH), 6.68 (dd, *J* = 9.1, 2.5, 1H, C-CH-*CH*-C-N-Et$_2$), 6.55 (d, *J* = 2.5, 1H, C-*CH*-C-N-Et$_2$), 6.08 (t, *J* = 1.3, 1H, O-C(O)-*CH*-C), 5.25 and 5.25 (2 × dd, *J* = 16.1, 1.3, 2 × 1H, O-*CH$_2$*-coumarin), 5.11 and 5.16 (2 × d, *J* = 13.0, 2 × 1H, O-*CH$_2$*-thiazole), 4.15 (bm, 1H, *CH*-NH-Val), 3.80 (bm, 1H, NH-*CH*-CH-OH), 3.78 (dd, *J* = 9.2, 7.3, 1H, NH-C(O)-*CH*(iPr)-NH), 3.59 (td, *J* = 6.7, 2.1, 1H, NH-CH-*CH*-OH), 3.42 (q, *J* = 7.0, 4H, *CH$_2$*-CH$_3$), 2.69 (bdd, *J* = 13.5, 4.9, 1H, *CH$_2$*-CH-NH-Val), 2.67 (bd, *J* = 7.6, 2H, *CH$_2$*-CH-NH-C(O)o-thiazole), 2.59 (bdd, *J* = 13.5, 8.0, 1H, *CH$_2$*-CH-NH-Val), 1.85 (dsept, *J* = 7.3, 6.8, 1H, -*CH*(CH$_3$)$_2$), 1.45 (m, 2H, OH-CH-*CH$_2$*-CH-NH), 1.11 (t, *J* = 7.0, 6H, CH$_2$-*CH$_3$*), 0.76 and 0.79 (2 × d, *J* = 6.8, 6H, -CH(*CH$_3$*)$_2$). ^{13}C NMR (125.7 MHz, DMSO-*d6*):*δ* 161.01 (NH-*(O)CVal*-NH), 155.92 (O-*C*-CH-C-N-Et$_2$), 155.79 (thizaole-O-*C*-N), 155.74 (N-*CH*-S), 155.53 (Val-NH-*C*(O)-O), 152.07 (Val-NH-C(O)-O -CH$_2$-*C*), 150.58 (**C**-N-Et$_2$), 143.21 (S-C-*CH*-N), 139.640 (i-*Ph*-CH$_2$-CH-NH-thiazol), 138.86 (i-*Ph*-CH$_2$-CH-NH-Val), 134.29 (S-C-CH-N), 129.19 and 129.52 (2 × o-*Ph*), 128.18 and 128.03 (2 × m-*Ph*), 126.00 and 125.94 (2 × p-*Ph*), 125.50 (C-*CH*-CH-C-N-Et$_2$), 108.91 (C-CH-*CH*-C-N-Et$_2$), 105.43 (**C**-CH-CH-C-N-Et$_2$), 104.63 (O-C(O)-*CH*-C), 97.05 (C-*CH*-C-N-Et$_2$), 69.15 (HO-*CH*), 61.16 (O-*CH$_2$*-coumarin), 60.57 (NH-C(O)-*CH*(iPr)-NH), 57.37 (C(O)O-*CH$_2$*-thiazole), 55.73 (NH-*CH*-CH-OH), 47.30 (OH-CH-CH$_2$-*CH*-NH), 44.20 (*CH$_2$*-CH$_3$), 39.53 (Val-NH-CH-*CH$_2$*-Ph), 38.29 (OH-CH-*CH$_2$*-CH-NH), 37.34 (*CH$_2$*-CH-NH-C(O)o-thiazole), 30.55 (*CH*(CH$_3$)$_2$), 19.43 and 18.33 (2 × *CH$_3$*), 12.50 (CII$_2$-*CII$_3$*). IIRMS (m/z; ESI+): calculated for $C_{43}I_{51}O_8N_5S$ [MNa]$^+$ 820.33506; found 820.33470.

Purification of HIV PR. The recombinant PR was overexpressed in *Escherichia coli* BL21(DE3) RIL (Novagen). Protein expression and isolation of inclusion bodies were carried out as previously described[34]. Inclusion bodies were solubilized in 67% (v/v) acetic acid and refolded by dilution into a 25-fold excess of water, followed by overnight dialysis at 4 °C against water and then against 50 mM MES (pH 5.8), 10% (v/v) glycerol, 1 mM EDTA and 0.05% (v/v) 2-mercaptoethanol. The PR was purified by cation exchange chromatography using MonoSFPLC (Pharmacia). The enzyme was stored at 70 °C until further use[34].

Inhibition of HIV-1 PR. K_i values were determined by spectrophotometric assay using purified recombinant HIV-1 PR and the chromogenic substrate KARVN-leNphEaNle-NH$_2$. Data were analyzed using the Morrison equation[35].

Crystallization experiments. The HIV PR-compound **1** complex was prepared by mixing the enzyme with an equimolar amount of **1** dissolved in DMSO. The protein was pre-concentrated to 4 mg ml^{-1} by ultrafiltration using Microcon-10 filters (Millipore, Billerica, MA, USA). The complex was then centrifuged for 25 min at 16,000 *g* to reduce the number of crystallization nuclei. Crystals were then grown by the hanging drop vapour diffusion technique at 19 °C. The crystallization drops contained 2 µl protein-inhibitor complex and 1 µl reservoir solution (0.2 M lithium sulfate, 0.1 M phosphate/citrate pH 4.2 and 20% (w/v) PEG 1000; JSCG + condition 6). The HIV PR-compound **2** complex was prepared by incubation HIV PR with fourfold molar excess of **2** for 30 min and it was then concentrated to a protein concentration of 4 mg ml^{-1} by the above described procedure. Crystals were grown as described above. The reservoir solution was 0.2 M magnesium chloride, 0.1 M Tris pH 8.5 and 20% (w/v) PEG 8000. For diffraction measurements, crystals were soaked in reservoir solution supplemented with 25% (v/v) glycerol and cooled in liquid nitrogen. The diffraction data collection and structure refinement are described in Supplementary Information in chapter 3.3.

Photolysis of the inhibitor. Irradiation was performed in two distinct set ups.

Cuvette set up. A 1 ml reaction mixture (8 nM purified recombinant HIV-1 PR in cleavage buffer—100 mM sodium acetate, 0.3 M NaCl, 4 mM EDTA, pH 4.7, various concentrations of inhibitor) at 4 °C was irradiated with two defocused 405 nm lasers (130 and 170 mW) in a quartz cuvette for various periods of time. The cuvette was then equlibrated to 37 °C, and the enzymatic reaction was started by adding 4 µl of 3.8 µM chromogenic substrate (KARVNleNphEaNle-NH$_2$)[27]. The enzyme activity (and thus the efficacy of photodegradation) was followed by the decrease in absorbance at 305 nm.

Capillary set up. Two 405 nm focusable lasers (130 and 170 mW, checked for both intensity and wavelength before use) were used for irradiation in a capillary set up. The solution (either purified HIV-1 PR or a suspension of immature virions) was linearly pumped through a 250 µm glass capillary (Hirschmann ring caps) at which both laser beams were focused (for an illustrative photo, see Supplementary Fig. 4). To 47.5 µl of cleavage buffer (100 mM sodium acetate, 0.3 M NaCl, 4 mM EDTA, pH 4.7) on ice, 2 µl of 4 µM HIV-1 PR and 0.5 µl of 200 µM compound **1** were added. The solution was irradiated at different flow rates, diluted in a 1 ml cuvette with 950 µl of cleavage buffer (100 mM sodium acetate, 0.3 M NaCl, 4 mM EDTA, pH 4.7, 37 °C) and the enzymatic reaction was started by adding 4 µl of 3.8 µM chromogenic substrate.

Analysis of photodegradation products. The photodegradation of the inhibitor was analyzed with an analytical Jasco PU-1580 HPLC (flow rate 1 ml min^{-1}, invariable gradient 2–100% ACN in 30 min, Watrex C18 Analytical Column, 5 µm, 250 × 5 mm), and the retention times were compared with those of synthetic standards (the degradation product was also an intermediate during synthesis of compound **1**).

Plasmids and cell cultures. Proviral plasmid pNL4-3 (obtained through the NIH AIDS Reagent Program from Dr Malcolm Martin) has been described before[36]. Plasmid pCHIV, which encodes all HIV-1 NL4-3 proteins except Nef, but lacks both long terminal repeat regions required for infectivity, has also been described[37]. HEK293T cells were kept in high-glucose Dulbecco's modified Eagle's medium (DMEM, Life Technologies) supplemented with penicillin/streptomycin and 10% foetal calf serum at 37 °C, 5% CO_2. For the analysis of inhibitor activity on viral particle processing, HEK293T cells were transfected with pNL4-3 using calcium phosphate, and inhibitor was added at the indicated concentrations. At 48 h post transfection, supernatants were harvested, cleared by filtration through a 0.45-µm filter and concentrated by ultracentrifugation through a 20% (w/w) sucrose cushion.

Photoactivation of HIV-1 PR *in situ*. HEK293T cells were seeded in six-well plates in high-glucose, phenol red-free DMEM supplemented with penicillin/streptomycin and 10% foetal calf serum. On the following day, cells were transfected with plasmid pCHIV[37] using polyethyleneimine according to standard procedures. A final concentration of 2 µM compound **1** or DMSO (vehicle) was added to the tissue culture medium at the time of transfection. At 44 h post transfection, tissue culture supernatants were harvested, adjusted to pH 6.0 using PR buffer (50 mM MES, pH 6.0, 150 mM NaCl, 2 mM DTT, 1 mM EDTA). Alternatively, supernatants were harvested, filtered, inhibitor was removed by two successive ultracentrifugation steps through a 20% sucrose cushion and the particle pellet was resuspended in PR buffer. In both cases, samples were then split into two aliquots, one of which was subjected to ultraviolet irradiation using the capillary set up described above, whereas the control aliquot was pumped through the capillary set up without ultraviolet irradiation. Subsequently, samples were incubated at 37 °C, and 20 µl aliquots were taken before incubation (t = 0) and at t = 15, 30, 60, 90 and 360 min. At these time points, the processing reaction was stopped by addition of SDS sample buffer and heat treatment (5 min, 90 °C).

Analysis of HIV polyprotein processing by immunoblot. Samples were separated by SDS–PAGE (17.5%; acrylamide:bisacrylamide 200:1), and proteins were transferred to a nitrocellulose membrane by semi-dry blotting. HIV-1 Gag-derived proteins were detected using rabbit polyclonal antiserum raised against HIV-1 CA, followed by fluorescently labelled goat-anti rabbit secondary antibody (LiCor). Quantification of anti-CA reactive bands was performed using an infrared imaging system (LiCor Odyssey) and Image Studio Lite software. Data were analyzed with GraphPad prism.

References

1. Krausslich, H. G. *et al.* Activity of purified biosynthetic proteinase of human immunodeficiency virus on natural substrates and synthetic peptides. *Proc. Natl Acad. Sci. USA* **86,** 807–811 (1989).
2. Pokorna, J., Machala, L., Rezacova, P. & Konvalinka, J. Current and novel inhibitors of HIV protease. *Viruses* **1,** 1209–1239 (2009).
3. Krausslich, H. G. Human immunodeficiency virus proteinase dimer as component of the viral polyprotein prevents particle assembly and viral infectivity. *Proc. Natl Acad. Sci. USA* **88,** 3213–3217 (1991).

4. Wiegers, K. *et al.* Sequential steps in human immunodeficiency virus particle maturation revealed by alterations of individual Gag polyprotein cleavage sites. *J. Virol.* **72,** 2846–2854 (1998).
5. Debouck, C. *et al.* Human immunodeficiency virus protease expressed in Escherichia coli exhibits autoprocessing and specific maturation of the gag precursor. *Proc. Natl Acad. Sci. USA* **84,** 8903–8906 (1987).
6. Krausslich, H. G., Nicklin, M. J., Lee, C. K. & Wimmer, E. Polyprotein processing in picornavirus replication. *Biochimie* **70,** 119–130 (1988).
7. Manchester, M., Everitt, L., Loeb, D. D., Hutchison, 3rd C. A. & Swanstrom, R. Identification of temperature-sensitive mutants of the human immunodeficiency virus type 1 protease through saturation mutagenesis. Amino acid side chain requirements for temperature sensitivity. *J. Biol. Chem.* **269,** 7689–7695 (1994).
8. Konvalinka, J. Structural and molecular biology of protease function and inhibition. *J. Cell Biochem.* **56,** 117–177 (1994).
9. Mattei, S. *et al.* Induced maturation of human immunodeficiency virus. *J. Virol.* **88,** 13722–12731 (2014).
10. Engels, J. & Schlaeger, E. J. Synthesis, structure, and reactivity of adenosine cyclic 3′,5′-phosphate benzyl triesters. *J. Med. Chem.* **20,** 907–911 (1977).
11. Kaplan, J. H., Forbush, 3rd B. & Hoffman, J. F. Rapid photolytic release of adenosine 5'-triphosphate from a protected analogue: utilization by the Na:K pump of human red blood cell ghosts. *Biochemistry* **17,** 1929–1935 (1978).
12. Ellis-Davies, G. C. Neurobiology with caged calcium. *Chem. Rev.* **108,** 1603–1613 (2008).
13. Makings, L. R. & Tsien, R. Y. Caged nitric oxide. Stable organic molecules from which nitric oxide can be photoreleased. *J. Biol. Chem.* **269,** 6282–6285 (1994).
14. Cruz, F. G., Koh, J. T. & Link, K. H. Light-activated gene expression. *J. Am. Chem. Soc.* **122,** 8777–8778 (2000).
15. Lin, W., Albanese, C., Pestell, R. G. & Lawrence, D. S. Spatially discrete, light-driven protein expression. *Chem. Biol.* **9,** 1347–1353 (2002).
16. Breitinger, H. G., Wieboldt, R., Ramesh, D., Carpenter, B. K. & Hess, G. P. Synthesis and characterization of photolabile derivatives of serotonin for chemical kinetic investigations of the serotonin 5-HT(3) receptor. *Biochemistry* **39,** 5500–5508 (2000).
17. Callaway, E. M. & Yuste, R. Stimulating neurons with light. *Curr. Opin. Neurobiol.* **12,** 587–592 (2002).
18. Mikat, V. & Heckel, A. Light-dependent RNA interference with nucleobase-caged siRNAs. *RNA* **13,** 2341–2347 (2007).
19. Shah, S., Jain, P. K., Kala, A., Karunakaran, D. & Friedman, S. H. Light-activated RNA interference using double-stranded siRNA precursors modified using a remarkable regiospecificity of diazo-based photolabile groups. *Nucleic Acids Res.* **37,** 4508–4517 (2009).
20. Nadler, A. *et al.* The fatty acid composition of diacylglycerols determines local signaling patterns. *Angew. Chem. Int. Ed.* **52,** 6330–6334 (2013).
21. Hiraoka, T. & Hamachi, I. Caged RNase: photoactivation of the enzyme from perfect off-state by site-specific incorporation of 2-nitrobenzyl moiety. *Bioorg. Med. Chem. Lett.* **13,** 13–15 (2003).
22. Chang, C. Y., Fernandez, T., Panchal, R. & Bayley, H. Caged catalytic subunit of cAMP-dependent protein kinase. *J. Am. Chem. Soc.* **120,** 7661–7662 (1998).
23. Riggsbee, C. W. & Deiters, A. Recent advances in the photochemical control of protein function. *Trends Biotechnol.* **28,** 468–475 (2010).
24. Brieke, C., Rohrbach, F., Gottschalk, A., Mayer, G. & Heckel, A. Light-controlled tools. *Angew. Chem. Int. Ed.* **51,** 8446–8476 (2012).
25. Lee, H. M., Larson, D. R. & Lawrence, D. S. Illuminating the chemistry of life: design, synthesis, and applications of "caged" and related photoresponsive compounds. *ACS Chem. Biol.* **4,** 409–427 (2009).
26. Li, H., Hah, J. M. & Lawrence, D. S. Light-mediated liberation of enzymatic activity: "small molecule" caged protein equivalents. *J. Am. Chem. Soc.* **130,** 10474–10475 (2008).
27. Porter, N. A., Bush, K. A. & Kinter, K. S. Photo-reversible binding of thrombin to avidin by means of a photolabile inhibitor. *J. Photochem. Photobiol. B* **38,** 61–69 (1997).
28. Kempf, D. J. *et al.* ABT-538 is a potent inhibitor of human immunodeficiency virus protease and has high oral bioavailability in humans. *Proc. Natl Acad. Sci. USA* **92,** 2484–2488 (1995).
29. Sundquist, W. I. & Krausslich, H. G. HIV-1 assembly, budding, and maturation. *Cold Spring Harb. Symp. Quant. Biol.* **2,** a006924 (2012).
30. Muller, B. *et al.* HIV-1 Gag processing intermediates trans-dominantly interfere with HIV-1 infectivity. *J. Biol. Chem.* **284,** 29692–29703 (2009).
31. Kaplan, A. H. *et al.* Partial inhibition of the human immunodeficiency virus type 1 protease results in aberrant virus assembly and the formation of noninfectious particles. *J. Virol.* **67,** 4050–4055 (1993).
32. Konnyu, B. *et al.* Gag-Pol processing during HIV-1 virion maturation: a systems biology approach. *PLoS Comput. Biol.* **9,** e1003103 (2013).
33. Dale, B. M. *et al.* Cell-to-cell transfer of HIV-1 via virological synapses leads to endosomal virion maturation that activates viral membrane fusion. *Cell Host Microbe* **10,** 551–562 (2011).
34. Saskova, K. G. *et al.* Enzymatic and structural analysis of the I47A mutation contributing to the reduced susceptibility to HIV protease inhibitor lopinavir. *Protein Sci.* **17,** 1555–1564 (2008).
35. Richards, A. D. *et al.* Sensitive, soluble chromogenic substrates for HIV-1 proteinase. *J. Biol. Chem.* **265,** 7733–7736 (1990).
36. Adachi, A. *et al.* Production of acquired immunodeficiency syndrome-associated retrovirus in human and nonhuman cells transfected with an infectious molecular clone. *J. Virol.* **59,** 284–291 (1986).
37. Lampe, M. *et al.* Double-labelled HIV-1 particles for study of virus-cell interaction. *Virology* **360,** 92–104 (2007).

Acknowledgements

We would like to thank Hana Prouzová for expert technical help, Hillary Hoffman for language editing, and Petr Klán for insightful advice in field of caged compounds. We also acknowledge the Grant Agency of the Czech Republic, Grant No. P208-12-G016 (Center of Excellence), BIOCEV; Grant number: CZ.1.05/1.1.00/02.0109 and Inter-BioMed Project LO1302 from the Ministry of Education of the Czech Republic for financial support. This work was funded in part by grants from the Deutsche Forschungsgemeinschaft to B.M. (MU885/5-1) and H.-G.K. (DFG grant number KR906/7-1). H.-G.K. and B.M. are investigators of the CellNetworks Cluster of Excellence (EXC81).

Author contributions

J.S. designed the compounds; J.S. with P.M. and P.C. synthesized the compounds; J.S. evaluated the compounds in vitro; J.W., M.P., M.A. and B.M. analyzed the antiviral activity and inhibition of polyprotein processing; J.S. and P.Š. designed the irradiation apparatus; J.S., P.P. and P.Ř. crystallized the PR complexes and solved the structures; M.A., J.S., B.M. and H.-G.K. analyzed the polyprotein processing by photoactivation; J.K. conceived and lead the project; J.S., J.K., H.-G.K. and B.M. analyzed the data, J.S., H.-G.K., P.Ř., B.M. and J.K. wrote the manuscript.

Additional information

Accesion codes: Atomic coordinates and experimental structure factors have been deposited in the Protein Data Bank under codes 4U7Q and 4U7V for complexes with compounds **1** and **2**, respectively.

Supplementary Information accompanies this paper at http://www.nature.com/naturecommunications

Competing financial interests: The authors declare no competing financial interests.

Reprints and permission information is available online at http://npg.nature.com/reprintsandpermissions/

How to cite this article: Schimer, J. *et al.* Triggering HIV polyprotein processing by light using rapid photodegradation of a tight-binding protease inhibitor. *Nat. Commun.* 6:6461 doi: 10.1038/ncomms7461 (2015).

5.3 Rational Design of Urea-based Glutamate Carboxypeptidase II (GCPII) Inhibitors as Versatile Tools for Specific Drug Targeting and Delivery

Background:

Besides being a prostate cancer marker, GCPII is also a proteolytic enzyme. During the past three decades a number of high affinity inhibitors have been developed (chapter 3.2.6). These GCPII inhibitors can be utilized in imaging of the prostate carcinoma, and have been studied thoroughly in the past. However, it should be noted that imaging through radio-labeled or fluorescently-labeled monoclonal antibodies is predominant in this field (chapter 3.2.8).

Due to GCPII active site architecture, with its relatively wide entrance tunnel, GCPII inhibitors could be also utilized to anchor various nanoparticles, that could be used for example for targeting therapeutics into the prostate carcinoma cells. To prepare an inhibitor, which would be able to facilitate the interaction between GCPII and the chosen nanoparticle, an appropriate linker reaching outside of the GCPII active site to the surface of the protein is needed.

Summary:

In the presented study we set out to design GCPII inhibitor with linker reaching outside GCPII terminated with D-biotin to enable facile modification of various nanoparticles. Additionally, we performed structure-assisted inhibitor design to target GCPII exosites thus increasing the binding potency of the inhibitors. The overall strategy of the project is illustrated in Figure 16 (p. 57).

Through structure-activity relationship (SAR) study we were able design and target GCPII exosite which resulted in 7-fold improvement of final inhibitor *Ki* value compared to parental molecule. Additionally, we optimized the length of the inhibitor linker for effective attachment to a biotin-binding molecule and showed that the optimized inhibitor could be used to a facile preparation of GCPII-specific nanoparticles which are able to visualize prostate cancer cells.

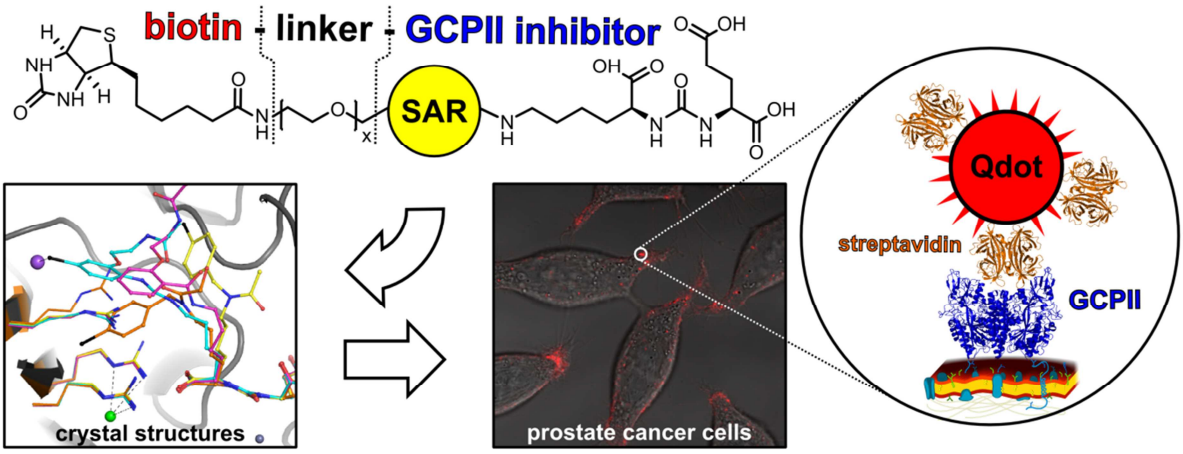

Figure 16: Overall strategy of GCPII targeting inhibitor design and utilization. Using established urea-based inhibitor scaffold we conducted structure-activity relationship (SAR) study of linker moiety to target GCPII exosite thus increasing potency of the final inhibitor. Such inhibitor then enables easy modification of various nanoparticles (e.g., commercially available quantum dots (Qdots)) through terminal D-biotin yielding nanoparticles, which specifically recognize the GCPII protein.

My contribution:

I prepared all the compounds, participated in measurement of inhibition constants and contributed to the preparation of the manuscript.

Tykvart, J., Schimer, J., Barinkova, J., Pachl, P., Postova-Slavetinska, L., Majer, P., Konvalinka, J., and Sacha, P., **Rational design of urea-based glutamate carboxypeptidase II (GCPII) inhibitors as versatile tools for specific drug targeting and delivery**. Bioorg Med Chem, 2014. **22**(15): p. 4099-4108.

Bioorganic & Medicinal Chemistry 22 (2014) 4099–4108

Contents lists available at ScienceDirect

Bioorganic & Medicinal Chemistry

journal homepage: www.elsevier.com/locate/bmc

Rational design of urea-based glutamate carboxypeptidase II (GCPII) inhibitors as versatile tools for specific drug targeting and delivery

Jan Tykvart [a,b,†], Jiří Schimer [a,b,†], Jitka Bařinková [a], Petr Pachl [a,c], Lenka Poštová-Slavětínská [a], Pavel Majer [a], Jan Konvalinka [a,b], Pavel Šácha [a,b,*]

[a] Gilead Sciences and IOCB Research Centre, Institute of Organic Chemistry and Biochemistry, Academy of Sciences of the Czech Republic, v.v.i., Flemingovo n. 2, Prague 6, 166 10 Czech Republic
[b] Department of Biochemistry, Faculty of Natural Science, Charles University, Albertov 6, Prague 2, Czech Republic
[c] Institute of Molecular Genetics, Academy of Sciences of the Czech Republic, Vídeňská 1083, Prague 4, Czech Republic

ARTICLE INFO

Article history:
Received 20 January 2014
Revised 26 May 2014
Accepted 28 May 2014
Available online 5 June 2014

Keywords:
GCPII
PSMA
Structure-aided drug design
Specific drug targeting

ABSTRACT

Glutamate carboxypeptidase II (GCPII), also known as prostate specific membrane antigen (PSMA), is an established prostate cancer marker and is considered a promising target for specific anticancer drug delivery. Low-molecular-weight inhibitors of GCPII are advantageous specific ligands for this purpose. However, they must be modified with a linker to enable connection of the ligand with an imaging molecule, anticancer drug, and/or nanocarrier. Here, we describe a structure–activity relationship (SAR) study of GCPII inhibitors with linkers suitable for imaging and drug delivery. Structure-assisted inhibitor design and targeting of a specific GCPII exosite resulted in a 7-fold improvement in K_i value compared to the parent structure. X-ray structural analysis of the inhibitor series led to the identification of several inhibitor binding modes. We also optimized the length of the inhibitor linker for effective attachment to a biotin-binding molecule and showed that the optimized inhibitor could be used to target nanoparticles to cells expressing GCPII.

1. Introduction

Prostate carcinoma (PCa) is the most commonly diagnosed cancer and the second leading cause of cancer death among men in the USA; the number of diagnoses and deaths exceeded 240,000 and 28,000, respectively, in 2012.[1] Identification of a molecule that would enable early diagnosis and reliable detection of PCa metastases, as well as function as a possible target for specific therapy, is crucial for effective treatment of this cancer. Evidence suggests that glutamate carboxypeptidase II (GCPII), also known as prostate specific membrane antigen (PSMA), is a promising candidate for this purpose.[2,3]

GCPII, a 750-amino-acid type II transmembrane di-zinc metallopeptidase, possesses two distinct endogenous substrates in the human body. In the brain, it is responsible for degradation of the peptide neurotransmitter *N*-acetyl-L-aspartyl-L-glutamate,[4] and in the small intestine, it cleaves terminal glutamates from poly-γ-glutamylated folate.[5] In addition to its enzymatic roles, GCPII is studied for its overexpression in PCa.[6] Recently, it has been shown that GCPII is also expressed at the neovasculature of solid tumors,[7] which makes it even more interesting as a diagnostic/therapeutic target. Furthermore, the facts that GCPII is a transmembrane protein, with a large extracellular domain, and is internalized upon ligand binding[8] make GCPII even more suitable for specific cancer cell targeting.

Antibodies, small-molecule inhibitors, and aptamers have been studied as tools for specific targeting of GCPII. At present, only one molecule, radioisotope-antibody conjugate ^{111}In-7E11-C5.3, has made it through the development pipeline into practical use as the imaging agent ProstaScint™.[9] New generations of diagnostic and therapeutic radiolabeled antibodies targeting the extracellular

Abbreviations: Avi-GCPII, extracellular portion (amino acids 44–750) of recombinant human GCPII with N-terminal Avi-tag followed by a TEV cleavage site; GCPII, glutamate carboxypeptidase II; Qdot, quantum dot; LNCaP, lymph node carcinoma of the prostate; 2-MPPA, 2-(3-mercaptopropyl)pentanedioic acid; PCa, prostate carcinoma; 2-PMPA, 2-(phosphonomethyl)pentanedioic acid; PSMA, prostate specific membrane antigen; rhGCPII, extracellular portion (amino acids 44–750) of recombinant human GCPII; SAR, structure–activity relationship; SPR, surface plasmon resonance; TEV, tobacco etch virus.

* Corresponding author. Tel.: +420 220 183 452; fax: +420 220 183 578.
E-mail address: pavelsacha@gmail.com (P. Šácha).
† These authors contributed equally to the presented work.

http://dx.doi.org/10.1016/j.bmc.2014.05.061
0968-0896/

portion of GCPII are in various stages of clinical trials, and diverse radiolabeled small-molecule inhibitors also have been intensively investigated.[2,10–12] Beside radiolabeling approach, a small-molecule inhibitors and in some extent also antibodies modified with various organic dyes have been intensively investigated as a potential diagnostic agents.[13,14]

In addition to their applications in direct labeling with radioisotope or organic dye, GCPII-specific antibodies, small-molecule inhibitors, and aptamers also could be used for targeted delivery of various nanoparticles,[15] such as gold nanoparticles,[16,17] polymers,[18–21] nanorods,[22] and nanobubbles.[23]

Generally, low-molecular-weight ligands have a number of advantages over antibodies, which are still used more frequently for specific targeting. Small-molecule ligands are easy to prepare on a large scale, could have very favorable pharmacokinetic properties (such as bioavailability, half-life, etc.), and might penetrate the blood–brain barrier.[24] Moreover, numerous modified analogs of a particular small-molecule ligand can be easily prepared. Such modifications may lead to enhanced specificity and affinity.

A number of potent (low nanomolar) inhibitors of GCPII have been described in the literature. Generally, these GCPII inhibitors contain a glutamate residue or analog, which binds very specifically in the P1′ site, and a zinc binding group. Based on the nature of the zinc binding group, GCPII inhibitors can be divided into three groups: (1) phosphonate-, phosphate-, and phosphoramide-based (e.g., 2-PMPA[25]); (2) thiol-based (e.g., 2-MPPA[26]); and (3) urea-based inhibitors (e.g., Glu-NH-C(O)-NH-Glu[27]). For more detailed information, see a recent review summarizing current knowledge about GCPII inhibitors.[28]

The structure of GCPII has been extensively studied during the past several years, resulting in deposition of more than 20 X-ray structures, the majority of them solved by the Barinka and Konvalinka groups. GCPII likely forms homodimer under physiological conditions, and its substrate binding site has strong specificity in the P1′ pocket, while the P1 pocket is more flexible. Therefore, greater molecular variability is possible in the part of the inhibitor molecule that binds to the P1 site. Additionally, a deep accessory funnel-shaped tunnel contains several more exosites that could be utilized in design of more potent inhibitors. For more detailed information, see a recently published structural description of GCPII molecule.[29]

In this work, we designed novel inhibitors based on the established urea-based scaffold.[27] We performed a structure–activity relationship (SAR) study to utilize the arginine patch exosite near the S1 site that is able, through conformational change of Arg463, to create a so-called 'S1-accessory hydrophobic pocket'.[30,31] To maximize inhibitor binding affinity, we also attempted to exploit a previously described positive effect of halogens attached to the aromatic moiety of the inhibitor.[32]

We set out to prepare a generally applicable inhibitor of GCPII that could be used for facile modification of various nanoparticles using a streptavidin–biotin interaction since it has been already shown that such modified inhibitors can bind to GCPII.[17,33]

2. Materials and methods

2.1. Preparation of recombinant GCPII

For SPR measurements, the extracellular part of recombinant human GCPII (rhGCPII) containing amino acids 44–750 was prepared as previously described.[34] For inhibition constant measurements and crystallization trials, the extracellular part of recombinant human GCPII with an N-terminal Avi-tag (Avi-GCPII) was prepared as previously described.[35]

2.2. Determination of inhibition constants by HPLC

IC_{50} values for all inhibitors were determined using an HPLC-based assay. In a 96-well plate, 0.2 ng of Avi-GCPII in 25 mM Bis-Tris propane, 150 mM NaCl, 0.001% (w/w) octaethylene glycol monododecyl ether (Affymetrix), pH 7.4, and inhibitors were mixed together in a final volume of 180 μL. Ten inhibitor concentrations were used (4 times serial dilution) to obtain a full inhibition curve. Reactions were pre-incubated at 37 °C for 5 min, started by addition of 20 μL of 4 μM pteroyl-di-L-glutamate (Schircks Laboratories) and incubated at 37 °C for 20 min. The reactions were stopped with 20 μL of 25 μM 2-PMPA.

Subsequently, 100 μL of reaction mixture was injected into and analyzed on an Agilent 1200 Series system using an Acquity UPLC HSS T3 1.8 μm column (2.1 × 100 mm, Waters). The HPLC analysis was run isocratically in 2.7% ACN and 97.3% 20 mM phosphate, pH 6.0. Absorbance of both substrate and product were detected at 281 nm. Afterwards, data were processed, and IC_{50} values were obtained using GraFit v.5.0.11 (Erithacus Software Ltd.).

Kinetic parameters (K_M and k_{cat}) of pteroyl-di-L-glutamate cleavage by Avi-GCPII in the reaction buffer used for IC_{50} measurement were determined as described above but without addition of inhibitor and with substrate concentrations ranging from 15 nM to 400 nM (substrate conversions for all reactions were 13 ± 2%). From the kinetic parameters of pteroyl-di-L-glutamate cleavage and by assuming a competitive mode of inhibition, the K_i value for each inhibitor was calculated using the Cheng–Prusoff equation.[36]

2.3. Surface plasmon resonance measurements

All surface plasmon resonance measurements were performed on a four-channel SPR sensor platform developed at the Institute of Photonics and Electronics, Prague.[37,38] In a typical experiment, the SPR chip (provided by the IPE) was loaded into a pure ethanol mixture of HS-$(CH_2)_{11}$-PEG_4-OH and HS-$(CH_2)_{11}$-PEG_6-O-CH_2-COOH alkanethiols (molar ratio 7:3, Prochimia) with a final concentration of 0.2 mM and incubated for 1 h at 37 °C. The chip was rinsed with UV ethanol and deionized water and subsequently dried with flow of nitrogen. Then, the chip was mounted to the prism on the SPR sensor. The experiment was performed at 25 °C.

The activation of carboxylic terminal groups on the sensor surface was performed in situ by injecting a 1:1 mixture of 11.51 mg/mL *N*-hydroxysuccinimide (NHS) and 76.68 mg/mL 1-ethyl-3-(3-dimethylaminopropyl)-carbodiimide hydrochloride (EDC) in deionized water (Biacore) for 5 min at a flow rate of 20 μL/min. The remainder of the experiment was performed at a flow rate of 30 μL/min. Afterwards, a 0.02 mg/mL neutravidin solution (for qualitative experiments) or a mixture of neutravidin with BSA (molar ratio 1:50) at a final concentration of 0.04 mg/mL in 10 mM sodium acetate buffer, pH 5.0 (for kinetic experiments), was loaded for 8 min. Then, high ionic strength solution (PBS with 0.5 M NaCl) was used to wash out noncovalently bound neutravidin molecules, followed by 1 M ethanolamine (Biacore) for deactivation of residual activated carboxylic groups.

A 1 μM solution of inhibitor in TBS was immobilized on prepared gold chips with neutravidin or neutravidin/BSA layer in TBS to saturate all biotin binding sites. Afterwards, rhGCPII (in the same or various concentrations) in TBS was injected for several minutes (association), and then TBS alone was injected (dissociation).

Kinetic curves of binding were exported and subsequently fitted in TraceDrawer v.1.5 (Ridgeview Instruments AB) to obtain k_{on} and k_{off} parameters.

2.4. Crystallization and data collection

Avi-GCPII stock solution (15 mg/mL) was mixed in a 1:1 ratio with 1–10 mM inhibitor. The crystallization droplets were prepared by combining 1 μL of the protein/inhibitor solution with 1 μL of the precipitation solution containing 33% pentaerythritol propoxylate (Hampton Research), 1–2% PEG 3350 (Fluka), and 100 mM Tris–HCl, pH 8.0. In some cases, micro-seeding was used to obtain crystals of sufficient size for diffraction. The micro-seeding solution was prepared by fishing out several smaller crystals, vortexing them in 100 μL of precipitation solution, and further diluting the solution 20- to 100-fold in precipitation solution. Crystals were grown by the hanging drop vapor diffusion method at 291 K. Crystals were flash-frozen in liquid nitrogen, and the diffraction data were collected either at 100 K at beamlines BL14.1 and BL14.2 of BESSY, Berlin, Germany[39] or at 120 K using an in-house diffractometer (Nonius FR 591 generator, 345-mm MarResearch Image Plate detector). Complete datasets were collected from single crystals. The diffraction data to resolution were integrated and reduced using XDS[40] and its graphical interface XDSAPP.[41]

2.5. Structure determination and refinement

Structure determination was performed by molecular replacement using the program Molrep in CCP4 software package.[42,43] The previously solved structure of rhGCPII in complex with the inhibitor 2-PMPA (PDB entry 2PVW)[44] without the inhibitor and without water molecules was used as the starting model for structural refinement based on the X-ray data collected from crystals of the Avi-GCPII/inhibitor complexes. Calculations were performed with the program Refmac 5.7,[45] and the refinement protocol was interspersed with manual corrections to the model using WinCoot v.0.7.[46] The final models, together with experimental amplitudes, were deposited into the RCSB Protein DataBank. A summary of structural parameters is displayed in Table S1.

2.6. Preparation of nanocarriers specifically recognizing GCPII

A 25 μL aliquot of a 250 nM solution of Qdot® 605 streptavidin conjugate (Life Technologies) was mixed with a 40-fold molar excess of **22b** in TBS and incubated overnight at 4 °C. Excess unbound **22b** was removed by six 10x dilution/concentration cycles using Amicon Ultra-0.5 mL 30 K filters (Millipore). Subsequently, the solution was diluted to 100 nM and used as a stock solution for subsequent experiments.

2.7. Testing of specific targeting towards prostate cancer cell lines by confocal microscopy

LNCaP and PC-3 cells were grown in 4-Chamber 35 mm Glass Bottom Dishes (In Vitro Scientific). LNCaP cells were grown in RPMI-1640 medium (Sigma–Aldrich) with addition of FBS (final concentration of 10%) while PC3 cells were grown in DMEM-High Glucose medium (GE Healthcare) with addition of L-glutamine (final concentration of 4 mM) and FBS (final concentration of 10%). After two days, the medium was aspirated from all chambers, and cells were washed once with TBS. Afterwards, the 10 nM solution of appropriate Qdot® 605 streptavidin conjugate in TBS was added to each chamber and the live cells were incubated for 15 min at 37 °C. Then, confocal images (pinhole 1 Airy unit) of cells in each chamber were taken with a Zeiss LSM 780 confocal microscope (Carl Zeiss Microscopy) using an oil-immersion objective (Plan-Apochromat 63×/1.40 Oil DIC M27). The fluorescent images were collected at room temperature using 2% of the 405 nm diode laser (max. power 30 mW) for excitation and emission spectral detector in the 578–639 nm range (voltage on detector: 834 V). Simultaneously bright field images were taken using transmission detector (voltage 342 V). All the images were taken using the same settings. The microscope was operated and the images were processed by ZEN 2011 software (Carl Zeiss Microscopy).

3. Experimental section

3.1. Organic synthesis

All chemicals were purchased from Sigma–Aldrich unless otherwise stated. All inhibitors tested in biological assays were purified using preparative scale HPLC with a Waters Delta 600 system (flow rate 7 mL/s, gradient shown for each compound–including ^tR) using a Waters SunFire C18 OBD Prep Column, 5 μm, 19 × 150 mm. The purity of compounds was tested with an analytical Jasco PU-1580 HPLC (flow rate 1 mL/s, invariable gradient: 2–100% ACN in 30 min, ^tR shown for each compound) using a Watrex C18 Analytical Column, 5 μm, 250 × 5 mm. The purity of all tested inhibitors was at least 99%. The structures of inhibitors were further confirmed by HRMS on LTQ Orbitrap XL (Thermo Fisher Scientific) and by NMR (Bruker Avance I™ 500 MHz equipped with Cryoprobe or Bruker Avance I™ 400 MHz).

The general procedure for preparation of *para*-substituted branched inhibitors (shown for the *para*-bromo derivative) is depicted in Scheme 1. Preparation of other inhibitors is described in Supplementary materials.

3.1.1. Compound 21: Di-*tert*-butyl 2-(3-(6-((4-bromobenzyl)amino)-1-(*tert*-butoxy)-1-oxohexan-2-yl)ureido)pentanedioate

Di-*tert*-butyl 2-(3-(6-amino-1-(*tert*-butoxy)-1-oxohexan-2-yl)ureido)pentanedioate (300 mg, 0.615 mmol, 1.0 equiv; prepared as described in[47]) and 120 mg (0.646 mmol, 1.05 equiv) of 4-bromobenzaldehyde were dissolved in 5 mL methanol in a round-bottom flask. Glacial acetic acid (50 μL) was added, and 120 mg (1.85 mmol, 3.0 equiv) of sodium cyanoborohydride were added in one portion with vigorous stirring. After 12 h, the reaction mixture was quenched by addition of 10 mL water. The reaction mixture was further diluted after 10 min with 50 mL water and was extracted with ethyl acetate (EtOAc; 3 × 25 mL). The organic phase was dried and evaporated, and crude product was purified by chromatography on silica (mobile phase: EtOAc + 1% saturated ammonia in water, TLC R_f = 0.55). Pure product was isolated in 48% yield (395 mg). Analytical HPLC (gradient: 2–100% ACN in 30 min) ^tR = 23.4 min. HRMS (ESI+): calculated for $C_{31}H_{51}O_7N_3Br$ $[M]^+$ 656.29049. Found 656.29062. ^{1}H NMR (500 MHz, DMSO-d_6): δ 7.47 (m, 2H, ***m*-Ph**), 7.27 (m, 2H, ***o*-Ph**), 6.29 (d, 1H, J = 8.5 Hz, **HN**-Glu-2), 6.24 (d, 1H, J = 8.4 Hz, **HN**-Lys-2), 4.02 (btd, 1H, J_1 = 8.6, J_2 = 5.1 Hz, **Glu-2**), 3.96 (td, 1H, J_1 = 8.1, J_2 = 5.4 Hz, **Lys-2**), 3.62 (s, 2H, CH_2-Ph), 2.41 (t, 2H, J = 7.1 Hz, **Lys-6**), 2.25 (ddd,1 H, J_1 = 16.6, J_2 = 8.8, J_3 = 6.8 Hz, **Glu-4b**), 2.18 (ddd, 1H, J_1 = 16.6, J_2 = 8.8, J_3 = 6.1 Hz, **Glu-4a**), 1.86 (m, 1H, **Glu-3b**), 1.66 (m, 1H, **Glu-3a**), 1.57 (m, 1H, **Lys-3b**), 1.49 (m, 1H, **Lys-3a**), 1.40 (m, 2H, **Lys-5**), 1.38 (br s, 27 H, (C(CH_3)$_3$), 1.29 (m, 2H, **Lys-4**). ^{13}C NMR (125.7 MHz, DMSO-d_6): δ 172.50 (**Lys-1**), 172.11 (**Glu-1**), 171.63 (**Glu-5**), 157.31 (NH-*CO*-NH), 140.83 (***i*-Ph**), 131.07 (***m*-Ph**), 130.26 (***o*-Ph**), 119.52 (***p*-Ph**), 80.76 (*CH*(CH_3)$_3$), 80.45 (*CH*(CH_3)$_3$), 79.95 (*CH*(CH_3)$_3$), 53.18 (**Lys-2**), 52.38 (CH_2-Ph), 52.36 (**Glu-2**), 48.49 (**Lys-6**), 32.17 (**Lys-3**), 31.07 (**Glu-4**), 29.24 (**Lys-5**), 27.93 (CH(CH_3)$_3$), 27.84 (CH(CH_3)$_3$),27.82 (CH(CH_3)$_3$), 27.77 (**GLu-3**), 23.03 (**Lys-4**).

3.1.2. Compound 22a: 2-(3-(5-(*N*-(4-Bromobenzyl)acetamido)-1-carboxypentyl)ureido)pentanedioic acid

Compound **21** (63 mg, 95.9 μmol, 1.0 equiv) was dissolved in 0.5 mL DMF, and 23 mg (144 μmol, 1.5 equiv) of N-acetoxysuccinimide were added in one portion along with 25 μL (144 μmol,

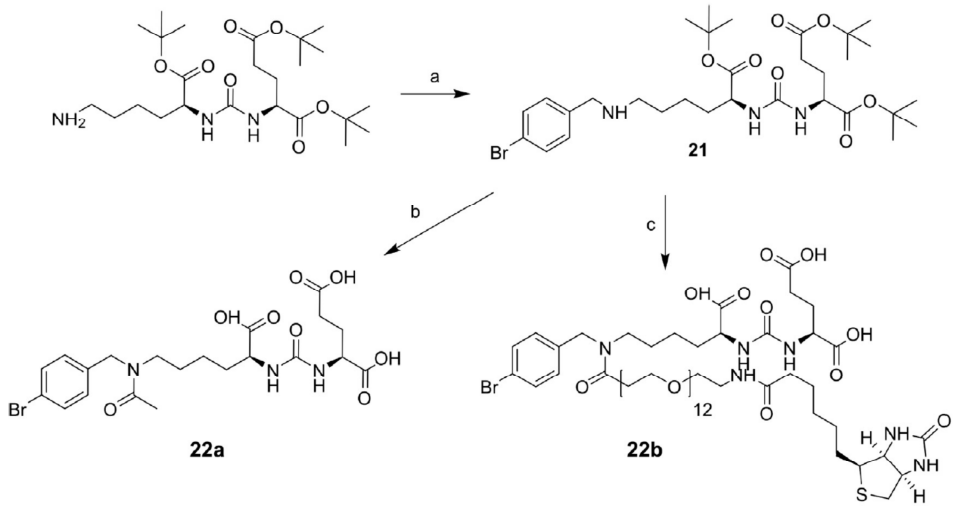

a) 4-bromobenzaldehyde, $NaBH_3CN$, MeOH + 1% AcOH; b) 1) N-acetoxysuccinimide, DIEA, DMF; 2) TFA; c) 1) HOOC-PEG_{12}-Biotin, TBTU, DIEA, DMF; 2) TFA

Scheme 1. Preparation of *para*-bromo substituted branched inhibitor.

1.5 equiv) DIEA. The reaction mixture was stirred at room temperature overnight. All volatiles were removed in vacuum, and the crude product was treated with 0.5 mL TFA, then alternately stirred and sonicated for 15 min. TFA was removed by flow of nitrogen, and the oily product was purified using preparative HPLC (gradient: 15–50% ACN in 60 min, ^tR = 38 min). Sixteen milligrams of product were obtained (isolated yield = 31%). Analytical HPLC (gradient: 2–100% ACN in 30 min) ^tR = 18.0 min. HRMS (ESI+): calculated for $C_{21}H_{29}O_8N_3Br$ $[M]^+$ 530.11325. Found 530.11286. There are two possible rotamers; some atoms give two signals in NMR spectra. In these cases, the two signals are connected with the conjunction and ^{1}H NMR (500 MHz, DMSO-d_6): δ 7.56 and 7.49 (m, 2H, ***m*-Ph**), 7.17 and 7.16 (m, 2H, ***o*-Ph**), 6.37–6.25 (m, 2H, **NH**-Lys-2, **NH**-Glu-2), 4.51 and 4.44–4.43 (s and m, 2H, CH_2-Ph), 4.13–4.00 (m, 2H, **Glu-2**, **Lys-2**), 3.21–3.13 (m, 2H, **Lys-6**), 2.31–2.16 (m, 2H, **Glu-4**), 2.06 and 1.97 (s, 3H, CH_3-CO), 1.96–1.86 (m, 1H, **Glu-3b**), 1.75–1.57 (m, 2H, **Glu-3a**, **lys-3b**), 1.57–1.36 (m, 3H, **Lys-3a**, **Lys-5**), 1.28–1.16 (m, 2H, **Lys-4**). ^{13}C NMR (125.7 MHz, DMSO-d_6): δ 174.72 and 174.68 (**Lys-1**), 174.41 (**Glu-1**), 173.95 (**Glu-5**), 170.07 and 169.90 (CH_3-*CO*), 157.47 (NH-*CO*-NH), 138.12 and 137.64 (***i*-Ph**), 131.77 and 131.42 (***m*-Ph**), 129.97 and 128.98 (***o*-Ph**), 120.37 and 120.13 (***p*-Ph**), 52.39 and 52.24 (**Lys-2**), 51.85 and 51.83 (**Glu-2**), 50.60 and 46.99 (CH_2-Ph), 47.67 and 45.09 (**Lys-6**), 32.00 and 31.97 (**Lys-3**), 30.11 (**Glu-4**), 27.73 (**Glu-3**), 27.69 and 26.89 (**Lys-5**), 22.66 and 22.47 (**Lys-4**), 21.77 and 21.38 (CH_3-CO).

3.1.3. Compound 22b: (3*S*,7*S*)-12-(4-Bromobenzyl)-5,13,54-trioxo-59-((3a*R*,4*R*,6a*S*)-2-oxohexahydro-1*H*-thieno[3,4-*d*]imidazol-4-yl)-17,20,23,26,29,32,35,38,41,44,47,50-dodecaoxa-4,6,12,53-tetraazanonapentacontane-1,3,7-tricarboxylic acid

HOOC-PEG_{12}-biotin (38 mg, 45.7 μmol, 1.0 equiv; IRIS biotech) was dissolved in 0.5 mL DMF, and 16 mg (49.8 μmol, 1.1 equiv) TBTU along with 10 μL DIEA (57.4 μmol, 1.25 equiv) were added. The reaction mixture was stirred for 15 min, and 30 mg (45.7 μmol, 1.0 equiv) of **21** (dissolved in 0.2 mL DMF) was added to the reaction mixture in one portion. The reaction proceeded at room temperature overnight, and the mixture was rotary evaporated to dryness. TFA (0.5 mL) was added, and the reaction mixture was alternately sonicated and stirred for 15 min. TFA was then removed by flow of nitrogen, and the product was purified using preparative HPLC (gradient: 30–80% ACN in 60 min, ^tR = 18 min). Eighteen milligrams of product were obtained (isolated yield = 33%). Analytical HPLC (gradient: 2–100% ACN in 30 min) ^tR = 19.0 min. HRMS (ESI+): calculated for $C_{56}H_{92}O_{22}N_6BrS$ $[M]^+$ 1311.5174. Found 1311.5164.

4. Results

4.1. Effect of -amino group modification and optimization of PEG linker length

First, we prepared several compounds to map the effects of modification at the ε-amine lysine of the inhibitor scaffold Glu-NH-C(O)-NH-Lys (see Fig. 1A). Exchange of a hydrogen atom (**2**) for an acetyl group (**3**) at the ε-amino group resulted in a 2-order-of-magnitude decrease in K_i value (K_i(**2**) = 44.3 ± 2.4 nM vs K_i(**3**) = 0.174 ± 0.033 nM). However, substitution of the acetyl group with a PEG linker with biotin (**4**, **5**) led to major drop in inhibitor potency, showing a negative correlation with the number of PEG units. To determine the minimal length of the PEG linker (necessary to connect GCPII and biotin-binding molecule), we used surface plasmon resonance (SPR) to analyze the ability of these inhibitors, attached via biotin to immobilized neutravidin, to bind GCPII (see Fig. 1B). The difference in association curves as well as saturation signals (4 nm for **5** vs 0.75 nm for **4**) clearly shows that PEG_{12}-biotin but not PEG_8-biotin ensures efficient connection of GCPII and neutravidin.

4.2. Reaching the exosite: Connection of the aromatic moiety to the inhibitor scaffold

To further improve inhibitor potency, we attempted to utilize the previously described 'S1-accessory hydrophobic pocket'.[30] We designed four possible connections of an aromatic moiety, intended to interact with this pocket, to the inhibitor scaffold. First,

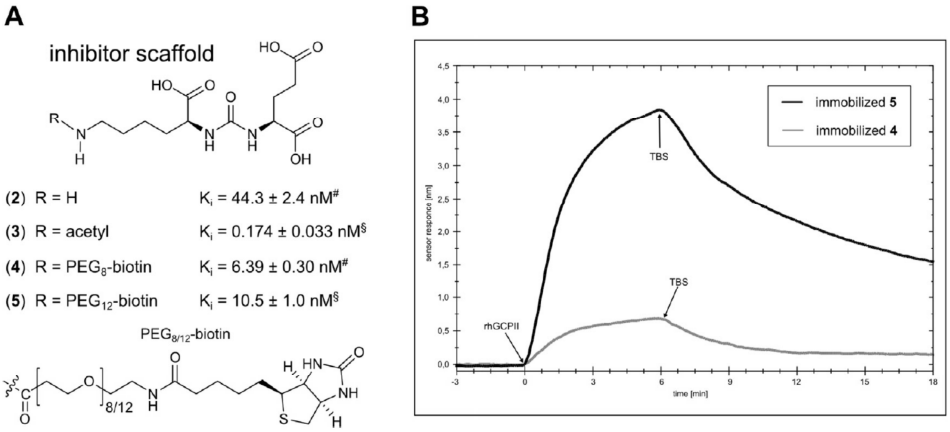

Figure 1. Kinetic characterization of ε-amino group derivatization of the Glu-NH-C(O)-NH-Lys inhibitor scaffold and optimization of the PEG linker length. (A) K_i values for modified inhibitors with acetyl or PEG chains of different lengths. The K_i values are presented as mean ± standard deviation. #measurements performed in duplicate. §measurements performed in at least tetraplicate. (B) Comparison of recombinant human GCPII (rhGCPII) binding to immobilized inhibitors **4** and **5** by surface plasmon resonance (SPR). The inhibitors were immobilized on gold chips via interaction with neutravidin (data not shown). At 0 min, rhGCPII in TBS (29.4 nM) was injected to both flow-channels (association phase), and at 6 min, TBS was applied to both channels to wash out bound rhGCPII molecules (dissociation phase). SPR data were processed by TraceDrawer v.1.5 (Ridgeview Instruments AB).

we tried a branching setup at the ε-amino group, substituting hydrogen atom with a benzyl moiety and the second hydrogen with a linker (acetyl, **15a**, or PEG_{12}-biotin, **15b**). Second, we used a linear setup connecting the aromatic moiety to the inhibitor scaffold via a methylene carbonyl (**9a**, **9b**), amide (**13a**, **13b**), or carbonyl group (**20$_{(H)}$a**, **20$_{(H)}$b**) with the linker (acetyl or PEG_{12}-biotin) emerging from the aromatic ring at the *ortho* position. We compared the K_i values for all these compounds (see Fig. 2). We noted an increase in K_i values when comparing the original acetylated compound (**3**) to acetylated inhibitors containing an aromatic moiety (**9a**, **20$_{(H)}$a**, **13a**, **15a**). On the other hand, when we compared inhibitors with PEG linkers with the original compound with PEG linker (K_i(**5**) = 10.5 ± 1.0 nM), we observed improvements in inhibitor potency when the aromatic moiety is attached in the branched setup (K_i(**15b**) = 3.42 ± 0.47 nM) and in the linear setup connected via amide group (K_i(**13b**) = 7.6 ± 1.2 nM).

4.3. Effect of halogen substitution at the *para* position of the aromatic ring

Based on previously reported data,[32] we investigated the possible effect of introduction of halogen atoms at the *para* position of the aromatic moiety. We prepared and kinetically characterized a panel of halogenated inhibitors with the aromatic moiety linked

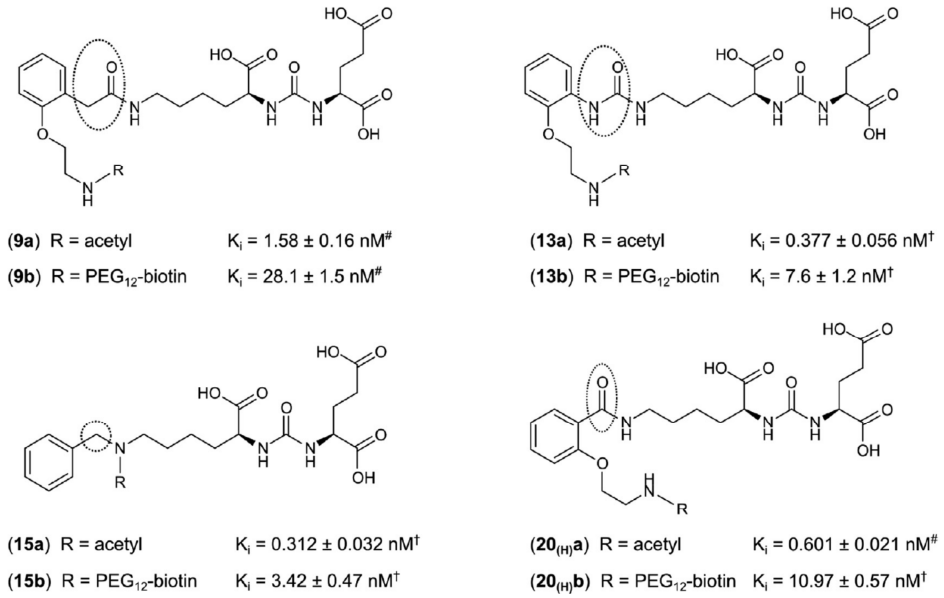

Figure 2. Kinetic characterization of inhibitors with aromatic moieties. Inhibitors with various attachments of an aromatic ring (circled)—methylene carbonyl (**9a**, **9b**), amide (**13a**, **13b**), methylene (**15a**, **15b**), and carbonyl (**20$_{(H)}$a**, **20$_{(H)}$b**) linkers—were synthesized and their K_i values for GCPII determined. The K_i values are presented as mean ± standard deviation. #measurements performed in duplicate. †measurements performed in triplicate. The PEG_{12}-biotin formula is shown in Figure 1.

via a carbonyl group (see Fig. 3). The carbonyl attachment of the aromatic ring was chosen for its synthetic availability. In general, halogen substitution showed a negligible effect on K_i values, with the exception of the bromine derivative. Bromine substitution led to a two-fold increase in inhibitor potency (K_i(**20**$_{(Br)}$**a**) = 0.268 ± 0.060 nM vs K_i(**20**$_{(H)}$**a**) = 0.601 ± 0.021 nM).

Based on these results, we chose the inhibitors with the two most favorable aromatic moiety linkers and modified them by adding a bromine moiety in the *para* position of the aromatic ring (see Fig. 4A). Both inhibitors showed superior inhibition potency compared to their non-halogenated counterparts in both acetylated and PEGylated forms. 4-bromobenzyl modification with branched attachment of PEG_{12}-biotin moieties at the ε-amino group had the lowest K_i value (K_i(**22b**) = 1.570 ± 0.071 nM) of all the PEGylated inhibitors. This combination of the most favorable aromatic moiety connection and halogen derivatization led to a 7-fold improvement in inhibitor potency compared to the lead structure (K_i(**5**) = 10.5 ± 1.0 nM). Additionally, we confirmed the ability of **22b** to mediate the GCPII–neutravidin interaction and determined its association and dissociation rates by SPR, yielding a K_D value of 1.85 ± 0.42 nM (see Fig. 4B).

4.4. Binding modes of inhibitors to GCPII

We determined X-ray structures of GCPII in complex with several inhibitors [**13b** (PDB code 4NGS), **22a** (4NGM), **22b** (4NGQ), **28b** (4NGT), **20**$_{(H)}$**b** (4NGP), **20**$_{(Br)}$**a** (4NGN), and **9b** (4NGR)] to investigate how different connections of aromatic moieties (both unmodified and halogenated) and the presence of the PEG linker influence inhibitor binding into the GCPII substrate binding pocket (for information about data collection and refinement statistics, see Table S1). In all structures, the basic inhibitor scaffold binds into the S1′ and S1 sites as previously described.[30] In general, the accessory tunnel of GCPII exhibited a high degree of flexibility, enabling several modes of inhibitor binding (see Fig. 5A).

Comparison of the structures of GCPII in complex with **22a** and **22b** revealed different binding modes of the 4-bromobenzyl moiety (see Fig. 5B and C). In the case of PEGylated inhibitor **22b**, the 4-bromobenzyl group is located within the arginine patch of GCPII created by arginines 463, 534, and 536. The formation of this cavity is enabled by a 2 Å shift of the Arg463 side chain. The conformation is stabilized by a π–cationic interaction between the guanidinium group of Arg463 and the aromatic ring and also

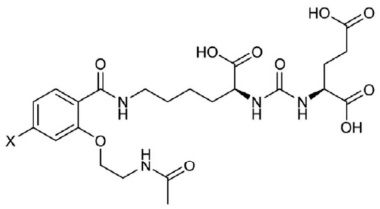

(**20**$_{(H)}$**a**) X = H K_i = 0.601 ± 0.021 nM#
(**20**$_{(F)}$**a**) X = F K_i = 1.012 ± 0.040 nM#
(**20**$_{(Cl)}$**a**) X = Cl K_i = 0.722 ± 0.053 nM#
(**20**$_{(Br)}$**a**) X = Br K_i = 0.268 ± 0.060 nM†
(**20**$_{(I)}$**a**) X = I K_i = 0.600 ± 0.027 nM#

Figure 3. Kinetic characterization of inhibitors with various halogen substitutions at the *para* position of the aromatic ring. The K_i values are presented as mean ± standard deviation. #measurements performed in duplicate. † measurements performed in triplicate.

by hydrogen bonding of the inhibitor's carbonyl linker with Arg463 κ-NH1 (see Fig. 5B). In contrast, the 4-bromobenzyl group of the acetylated inhibitor (**22a**) adopted a different conformation outside the arginine patch. In this case, the 4-bromobenzyl moiety extrudes into accessory tunnel of the GCPII binding site with no obvious interaction with the protein (except a water-mediated hydrogen bond between the inhibitor carbonyl group and ε-O of Gln254). The arginine patch adopts a more energetically favorable conformation in which the guanidinium group of Arg463 interacts with the carboxyl groups of Glu457 and Asp465 (see Fig. 5C).

Structures of GCPII in complex with inhibitors with linearly attached linker moieties (**13b**, **20**$_{(H)}$**b**, **28b**, **20**$_{(Br)}$**a**) revealed that these have a different binding mode than inhibitors with branched attachment of the linker and aromatic moiety (**22a**,**b**). In both acetylated and PEGylated forms, the aromatic moiety did not enter the arginine patch, indicating that the location of the linker connection at the *ortho* position of the aromatic ring likely sterically disables this mode of binding (see Fig. 5A).

PEGylated inhibitors with amide (**13b**, **28b**) and carbonyl (**20**$_{(H)}$**b**) connections showed similar modes of binding to GCPII. The aromatic moieties of these inhibitors were located in the hydrophobic pocket created by the side chains of Trp541 and Phe546. Trp541 and Phe546 are part of the so-called GCPII 'entrance lid', which in these complexes is in closed conformation, enabling the creation of this exosite (see Fig. 5D). Addition of bromine (**28b**) led to slight movement of the aromatic ring towards the protein backbone. This inhibitor was found in two different conformations. These conformations were stabilized either by π–cationic interaction of the 4-bromobenzyl moiety with the guanidinium group of Arg463 and bromine ionic interaction with a sodium cation (**28b**–cyan) or by interaction of bromine with the carbonyl oxygen of Lys539 by halogen bond and with γ-O of Thr538 by hydrogen bond (**28b**–green) (see Fig. 5E).[48] In the case of PEGylated inhibitor with methylene carbonyl connection of the aromatic ring (**9b**), the electron density for the aromatic moiety was not visible in the structure, suggesting that this moiety is not bound in one stable conformation (data not shown). This observation might explain the lower inhibition potency we observed for inhibitors with methylene carbonyl connections.

The structure of GCPII in complex with **20**$_{(Br)}$**a** (**20**$_{(H)}$**a** modified with bromine in the *para* position) revealed yet another conformation of the aromatic moiety. The 'entrance lid' in this structure is highly disordered, and the inhibitor position is stabilized by bromine interactions with water molecules and by a hydrogen bond between the inhibitor's terminal carbonyl group and the Tyr234 hydroxyl group (data not shown).

4.5. Visualization of GCPII on cancer cells using specific nanocarriers

We prepared GCPII-specific nanocarriers from commercially available Qdot® 605 streptavidin conjugate and **22b**. As shown in Figure 6, such nanoparticles specifically recognized LNCaP cells (endogenously expressing GCPII) and not PC-3 cells (lacking GCPII expression). Additionally, Qdots without **22b** bound to neither LNCaP nor PC-3 cells. These results support the concept that a small-molecule GCPII inhibitor could be used for nanoparticle targeting and visualization of GCPII-positive cells.

5. Discussion

We set out to develop low-molecular weight inhibitor of GCPII as a molecular recognition tag suitable for facile modification of various nanoparticles through well-established biotin–avidin

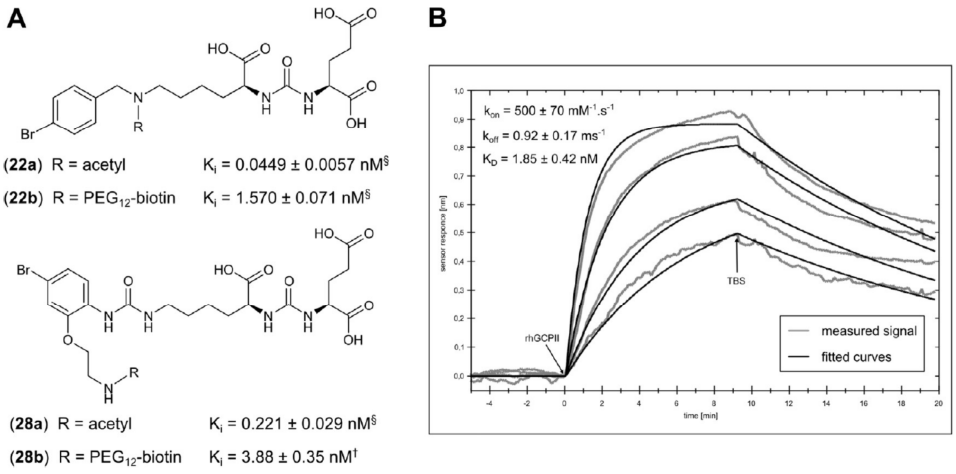

Figure 4. Kinetic characterization of two inhibitors with different connections of the 4-bromobenzyl moiety. (A) A branched connection or linear connection via amide linker and bromine placed in the *para* position of the aromatic ring showed a synergic effect and provided the tightest binding inhibitors in the panel studied. The K_i values are presented as mean ± standard deviation. †measurements performed in triplicate. §measurements performed in at least tetraplicate. The PEG_{12}-biotin formula is shown in Figure 1. (B) Kinetic characterization of the neutravidin–rhGCPII interaction mediated by inhibitor **22b** measured by surface plasmon resonance (SPR). Compound **22b** was immobilized on a gold chip via its interaction with neutravidin (data not shown). At 0 min, four samples with different rhGCPII concentrations (3.675 nM, 7.35 nM, 14.7 nM, and 29.4 nM) were injected into 4 different flow-channels (association phase), and after 9 min, TBS was applied to all channels to wash out bound rhGCPII molecules (dissociation phase). Values of association (k_{on}) and dissociation (k_{off}) rates displayed here were obtained by fitting four independent measurements using TraceDrawer v.1.5 (Ridgeview Instruments AB) and represent mean ± standard deviation. The dissociation constant (K_D) was calculated from k_{on} and k_{off}. For visual clarity, one representative example of this kinetic measurement is presented.

interaction. We performed structure-assisted design of this tag in order to maximize its affinity towards GCPII upon binding to the nanoparticle.

First, we mapped the effects of modifying our inhibitor scaffold, Glu-NH-C(O)-NH-Lys (**2**), at the lysine ε-amino group. Acetylation of the amine led to a major improvement in inhibitor potency, confirming the fact that GCPII does not favor positively charged amino acids in the P1 and P1′ positions.[34] In agreement with the findings of Zhang et al.,[49] we observed a drop in inhibitory activity after addition of a PEG linker (in proportion to the number of PEG units). Most likely, the long disordered PEG chain entropically disfavors inhibitor binding to GCPII. We attempted to reduce the negative effect of the PEG chain linker by shortening it to a minimal length. It has already been shown that 12 PEG units are sufficient and 4 PEG units are insufficient for interaction of GCPII with streptavidin.[17,33] In this work, we found out that even 8 PEG units in the linker chain are insufficient to mediate proper connection of GCPII and the biotin-binding molecule.

To further improve inhibitor potency, we attempted to utilize the 'S1-accessory hydrophobic pocket'.[30] We chose two different approaches (branched and linear) to introduce an aromatic moiety and PEG linker or acetyl moiety into the inhibitor molecule. In the linear setup, we chose 3 different moieties to link the aromatic ring with the inhibitor scaffold. These moieties differ in length (1 atom for the carbonyl vs 2 atoms for the amide and methylene carbonyl moieties), rigidity (planar carbonyl and amide vs methylene carbonyl), and hybridization. Amide attachment of the aromatic ring yielded inhibitors (acetylated and PEGylated) with the best potencies, showing that 2 atoms and a more rigid linker improves inhibitor potency (additionally, the nitrogen atom may participate in hydrogen bonding). This observation is in agreement with previously published data.[32] The PEG linker was attached to the *ortho* position of the aromatic moiety. We chose the *ortho* position based on visual examination of the published crystal structure of GCPII in complex with the inhibitor DCIBzL (PDB entry 3D7H).[30]

Halogen bonds are increasingly recognized as important contributors to the specific binding of drug-like molecules to their targets.[50,51] Maresca et al. showed that halogen substitution on the aromatic ring in urea-based inhibitors can lead to significant improvement of inhibitor potency.[32] Therefore, we prepared inhibitors with the aromatic ring modified in the *para* position with halogen atoms (for ease of synthesis, we decided to initially test the hypothesis with $\mathbf{20}_{(H)}\mathbf{a}$). Modification with bromine ($\mathbf{20}_{(Br)}\mathbf{a}$) gave the best results, suggesting that the positive effect of a halogen atom on inhibitor potency is spatially restricted. Even though the results from crystallographic studies showed quite different binding modes for $\mathbf{20}_{(Br)}\mathbf{a}$ compared to **22a**, **22b**, and **28b**, we also observed a positive effect of bromine addition to the aromatic ring for the latter compounds, suggesting that the effect of this substitution is generally applicable. Bromine substitutions could therefore be utilized in future design of GCPII inhibitors with similar scaffolds.

The X-ray structures of GCPII in complex with various inhibitors revealed that the aromatic moiety was targeted inside the arginine patch in only one case (**22b**). This inhibitor showed the best inhibitory activity among the PEGylated inhibitors. The acetylated form of this inhibitor (**22a**) had the lowest K_i value of all inhibitors tested. The 4-bromobenzyl moiety of **22a** does not bind inside the arginine patch, as aimed for, but protrudes into the wide accessory tunnel. The reason for this binding mode may be the fact that the opening of the arginine patch requires repositioning of the Arg463 side chain, which is typically strongly coordinated with the Glu457 and Asp465 side chains. Moreover, the 4-bromobenzyl moiety displaces several water molecules that would otherwise be strongly coordinated in the accessory tunnel, making this conformation entropically more favorable. In the case of **22b**, the long PEG chain forbids such a conformation (the acetyl moiety of **22a** points inside the accessory binding tunnel), and therefore, the 4-bromobenzyl moiety adopts another energetically favorable position—inside the arginine patch.

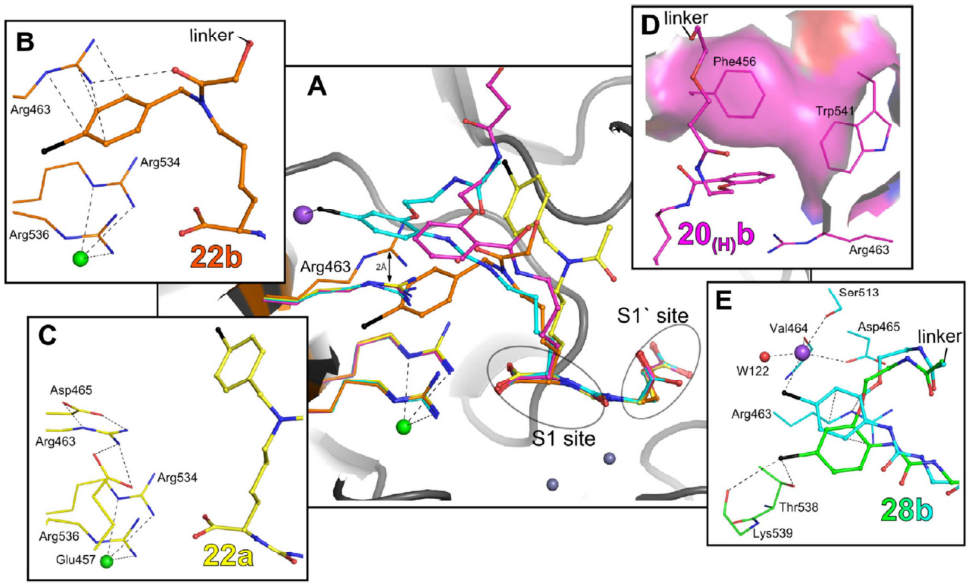

Figure 5. Structural analysis of several inhibitors binding into the GCPII active site. The backbone of GCPII is depicted in cartoon representation in gray. Interacting amino acid side chains are shown as lines, and inhibitor molecules are in ball-and-stick representation. The carbon atoms of interacting amino acid side chains and the inhibitor molecules are colored orange (**22b**), yellow (**22a**), magenta (**20$_{(H)}$b**), and cyan/green (**28b**). Oxygen atoms are depicted in red, nitrogen atoms in blue, and bromine atoms in black. Zinc ions are shown as gray spheres, chlorine ions as green spheres, sodium ions as a violet spheres, and water molecule as a red sphere. (A) An overlay of the crystal structures of inhibitors **22a**, **22b**, **20$_{(H)}$b**, and **28b** in complex with GCPII and their different binding modes into the accessory binding tunnel. The major conformational shift of the Arg463 side chain is indicated with a black arrow. The gray circles highlight the S1 and S1′ binding sites of the inhibitor molecules. For clarity, only one conformation of GCPII in complex with **28b** is shown (cyan). (B) The bromobenzyl group of **22b** is bound within the arginine patch and stabilized by π–cationic interaction with the Arg463 guanidinium group and by hydrogen bonding between κ-NH of Arg463 and the carbonyl oxygen of the inhibitor molecule. (C) The bromobenzyl moiety of **22a** is bound outside the arginine patch, which is in closed conformation with the Arg463 side chain stabilized by hydrogen bonding with the Glu457 and Asp465 carboxyl groups. (D) Binding of the **20$_{(H)}$b** aromatic moiety into the GCPII hydrophobic pocket created by the Phe546 and Trp541 side chains. The GCPII 'entrance lid' (Trp541-Gly548) adopts a closed conformation, enabling formation of this hydrophobic pocket. (E) Inhibitor **28b** was found in two different conformations (the inhibitor molecule, together with interacting amino acids, is depicted in cyan and green). In one conformation (cyan), the aromatic moiety is moved above the Arg463 side chain and stabilized by π–cationic interaction with its guanidinium group, and in addition, the bromine atom interacts with a sodium ion. The second conformation (green) is stabilized by bromine interaction with the Lys539 carbonyl oxygen of the protein backbone and with the hydroxyl group of the Thr538 side chain. In both conformations, the GCPII 'entrance lid' is in closed conformation, enabling additional stabilization by hydrophobic interactions of the aromatic ring with the side chains of Phe546 and Trp541 (not shown). Only the part of the inhibitor molecule for which the electron density could be mapped is shown in B, D, and E. The PEG chain is depicted schematically as 'linker'. The pictures were processed with PyMOL Molecular Graphics System, Version 1.3.0 Schrödinger, LLCPyMOL. (color reproduction in print).

Even though inhibitors with the PEG linker emerging from the aromatic ring (**9b**, **13b**, **20$_{(H)}$b**, **28b**) do not utilize the arginine patch, the most promising one (**28b**) possesses significantly more potent inhibitory activity than the lead structure (**5**). With the exception of **9b**, the electron density for the aromatic ring was visible in all the crystal structures. Generally, the binding mode of the aromatic moiety is mediated through the highly flexible GCPII 'entrance lid' (Trp541–Gly548), which in closed conformation creates a hydrophobic binding pocket for the inhibitor aromatic moiety, which can be stabilized by the side chains of Trp541 and Phe546. This observation is supported by the fact that, in structures with clearly defined electron density for the aromatic moiety (**13b**, **20$_{(H)}$b**, **28b**), the 'entrance lid' is found in closed conformation, while in the structure with poorly defined electron density of the aromatic moiety (**9b**), it adopts the open conformation. It should be noted that in all structures except the complex with **20$_{(H)}$b** the 'entrance lid' is highly flexible with high B factors and poor electron density maps of amino acid side chains. The various binding modes of the inhibitors studied clearly show and confirm the ability of the GCPII accessory binding tunnel (mainly the 'entrance lid') to adopt diverse conformations and thus form various transient exosites.

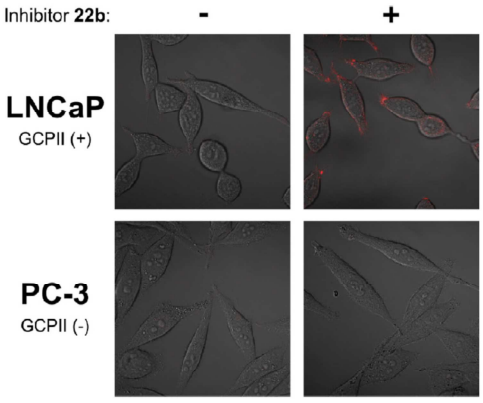

Figure 6. Confocal images of LNCaP and PC-3 cells treated with Qdot® 605 streptavidin conjugate (red color in the picture) with **22b** to visualize GCPII. Cells were treated with Qdots with or without bound inhibitor **22b** for 15 min. Confocal images were merged with bright field images and processed using ZEN 2011 software. All images were taken in the same microscope set-up. For more details, see the Section 3. (color reproduction in print).

Finally, we conducted a proof-of-concept experiment showing that small molecules can be used for nanoparticle targeting. We prepared GCPII-specific nanoparticles bearing the novel inhibitor **22b** as a homing device. We chose Qdot® 605 streptavidin conjugate for its commercial availability. After conjugation with **22b**, the nanoparticles were able to specifically bind GCPII. These nanoparticles specifically recognized GCPII on the surface of

prostate cancer cell lines endogenously expressing GCPII (LNCaP cells) and did not bind to a prostate cancer cell line that lacks GCPII expression (PC-3 cells; compare Fig. 6). This simple experiment confirms our initial assumption that our engineered inhibitors can function as simple GCPII-specific homing devices for nanoparticles.

Generally, nanoparticles using the inhibitors as specific targeting moieties will face the similar problem of cross-reactivity as the antibodies. For antibodies, the similarity of primary and secondary structures predetermines a possible cross-reactivity of their original antigen while in the case of inhibitor-guided nanoparticles, a substrate specificity will play a key role in assessing the possible cross-reactivities. In this particular case, we can expect that the close GCPII homologs which were shown to possess similar enzymatic activity (e.g., mouse GCPII (Knedlik et al. manuscript in preparation) or human GCPIII[52]) will most probably be also recognized by our engineered nanoparticles. On the other hand, even though the homologs have the same substrate binding side, they may differ slightly in the conformation of their exosites. Therefore by further fine-tuning of human GCPII specific inhibitors we may likely also diminish their cross-reactivity towards GCPII homologs.

The aim of this study, preparation of a more potent inhibitor that could utilize the arginine patch of GCPII and also enable functional connection of GCPII to a biotin-binding molecule, was successful. The final inhibitor **22b** possesses 7-fold greater inhibitory potency than the starting inhibitor **5**. Even though a 7-fold improvement in inhibitory activity may seem small, these types of inhibitors are intended to be used as part of a larger complex (e.g., nanoparticles) to ensure the specificity of the complex for its target (in this case, GCPII). Ideally, such a complex will contain more than one inhibitor molecule. In this scenario, due to the multiple binding effects, the final inhibitory potency of the complex is likely to be significantly higher than that of the inhibitor itself. Therefore, it can be expected that even a minor improvement in the small-molecule inhibitor's potency will lead to more significant improvement in the overall binding of the final complex.

6. Conclusion

We have prepared a series of GCPII inhibitors enabling effective connection of this molecule to any biotin-binding protein or nanoparticle. Through SAR study of the distal part of inhibitor we improved its affinity towards GCPII. The X-ray structure analysis showed that the accessory binding tunnel of GCPII is very flexible and is able to adopt several different conformations, thus creating various exosites that can bind the distal part of the inhibitor molecule. Finally, we successfully tested the ability of our designed inhibitor to effectively modified biotin-binding nanoparticle (Qdot) and function there as GCPII specific anchor.

Acknowledgments

The authors would like to thank Jana Starková and Karolína Šrámková for expert technical help and Hillary Hoffman for language editing. We also acknowledge the Ministry of Education of the Czech Republic, Grant no. P208-12-G016 (Center of Excellence) and OPPK Project CZ.2.16/3.1.00/24016 for financial support.

Supplementary data

Supplementary data associated with this article can be found, in the online version, at http://dx.doi.org/10.1016/j.bmc.2014.05.061. These data include MOL files and InChiKeys of the most important compounds described in this article.

References and notes

1. Siegel, R.; Naishadham, D.; Jemal, A. *J. Clin.* **2012**, *62*, 10.
2. Foss, C. A.; Mease, R. C.; Cho, S. Y.; Kim, H. J.; Pomper, M. G. *Curr. Med. Chem.* **2012**, *19*, 1346.
3. Ghosh, A.; Heston, W. D. W. *J. Cell. Biochem.* **2004**, *91*, 528.
4. Robinson, M. B.; Blakely, R. D.; Couto, R.; Coyle, J. T. *J. Biol. Chem.* **1987**, *262*, 14498.
5. Pinto, J. T.; Suffoletto, B. P.; Berzin, T. M.; Qiao, C. H.; Lin, S. L.; Tong, W. P.; May, F.; Mukherjee, B.; Heston, W. D. W. *Clin. Cancer Res.* **1996**, *2*, 1445.
6. Mhawech-Fauceglia, P.; Zhang, S.; Terracciano, L.; Sauter, G.; Chadhuri, A.; Herrmann, F. R.; Penetrante, R. *Histopathology* **2007**, *50*, 472.
7. Haffner, M. C.; Kronberger, I. E.; Ross, J. S.; Sheehan, C. E.; Zitt, M.; Muhlmann, G.; Ofner, D.; Zelger, B.; Ensinger, C.; Yang, X. M. J.; Geley, S.; Margreiter, R.; Bander, N. H. *Hum. Pathol.* **2009**, *40*, 1754.
8. Liu, H.; Rajasekaran, A. K.; Moy, P.; Xia, Y.; Kim, S.; Navarro, V.; Rahmati, R.; Bander, N. H. *Cancer Res.* **1998**, *58*, 4055.
9. Hinkle, G. H.; Burgers, J. K.; Neal, C. E.; Texter, J. H.; Kahn, D.; Williams, R. D.; Maguire, R.; Rogers, B.; Olsen, J. O.; Badalament, R. A. *Cancer* **1998**, *83*, 739.
10. Barinka, C.; Rojas, C.; Slusher, B.; Pomper, M. *Curr. Med. Chem.* **2012**, *19*, 856.
11. Mease, R. C.; Foss, C. A.; Pomper, M. G. *Curr. Top. Med. Chem.* **2013**, *13*, 951.
12. Tagawa, S. T.; Akhtar, N. H.; Nikolopoulou, A.; Kaur, G.; Robinson, B.; Kahn, R.; Vallabhajosula, S.; Goldsmith, S. J.; Nanus, D. M.; Bander, N. H. *Front Oncol.* **2013**, *3*, 214.
13. Chen, Y.; Pullambhatla, M.; Banerjee, S. R.; Byun, Y.; Stathis, M.; Rojas, C.; Slusher, B. S.; Mease, R. C.; Pomper, M. G. *Bioconjug. Chem.* **2012**, *23*, 2377.
14. Kovar, J. L.; Cheung, L. L.; Simpson, M. A.; Olive, D. M. *Prostate Cancer* **2014**, *2014*, 104248.
15. Sanna, V.; Sechi, M. *Maturitas* **2012**, *73*, 27.
16. Javier, D. J.; Nitin, N.; Levy, M.; Ellington, A.; Richards-Kortum, R. *Bioconjug. Chem.* **2008**, *19*, 1309.
17. Kasten, B. B.; Liu, T.; Nedrow-Byers, J. R.; Benny, P. D.; Berkman, C. E. *Bioorg. Med. Chem. Lett.* **2013**, *23*, 565.
18. Chen, Z.; Penet, M. F.; Nimmagadda, S.; Li, C.; Banerjee, S. R.; Winnard, P. T., Jr.; Artemov, D.; Glunde, K.; Pomper, M. G.; Bhujwalla, Z. M. *ACS Nano* **2012**, *6*, 7752.
19. Hrkach, J.; Von Hoff, D.; Mukkaram Ali, M.; Andrianova, E.; Auer, J.; Campbell, T.; De Witt, D.; Figa, M.; Figueiredo, M.; Horhota, A.; Low, S.; McDonnell, K.; Peeke, E.; Retnarajan, B.; Sabnis, A.; Schnipper, E.; Song, J. J.; Song, Y. H.; Summa, J.; Tompsett, D.; Troiano, G.; Van Geen Hoven, T.; Wright, J.; LoRusso, P.; Kantoff, P. W.; Bander, N. H.; Sweeney, C.; Farokhzad, O. C.; Langer, R.; Zale, S. *Sci. Transl. Med.* **2012**, *4*, 128ra39.
20. Liu, J.; Kopeckova, P.; Buhler, P.; Wolf, P.; Pan, H.; Bauer, H.; Elsasser-Beile, U.; Kopecek, J. *Mol. Pharm.* **2009**, *6*, 959.
21. Xu, W.; Siddiqui, I. A.; Nihal, M.; Pilla, S.; Rosenthal, K.; Mukhtar, H.; Gong, S. *Biomaterials* **2013**, *34*, 5244.
22. Schol, D.; Fleron, M.; Greisch, J. F.; Jaeger, M.; Frenz, M.; De Pauw, E.; De Pauw-Gillet, M. C. *Micron* **2013**, *50*, 68.
23. Wang, L.; Li, L.; Guo, Y.; Tong, H.; Fan, X.; Ding, J.; Huang, H. *Prostate* **2013**, *73*, 1147.
24. Imai, K.; Takaoka, A. *Nat. Rev. Cancer* **2006**, *6*, 714.
25. Jackson, P. F.; Cole, D. C.; Slusher, B. S.; Stetz, S. L.; Ross, L. E.; Donzanti, B. A.; Trainor, D. A. *J. Med. Chem.* **1996**, *39*, 619.
26. Majer, P.; Jackson, P. F.; Delahanty, G.; Grella, B. S.; Ko, Y. S.; Li, W.; Liu, Q.; Maclin, K. M.; Polakova, J.; Shaffer, K. A.; Stoermer, D.; Vitharana, D.; Wang, E. Y.; Zakrzewski, A.; Rojas, C.; Slusher, B. S.; Wozniak, K. M.; Burak, E.; Limsakun, T.; Tsukamoto, T. *J. Med. Chem.* **2003**, *46*, 1989.
27. Kozikowski, A. P.; Nan, F.; Conti, P.; Zhang, J.; Ramadan, E.; Bzdega, T.; Wroblewska, B.; Neale, J. H.; Pshenichkin, S.; Wroblewski, J. T. *J. Med. Chem.* **2001**, *44*, 298.
28. Ferraris, D. V.; Shukla, K.; Tsukamoto, T. *Curr. Med. Chem.* **2012**, *19*, 1282.
29. Pavlicek, J.; Ptacek, J.; Barinka, C. *Curr. Med. Chem.* **2012**, *19*, 1300.
30. Barinka, C.; Byun, Y.; Dusich, C. L.; Banerjee, S. R.; Chen, Y.; Castanares, M.; Kozikowski, A. P.; Mease, R. C.; Pomper, M. G.; Lubkowski, J. *J. Med. Chem.* **2008**, *51*, 7737.
31. Wang, H.; Byun, Y.; Barinka, C.; Pullambhatla, M.; Bhang, H. E.; Fox, J. J.; Lubkowski, J.; Mease, R. C.; Pomper, M. G. *Bioorg. Med. Chem. Lett.* **2010**, *20*, 392.
32. Maresca, K. P.; Hillier, S. M.; Femia, F. J.; Keith, D.; Barone, C.; Joyal, J. L.; Zimmerman, C. N.; Kozikowski, A. P.; Barrett, J. A.; Eckelman, W. C.; Babich, J. W. *J. Med. Chem.* **2009**, *52*, 347.
33. Liu, T.; Nedrow-Byers, J. R.; Hopkins, M. R.; Wu, L. Y.; Lee, J.; Reilly, P. T.; Berkman, C. E. *Bioorg. Med. Chem. Lett.* **2012**, *22*, 3931.
34. Barinka, C.; Rinnova, M.; Sacha, P.; Rojas, C.; Majer, P.; Slusher, B. S.; Konvalinka, J. *J. Neurochem.* **2002**, *80*, 477.
35. Tykvart, J.; Sacha, P.; Barinka, C.; Knedlik, T.; Starkova, J.; Lubkowski, J.; Konvalinka, J. *Protein Expr. Purif.* **2012**, *82*, 106.
36. Cheng, Y.; Prusoff, W. H. *Biochem. Pharmacol.* **1973**, *22*, 3099.
37. Hegnerova, K.; Bockova, M.; Vaisocherova, H.; Kristofikova, Z.; Ricny, J.; Ripova, D.; Homola, J. *Sens. Actuat. B-Chem.* **2009**, *139*, 69.
38. Pimkova, K.; Bockova, M.; Hegnerova, K.; Suttnar, J.; Cermak, J.; Homola, J.; Dyr, J. E. *Anal. Bioanal. Chem.* **2012**, *402*, 381.
39. Mueller, U.; Darowski, N.; Fuchs, M. R.; Forster, R.; Hellmig, M.; Paithankar, K. S.; Puhringer, S.; Steffien, M.; Zocher, G.; Weiss, M. S. *J. Synchrotron Radiat.* **2012**, *19*, 442.
40. Kabsch, W. *Acta Crystallogr. Sect. D Biol. Crystallogr.* **2010**, *66*, 125.

41. Krug, M.; Weiss, M. S.; Heinemann, U.; Mueller, U. *J. Appl. Crystallogr.* **2012**, *45*, 568.
42. Vagin, A.; Teplyakov, A. *Acta Crystallogr. D Biol. Crystallogr.* **2000**, *56*, 1622.
43. Bailey, S. *Acta Crystallogr. Sect. D Biol. Crystallogr.* **1994**, *50*, 760.
44. Barinka, C.; Rovenska, M.; Mlcochova, P.; Hlouchova, K.; Plechanovova, A.; Majer, P.; Tsukamoto, T.; Slusher, B. S.; Konvalinka, J.; Lubkowski, J. *J. Med. Chem.* **2007**, *50*, 3267.
45. Murshudov, G. N.; Skubak, P.; Lebedev, A. A.; Pannu, N. S.; Steiner, R. A.; Nicholls, R. A.; Winn, M. D.; Long, F.; Vagin, A. A. *Acta Crystallogr. Sect. D Biol. Crystallogr.* **2011**, *67*, 355.
46. Emsley, P.; Lohkamp, B.; Scott, W. G.; Cowtan, K. *Acta Crystallogr. Sect. D Biol. Crystallogr.* **2010**, *66*, 486.
47. Murelli, R. P.; Zhang, A. X.; Michel, J.; Jorgensen, W. L.; Spiegel, D. A. *J. Am. Chem. Soc.* **2009**, *131*, 17090.
48. Wilcken, R.; Zimmermann, M. O.; Lange, A.; Zahn, S.; Boeckler, F. M. *J. Comput. Aided Mol. Des.* **2012**, *26*, 935.
49. Zhang, A. X.; Murelli, R. P.; Barinka, C.; Michel, J.; Cocleaza, A.; Jorgensen, W. L.; Lubkowski, J.; Spiegel, D. A. *J. Am. Chem. Soc.* **2010**, *132*, 12711.
50. Hernandes, M. Z.; Cavalcanti, S. M.; Moreira, D. R.; De Azevedo Junior, W. F.; Leite, A. C. *Curr. Drug Targets* **2010**, *11*, 303.
51. Lu, Y.; Wang, Y.; Zhu, W. *Phys. Chem. Chem. Phys.* **2010**, *12*, 4543.
52. Hlouchova, K.; Barinka, C.; Klusak, V.; Sacha, P.; Mlcochova, P.; Majer, P.; Rulisek, L.; Konvalinka, J. *J. Neurochem.* **2007**, *101*, 682.

6 Discussion and Conclusion

HIV PR is still, even 25 years of its discovery and thousands of published papers, an interesting target for studies for both scientists and pharmaceutical companies. One of the reasons why the HIV PR is still in the spotlight of the scientists are the ever emerging drug resistances against the FDA approved PIs. The resistances are already spreading between the infected patients and will become more and more common. Therefore, the need for yet new generation of PIs combating these resistant strains will be growing. Another major reason for the need to identify new PIs is the seriousness of the side effects of the currently used medicine. The side effects occur more often than we would like to hear, and are decreasing the already surprisingly bad adherence of the patients to the medication. The bad adherence of the patients is creating a natural selection funnel for the mutated proteases, and this accelerates the foredescribed emergence of resistant strains. Secondly, even though the field of HIV PR has been studied thoroughly, we are still not sure how the enzyme exactly works. We do know it cleaves the polyprotein chains Gag and Gag-Pol into the functional proteins, and we know that both premature activations and inhibition of the enzymatic activity is detrimental for the virus. The question of how strictly time-regulated the process is arises immediately. Would it be possible to obtain fully mature virions if the protease was activated after the virus fully buds from the cell? Or is it more strictly controlled and does the protease have to start cleaving the polyprotein chains already at the site of the plasma membrane concomitantly to the budding process?

To answer the need of the novel PI scaffold we published a paper identifying novel class of PIs inhibitors - dibenzodiazepines. Benzodiazepines played an important role in the history during the development of various pharmaceutics. Originally the diazepines were used predominantly as compounds regulating the functions of the central nervous system. However, because their scaffold proved to be extremely well drugable, mainly because of its oral bioavailability, non-toxicity and over all good pharmocokinetic properties, the class spread across the medicinal field. Therefore we concluded that this new class of PIs is exceptionally interesting. The parental compound identified from the library screening was found to be occupying the active site of the HIV PR twice and this led us to the development of dimeric compounds which bind to the PR with stronger affinity (increase of activity by two orders of magnitude). We determined the binding mode of this new class of dimeric inhibitors to the active site of the PR and thus enabling further possible structure activity relationship studies, which could further potentiate the activity of the PIs. We have also reduced the

number of stereogenic centers from the original four to two, without any loss of activity, making the molecule synthetically more approachable. The most striking feature of this class of inhibitors is the innovative inhibitor core responsible for interaction with the catalytic aspartates. In the introductory part a special stress was put on various moieties used during the PIs development as potential interaction partners with the catalytic aspartates (chapter 3.1.8.2). The oxalyl linker was calculated to form strong hydrogen bonding and therefore present a new class of interacting partners with the protease core.

Subsequent studies, which were not presented in the paper, were focused to improve the preposterous insolubility of this new class of inhibitors. Unfortunately, we found out a strong negative correlation between the activity of the compounds and their solubility. This suggests that the formation of the PI-protease complex is mostly entropically driven, a quality which is rather unfavourable, and therefore further development of the new class of inhibitors was discontinued.

To address the more fascinating question concerning HIV PR, specifically the precise timing and enzymatic dynamics of polyprotein chain cleavage inside the virions we developed a novel tool how to synchronize the viral replication in the culture – namely a protease inhibitor which gets degraded at a define moment resulting in an activation of HIV PR. Two various approaches were considered, a photodegradable inhibitor and thermo-labile inhibitor. Because of the wealth accumulated in the literature concerning the photolabile moieties we set out this way.

The design and synthesis of the photodestructable inhibitor of HIV PR was a stepwise process with many dead ends along the way. The breaking point decision worth mentioning is probably the decision behind the use of photolabile 7-diethylamino-4-(hydroxymethyl) coumarin group. The number of identified groups which are able to break bond and release a target molecule is immense. However, only few of them fulfill the requirements we had. The major issue in development of the photolabile inhibitor was the yield of the photodegradation. In most of the biologically related published papers the effector molecule is caged, preventing it from its function. The photocleavage leads to release of the molecule and therefore the cleavage effectivity is not much of a concern in most of the cases, since the authors do not care if 50 % of the compound remains caged. Our situation was exactly the opposite, since we needed the yield of the inhibitor degradation to reach at least 98 %, because even 5 % of non-broken tight binding inhibitor would completely block the enzymatic activity. Another concern was the absorption wavelength of the moiety, which had to be as much red-shifted as

possible, not to damage the viral particles. Unfortunately, the red-shift correlates strongly with the number of double bonds in conjugation and/or aromatic moieties present and therefore also correlates with the size of the photolabile group as well as its insolubility. If the photolabile group was too large, HIV PR would not be able to accommodate it inside the catalytic site at the first place and the molecule would not inhibit the activity. At the end, two possible moieties were picked, *o*-nitrobenzyl derivatives and coumarine derivatives, out of which the coumarine inhibitor proved to be superior in both potency and ability to be destroyed by light.

Surprisingly, the photodegradation of the final inhibitor leads to a four order of magnitude loss of its activity, which is unprecedented in the literature (the only other known photolabile inhibitor in literature increases its K_i value by 50 fold).[181] We tried to address this exceptional loss of activity by structural studies. The inhibitor, unlike its degradation product, has a carbamate moiety between the P2 and P3 site of the inhibitor, which forms a strong hydrogen bond to the aspartate in position 29. This solely probably would not amount for the difference, which is further potentiated by the fact that the degradation product has a charged terminal amine. This positively charged amine moiety is probably strongly repelled from the active site, since charged residues are extremely unfavourable in the S2 sub-site of the enzyme.

The inhibitor was further shown to work as a photocage for the HIV PR even in the cell culture studies, which was demonstrated by the observation of the polyprotein processing in the virus-producing culture. After the irradiation, the Gag polyprotein was cleaved down to its functional proteins with half-life of 20-30 minutes. Even though this may seem like a long time for simple enzymatic peptide bond cleavage, one should consider several factors which are slowing down the process dramatically. The HIV PR is by itself still in form of a polyprotein chain (Gag-Pol), and has to form the enzymatically-active form by dimerization of the two long polyproteins, which further has to cleave out itself or cleave a third polyprotein. Either way, this process will be much slower, than the process we are observing with the purified HIV PR in the test tube. Furthermore, the concentration of the proteins is probably so high, that any dissociation will be also slowed, not to mention that the pH inside the virus could be also shifted from the pH optimum of the enzyme.

Even though the Gag processing is an important parameter that needed to be checked in the pilot studies, it will be needed in the future to analyze the viral infectivity, because this criterion directly correlates with the maturation process. If one does not regain infectivity, even though the Gag was fully processed, it will be needed to analyze also Gag-Pol

processing and subsequently the structure of the virus particles under cryo EM. These experiments will then finally shed the light on this topic.

As has been extensively reviewed in the second part of the introductory section, GCPII is a highly relevant pharmacological target mostly in respect toward the prostate carcinoma (PCa) diagnosis and its possible therapy. The small inhibitory molecules play relatively small part in the big picture of potential PCa therapeutics, being pushed out mostly by monoclonal antibodies and other analogous carriers such as aptamers. This is mostly because of the rapid clearance of the compounds from the organism, a quality that is inherent to them. This could be possibly circumvented by attaching the small inhibitor to a larger carrier which could potentially carry toxic agents, which get released upon internalization of the enzyme, killing thus the cell. In the last publication we investigated possible linkers reaching outside the binding cleft of the GCPII which could be utilized in recruitment of nanocarriers through widely used biotin-streptavidin interaction.

A straightforward attachment of the biotinylated ethylene glycol linker to the urea-based scaffold led to a dramatic decrease in the activity of the inhibitors by almost 100 fold. To compensate for this loss we approached to target the described exosites (chapter 3.2.5, figure 9, p. 28) of the enzyme, specifically the arginine patch structure. The arginine patch has been shown to be able to adopt a conformation with open cavity, which is readily able to tightly accommodate the 4-iodobenzyl moiety. We suggested branching off the linker from various sides of the benzyl moiety, to regain the lost activity. Subsequent synthesis and determination of crystal structure of the inhibitors in complex with GCPII showed surprising amount of possible conformations the benzyl group can adopt, with only one compound reaching the desired arginine patch region. However, the kinetic data showed that this particular inhibitors embodied highest inhibition potency with the overall 7-fold improvement compared to parental compound. Furthermore we showed that this inhibitor can be used to mediate the interaction between streptavidine labelled quantum dots (a model nanocarrier) and GCPII positive cells, which demonstrated the practical applicability of this compound to facile preparation of GCPII-specific nanocarriers.

To conclude, the presented papers in this dissertation thesis examine closely the novel class of HIV protease inhibitors discovered in our laboratory and establish basic knowledge about their inhibition potencies as well as their overall binding mode to the enzyme active site. To study the more basic questions concerning this fascinating enzyme we developed a tight binding inhibitor which upon irradiation decomposes and drops its inhibition potency by four orders of magnitude, thus working as a specific switch-on for the enzymatic activity. Using

this inhibitor we further showed that the processing of the Gag polyprotein chain inside the virion is possible even after its release from the cell, and leads to properly cleaved final products (capsid protein), with half-life of 20-30 minutes. We have also tried to employ novel GCPII inhibitors for the imaging, isolation and targeting GCPII-expressing cells by designing novel type of inhibitors with maximized binding potential to the entrance tunnel, making it specific towards GCPII. These inhibitors could be further used in drug targeting of small nanocarriers loaded with cytotoxic agents to the prostate carcinoma cells, decreasing the side effects of non-specific treatment.

7 References

1. Weiss, R.A., *How does HIV cause AIDS?* Science, 1993. **260**(5112): p. 1273-1279.
2. Carlson, L.A., Briggs, J.A., Glass, B., Riches, J.D., Simon, M.N., Johnson, M.C., Muller, B., Grunewald, K., and Krausslich, H.G., *Three-dimensional analysis of budding sites and released virus suggests a revised model for HIV-1 morphogenesis.* Cell Host Microbe, 2008. **4**(6): p. 592-599.
3. Levin, J.G., Mitra, M., Mascarenhas, A., and Musier-Forsyth, K., *Role of HIV-1 nucleocapsid protein in HIV-1 reverse transcription.* RNA Biol, 2010. **7**(6): p. 754-774.
4. Fiorentini, S., Marini, E., Caracciolo, S., and Caruso, A., *Functions of the HIV-1 matrix protein p17.* New Microbiol, 2006. **29**(1): p. 1-10.
5. Malim, M.H. and Emerman, M., *HIV-1 accessory proteins--ensuring viral survival in a hostile environment.* Cell Host Microbe, 2008. **3**(6): p. 388-398.
6. Sundquist W. I., K.H.G., *HIV-1 Assembly, Budding, and Maturation.* Cold Spring Harb Perspect Med, 2012. **2**(8): p. 1-24.
7. Hallenberger, S., Bosch, V., Angliker, H., Shaw, E., Klenk, H.D., and Garten, W., *Inhibition of furin-mediated cleavage activation of HIV-1 glycoprotein gp160.* Nature, 1992. **360**(6402): p. 358-361.
8. Tran, E.E., Borgnia, M.J., Kuybeda, O., Schauder, D.M., Bartesaghi, A., Frank, G.A., Sapiro, G., Milne, J.L., and Subramaniam, S., *Structural mechanism of trimeric HIV-1 envelope glycoprotein activation.* PLoS Pathog, 2012. **8**(7): p. e1002797.
9. Wyatt, R. and Sodroski, J., *The HIV-1 envelope glycoproteins: fusogens, antigens, and immunogens.* Science, 1998. **280**(5371): p. 1884-1888.
10. Frankel, A.D. and Young, J.A., *HIV-1: fifteen proteins and an RNA.* Annu Rev Biochem, 1998. **67**: p. 1-25.
11. Chan, D.C. and Kim, P.S., *HIV entry and its inhibition.* Cell, 1998. **93**(5): p. 681-684.
12. Goel, R., Beard, W.A., Kumar, A., Casas-Finet, J.R., Strub, M.P., Stahl, S.J., Lewis, M.S., Bebenek, K., Becerra, S.P., Kunkel, T.A., et al., *Structure/function studies of HIV-1(1) reverse transcriptase: dimerization-defective mutant L289K.* Biochemistry, 1993. **32**(48): p. 13012-13018.

13. Brass, A.L., Dykxhoorn, D.M., Benita, Y., Yan, N., Engelman, A., Xavier, R.J., Lieberman, J., and Elledge, S.J., *Identification of host proteins required for HIV infection through a functional genomic screen.* Science, 2008. **319**(5865): p. 921-926.
14. Debyser, Z., Christ, F., De Rijck, J., and Gijsbers, R., *Host factors for retroviral integration site selection.* Trends Biochem Sci, 2014.
15. Debyser Z., D.B.A., Taltynov O., Demeulemeester J., Christ F, *Validation of host factors of HIV integration as novel drug targets for anti-HIV therapy.* chemMedChem, 2014. **5**: p. 314-320.
16. Craigie, R. and Bushman, F.D., *HIV DNA integration.* Cold Spring Harb Perspect Med, 2012. **2**(7): p. a006890.
17. Ono, A. and Freed, E.O., *Plasma membrane rafts play a critical role in HIV-1 assembly and release.* Proc Natl Acad Sci U S A, 2001. **98**(24): p. 13925-13930.
18. de Marco, A., Muller, B., Glass, B., Riches, J.D., Krausslich, H.G., and Briggs, J.A., *Structural analysis of HIV-1 maturation using cryo-electron tomography.* PLoS Pathog, 2010. **6**(11): p. e1001215.
19. Barre-Sinoussi, F., Ross, A.L., and Delfraissy, J.F., *Past, present and future: 30 years of HIV research.* Nat Rev Microbiol, 2013. **11**(12): p. 877-883.
20. Cao, L., Song, W., De Clercq, E., Zhan, P., and Liu, X., *Recent progress in the research of small molecule HIV-1 RNase H inhibitors.* Curr Med Chem, 2014. **21**(17): p. 1956-1967.
21. Song, Y., Fang, Z., Zhan, P., and Liu, X., *Recent advances in the discovery and development of novel HIV-1 NNRTI platforms (Part II): 2009-2013 update.* Curr Med Chem, 2013. **21**(3): p. 329-355.
22. De Clercq, E., *The nucleoside reverse transcriptase inhibitors, nonnucleoside reverse transcriptase inhibitors, and protease inhibitors in the treatment of HIV infections (AIDS).* Adv Pharmacol, 2013. **67**: p. 317-358.
23. Sharma, M. and Walmsley, S.L., *Raltegravir as antiretroviral therapy in HIV/AIDS.* Expert Opin Pharmacother, 2014. **15**(3): p. 395-405.
24. Pommier, Y., Johnson, A.A., and Marchand, C., *Integrase inhibitors to treat HIV/AIDS.* Nat Rev Drug Discov, 2005. **4**(3): p. 236-248.
25. Dayam, R., Al-Mawsawi, L.Q., and Neamati, N., *HIV-1 integrase inhibitors: an emerging clinical reality.* Drugs R D, 2007. **8**(3): p. 155-168.
26. De Clercq, E., *New approaches toward anti-HIV chemotherapy.* J Med Chem, 2005. **48**(5): p. 1297-1313.

27. Biswas, P., Tambussi, G., and Lazzarin, A., *Access denied? The status of co-receptor inhibition to counter HIV entry.* Expert Opin Pharmacother, 2007. **8**(7): p. 923-933.
28. Blair, W.S., Pickford, C., Irving, S.L., Brown, D.G., Anderson, M., Bazin, R., Cao, J., Ciaramella, G., Isaacson, J., Jackson, L., Hunt, R., Kjerrstrom, A., Nieman, J.A., Patick, A.K., et al., *HIV capsid is a tractable target for small molecule therapeutic intervention.* PLoS Pathog, 2010. **6**(12): p. e1001220.
29. Shi, J., Zhou, J., Shah, V.B., Aiken, C., and Whitby, K., *Small-molecule inhibition of human immunodeficiency virus type 1 infection by virus capsid destabilization.* J Virol, 2010. **85**(1): p. 542-549.
30. Neira, J.L., *The capsid protein of human immunodeficiency virus: designing inhibitors of capsid assembly.* Febs J, 2009. **276**(21): p. 6110-6117.
31. Neira, J.L., *The capsid protein of human immunodeficiency virus: molecular recognition and design of antiviral agents.* Febs J, 2009. **276**(21): p. 6097.
32. Bartonova, V., Igonet, S., Sticht, J., Glass, B., Habermann, A., Vaney, M.C., Sehr, P., Lewis, J., Rey, F.A., and Krausslich, H.G., *Residues in the HIV-1 capsid assembly inhibitor binding site are essential for maintaining the assembly-competent quaternary structure of the capsid protein.* J Biol Chem, 2008. **283**(46): p. 32024-32033.
33. Seelmeier, S., Schmidt, H., Turk, V., and von der Helm, K., *Human immunodeficiency virus has an aspartic-type protease that can be inhibited by pepstatin A.* Proc Natl Acad Sci U S A, 1988. **85**(18): p. 6612-6616.
34. Kohl, N.E., Emini, E.A., Schleif, W.A., Davis, L.J., Heimbach, J.C., Dixon, R.A., Scolnick, E.M., and Sigal, I.S., *Active human immunodeficiency virus protease is required for viral infectivity.* Proc Natl Acad Sci U S A, 1988. **85**(13): p. 4686-4690.
35. Brierley, I. and Dos Ramos, F.J., *Programmed ribosomal frameshifting in HIV-1 and the SARS-CoV.* Virus Res, 2006. **119**(1): p. 29-42.
36. Tang, C., Louis, J.M., Aniana, A., Suh, J.Y., and Clore, G.M., *Visualizing transient events in amino-terminal autoprocessing of HIV-1 protease.* Nature, 2008. **455**(7213): p. 693-696.
37. Krausslich, H.G., Traenckner, A.M., and Rippmann, F., *Expression and characterization of genetically linked homo- and hetero-dimers of HIV proteinase.* Adv Exp Med Biol, 1991. **306**: p. 417-428.

38. Prabu-Jeyabalan, M., Nalivaika, E., and Schiffer, C.A., *Substrate shape determines specificity of recognition for HIV-1 protease: analysis of crystal structures of six substrate complexes.* Structure, 2002. **10**(3): p. 369-381.

39. Rognvaldsson, T., You, L., and Garwicz, D., *Bioinformatic approaches for modeling the substrate specificity of HIV-1 protease: an overview.* Expert Rev Mol Diagn, 2007. **7**(4): p. 435-451.

40. Beck, Z.Q., Morris, G.M., and Elder, J.H., *Defining HIV-1 protease substrate selectivity.* Curr Drug Targets Infect Disord, 2002. **2**(1): p. 37-50.

41. H.M. Berman, K.H., H. Nakamura *HIV PR structures.* 2003 [cited 2015 19.1.]; Available from: http://www.rcsb.org/pdb/results/results.do?qrid=FEF71EFD&tabtoshow=Current.

42. Kempf, D.J., Marsh, K.C., Denissen, J.F., McDonald, E., Vasavanonda, S., Flentge, C.A., Green, B.E., Fino, L., Park, C.H., Kong, X.P., et al., *ABT-538 is a potent inhibitor of human immunodeficiency virus protease and has high oral bioavailability in humans.* Proc Natl Acad Sci U S A, 1995. **92**(7): p. 2484-2488.

43. DeLano, W.L., *The PyMOL Molecular Graphics System, Delano Scientific, PAlo Alto, CA, USA.* 2002.

44. Wlodawer, A. and Vondrasek, J., *Inhibitors of HIV-1 protease: a major success of structure-assisted drug design.* Annu Rev Biophys Biomol Struct, 1998. **27**: p. 249-284.

45. Cooper, J.B., *Aspartic proteinases in disease: a structural perspective.* Curr Drug Targets, 2002. **3**(2): p. 155-173.

46. Hornak, V., Okur, A., Rizzo, R.C., and Simmerling, C., *HIV-1 protease flaps spontaneously open and reclose in molecular dynamics simulations.* Proc Natl Acad Sci U S A, 2006. **103**(4): p. 915-920.

47. Ishima, R., Freedberg, D.I., Wang, Y.X., Louis, J.M., and Torchia, D.A., *Flap opening and dimer-interface flexibility in the free and inhibitor-bound HIV protease, and their implications for function.* Structure, 1999. **7**(9): p. 1047-1055.

48. Todd, M.J., Semo, N., and Freire, E., *The structural stability of the HIV-1 protease.* J Mol Biol, 1998. **283**(2): p. 475-488.

49. Roberts, N.A., Martin, J.A., Kinchington, D., Broadhurst, A.V., Craig, J.C., Duncan, I.B., Galpin, S.A., Handa, B.K., Kay, J., Krohn, A., et al., *Rational design of peptide-based HIV proteinase inhibitors.* Science, 1990. **248**(4953): p. 358-361.

50. Thaisrivongs, S., Watenpaugh, K.D., Howe, W.J., Tomich, P.K., Dolak, L.A., Chong, K.T., Tomich, C.C., Tomasselli, A.G., Turner, S.R., Strohbach, J.W., et al., *Structure-based design of novel HIV protease inhibitors: carboxamide-containing 4-hydroxycoumarins and 4-hydroxy-2-pyrones as potent nonpeptidic inhibitors.* J Med Chem, 1995. **38**(18): p. 3624-3637.
51. Pokorna, J., Machala, L., Rezacova, P., and Konvalinka, J., *Current and Novel Inhibitors of HIV Protease.* Viruses, 2009. **1**(3): p. 1209-1239.
52. Capaldini, L., *Protease inhibitors' metabolic side effects: cholesterol, triglycerides, blood sugar, and "Crix belly." Interview with Lisa Capaldini, M.D. Interview by John S. James.* AIDS Treat News, 1997(No 277): p. 1-4.
53. Orman, J.S., Perry C.M., *Tipranavir: a review of its use in the management of HIV infection.* Drugs, 2008. **68**(10): p. 1435-1463.
54. Rittweger, M. and Arasteh, K., *Clinical pharmacokinetics of darunavir.* Clin Pharmacokinet, 2007. **46**(9): p. 739-756.
55. Katende-Kyenda, N.L., Lubbe, M.S., Serfontein, J.H., and Truter, I., *Prevalence of possible drug-drug interactions between antiretroviral agents in different age groups in a section of the private health care sector setting in South Africa.* J Clin Pharm Ther, 2008. **33**(4): p. 393-400.
56. Hazen, R., Harvey, R., Ferris, R., Craig, C., Yates, P., Griffin, P., Miller, J., Kaldor, I., Ray, J., Samano, V., Furfine, E., Spaltenstein, A., Hale, M., Tung, R., et al., *In vitro antiviral activity of the novel, tyrosyl-based human immunodeficiency virus (HIV) type 1 protease inhibitor brecanavir (GW640385) in combination with other antiretrovirals and against a panel of protease inhibitor-resistant HIV.* Antimicrob Agents Chemother, 2007. **51**(9): p. 3147-3154.
57. Cihlar, T., He, G.X., Liu, X., Chen, J.M., Hatada, M., Swaminathan, S., McDermott, M.J., Yang, Z.Y., Mulato, A.S., Chen, X., Leavitt, S.A., Stray, K.M., and Lee, W.A., *Suppression of HIV-1 protease inhibitor resistance by phosphonate-mediated solvent anchoring.* J Mol Biol, 2006. **363**(3): p. 635-647.
58. Koh, Y., Das, D., Leschenko, S., Nakata, H., Ogata-Aoki, H., Amano, M., Nakayama, M., Ghosh, A.K., and Mitsuya, H., *GRL-02031, a novel nonpeptidic protease inhibitor (PI) containing a stereochemically defined fused cyclopentanyltetrahydrofuran potent against multi-PI-resistant human immunodeficiency virus type 1 in vitro.* Antimicrob Agents Chemother, 2009. **53**(3): p. 997-1006.

59. Sham, H.L., Betebenner, D.A., Wideburg, N., Saldivar, A.C., Kohlbrenner, W.E., Craig-Kennard, A., Vasavanonda, S., Kempf, D.J., Clement, J.J., Erickson, J.E., et al., *Pseudo-symmetrical difluoroketones. Highly potent and specific inhibitors of HIV-1 protease.* FEBS Lett, 1993. **329**(1-2): p. 144-146.

60. Lu, D. and Vince, R., *Discovery of potent HIV-1 protease inhibitors incorporating sulfoximine functionality.* Bioorg Med Chem Lett, 2007. **17**(20): p. 5614-5619.

61. Lu, D., Sham, Y.Y., and Vince, R., *Design, asymmetric synthesis, and evaluation of pseudosymmetric sulfoximine inhibitors against HIV-1 protease.* Bioorg Med Chem, 2010. **18**(5): p. 2037-2048.

62. Specker, E., Bottcher, J., Brass, S., Heine, A., Lilie, H., Schoop, A., Muller, G., Griebenow, N., and Klebe, G., *Unexpected novel binding mode of pyrrolidine-based aspartyl protease inhibitors: design, synthesis and crystal structure in complex with HIV protease.* ChemMedChem, 2006. **1**(1): p. 106-117.

63. Fitzgerald, P.M., McKeever, B.M., VanMiddlesworth, J.F., Springer, J.P., Heimbach, J.C., Leu, C.T., Herber, W.K., Dixon, R.A., and Darke, P.L., *Crystallographic analysis of a complex between human immunodeficiency virus type 1 protease and acetyl-pepstatin at 2.0-A resolution.* J Biol Chem, 1990. **265**(24): p. 14209-14219.

64. Blum, A., Bottcher, J., Heine, A., Klebe, G., and Diederich, W.E., *Structure-guided design of C2-symmetric HIV-1 protease inhibitors based on a pyrrolidine scaffold.* J Med Chem, 2008. **51**(7): p. 2078-2087.

65. Lam, P.Y., Jadhav, P.K., Eyermann, C.J., Hodge, C.N., Ru, Y., Bacheler, L.T., Meek, J.L., Otto, M.J., Rayner, M.M., Wong, Y.N., et al., *Rational design of potent, bioavailable, nonpeptide cyclic ureas as HIV protease inhibitors.* Science, 1994. **263**(5145): p. 380-384.

66. Sham, H.L., Zhao, C., Marsh, K.C., Betebenner, D.A., Lin, S., Rosenbrook, W., Jr., Herrin, T., Li, L., Madigan, D., Vasavanonda, S., Molla, A., Saldivar, A., McDonald, E., Wideburg, N.E., et al., *Novel azacyclic ureas that are potent inhibitors of HIV-1 protease.* Biochem Biophys Res Commun, 1996. **225**(2): p. 436-440.

67. Sham, H.L., Zhao, C., Stewart, K.D., Betebenner, D.A., Lin, S., Park, C.H., Kong, X.P., Rosenbrook, W., Jr., Herrin, T., Madigan, D., Vasavanonda, S., Lyons, N., Molla, A., Saldivar, A., et al., *A novel, picomolar inhibitor of human immunodeficiency virus type 1 protease.* J Med Chem, 1996. **39**(2): p. 392-397.

68. Ax, A., Schaal, W., Vrang, L., Samuelsson, B., Hallberg, A., and Karlen, A., *Cyclic sulfamide HIV-1 protease inhibitors, with sidechains spanning from P2/P2' to P1/P1'.* Bioorg Med Chem, 2005. **13**(3): p. 755-764.
69. Palmer, S., Shafer, R.W., and Merigan, T.C., *Highly drug-resistant HIV-1 clinical isolates are cross-resistant to many antiretroviral compounds in current clinical development.* AIDS, 1999. **13**(6): p. 661-667.
70. Ala, P.J., DeLoskey, R.J., Huston, E.E., Jadhav, P.K., Lam, P.Y., Eyermann, C.J., Hodge, C.N., Schadt, M.C., Lewandowski, F.A., Weber, P.C., McCabe, D.D., Duke, J.L., and Chang, C.H., *Molecular recognition of cyclic urea HIV-1 protease inhibitors.* J Biol Chem, 1998. **273**(20): p. 12325-12331.
71. Cigler, P., Kozisek, M., Rezacova, P., Brynda, J., Otwinowski, Z., Pokorna, J., Plesek, J., Gruner, B., Doleckova-Maresova, L., Masa, M., Sedlacek, J., Bodem, J., Krausslich, H.G., Kral, V., et al., *From nonpeptide toward noncarbon protease inhibitors: metallacarboranes as specific and potent inhibitors of HIV protease.* Proc Natl Acad Sci U S A, 2005. **102**(43): p. 15394-15399.
72. Kona, J., *Theoretical study on the mechanism of a ring-opening reaction of oxirane by the active-site aspartic dyad of HIV-1 protease.* Org Biomol Chem, 2008. **6**(2): p. 359-365.
73. Meek, T.D., Dayton, B.D., Metcalf, B.W., Dreyer, G.B., Strickler, J.E., Gorniak, J.G., Rosenberg, M., Moore, M.L., Magaard, V.W., and Debouck, C., *Human immunodeficiency virus 1 protease expressed in Escherichia coli behaves as a dimeric aspartic protease.* Proc Natl Acad Sci U S A, 1989. **86**(6): p. 1841-1845.
74. Zhonghua Yu, C.P., McPhee F., De Voss J., Jones P., Burlingame A. L., Kuntz I., Craik C. S., Ortiz de Montellano P., *Irreversible Inhibition of the HIV-1 Protease: Targeting Alkylating Agents to the Catalytic Aspartate Groups.* J Am Chem Soc, 1996. **118**(25): p. 5846-5856.
75. Svicher, V., Ceccherini-Silberstein, F., Erba, F., Santoro, M., Gori, C., Bellocchi, M.C., Giannella, S., Trotta, M.P., Monforte, A., Antinori, A., and Perno, C.F., *Novel human immunodeficiency virus type 1 protease mutations potentially involved in resistance to protease inhibitors.* Antimicrob Agents Chemother, 2005. **49**(5): p. 2015-2025.
76. Ceccherini-Silberstein, F., Erba, F., Gago, F., Bertoli, A., Forbici, F., Bellocchi, M.C., Gori, C., D'Arrigo, R., Marcon, L., Balotta, C., Antinori, A., Monforte, A.D., and

Perno, C.F., *Identification of the minimal conserved structure of HIV-1 protease in the presence and absence of drug pressure.* AIDS, 2004. **18**(12): p. F11-19.

77. Zhang, Z.Y., Poorman, R.A., Maggiora, L.L., Heinrikson, R.L., and Kezdy, F.J., *Dissociative inhibition of dimeric enzymes. Kinetic characterization of the inhibition of HIV-1 protease by its COOH-terminal tetrapeptide.* J Biol Chem, 1991. **266**(24): p. 15591-15594.
78. Babe, L.M., Rose, J., and Craik, C.S., *Synthetic "interface" peptides alter dimeric assembly of the HIV 1 and 2 proteases.* Protein Sci, 1992. **1**(10): p. 1244-1253.
79. Schramm, H.J., Billich, A., Jaeger, E., Rucknagel, K.P., Arnold, G., and Schramm, W., *The inhibition of HIV-1 protease by interface peptides.* Biochem Biophys Res Commun, 1993. **194**(2): p. 595-600.
80. Vidu, A., Dufau, L., Bannwarth, L., Soulier, J.L., Sicsic, S., Piarulli, U., Reboud-Ravaux, M., and Ongeri, S., *Toward the first nonpeptidic molecular tong inhibitor of wild-type and mutated HIV-1 protease dimerization.* ChemMedChem, 2010. **5**(11): p. 1899-1906.
81. Bowman, M.J. and Chmielewski, J., *Sidechain-linked inhibitors of HIV-1 protease dimerization.* Bioorg Med Chem, 2009. **17**(3): p. 967-976.
82. Lee, S.G. and Chmielewski, J., *Cross-linked peptoid-based dimerization inhibitors of HIV-1 protease.* Chembiochem, 2010. **11**(11): p. 1513-1516.
83. Perryman, A.L., Lin, J.H., and McCammon, J.A., *Restrained molecular dynamics simulations of HIV-1 protease: the first step in validating a new target for drug design.* Biopolymers, 2006. **82**(3): p. 272-284.
84. Perryman, A.L., Zhang, Q., Soutter, H.H., Rosenfeld, R., McRee, D.E., Olson, A.J., Elder, J.E., and Stout, C.D., *Fragment-based screen against HIV protease.* Chem Biol Drug Des, 2010. **75**(3): p. 257-268.
85. Roberts, J.D., Bebenek, K., and Kunkel, T.A., *The accuracy of reverse transcriptase from HIV-1.* Science, 1988. **242**(4882): p. 1171-1173.
86. Domingo, E., Escarmis, C., Sevilla, N., Moya, A., Elena, S.F., Quer, J., Novella, I.S., and Holland, J.J., *Basic concepts in RNA virus evolution.* FASEB J, 1996. **10**(8): p. 859-864.
87. Kaplan, A.H., Michael, S.F., Wehbie, R.S., Knigge, M.F., Paul, D.A., Everitt, L., Kempf, D.J., Norbeck, D.W., Erickson, J.W., and Swanstrom, R., *Selection of multiple human immunodeficiency virus type 1 variants that encode viral proteases with*

decreased sensitivity to an inhibitor of the viral protease. Proc Natl Acad Sci U S A, 1994. **91**(12): p. 5597-5601.

88. Condra, J.H., Schleif, W.A., Blahy, O.M., Gabryelski, L.J., Graham, D.J., Quintero, J.C., Rhodes, A., Robbins, H.L., Roth, E., Shivaprakash, M., et al., *In vivo emergence of HIV-1 variants resistant to multiple protease inhibitors.* Nature, 1995. **374**(6522): p. 569-571.
89. Molla, A., Korneyeva, M., Gao, Q., Vasavanonda, S., Schipper, P.J., Mo, H.M., Markowitz, M., Chernyavskiy, T., Niu, P., Lyons, N., Hsu, A., Granneman, G.R., Ho, D.D., Boucher, C.A., et al., *Ordered accumulation of mutations in HIV protease confers resistance to ritonavir.* Nat Med, 1996. **2**(7): p. 760-766.
90. Quiñones-Mateu, M.E., Weber J., Rangel H.R., Chakraborty B., *HIV-1 fitness and antiretroviral drug resistance.* AIDS Rev, 2001. **3**: p. 223–242.
91. Vergne, L., Peeters, M., Mpoudi-Ngole, E., Bourgeois, A., Liegeois, F., Toure-Kane, C., Mboup, S., Mulanga-Kabeya, C., Saman, E., Jourdan, J., Reynes, J., and Delaporte, E., *Genetic diversity of protease and reverse transcriptase sequences in non-subtype-B human immunodeficiency virus type 1 strains: evidence of many minor drug resistance mutations in treatment-naive patients.* J Clin Microbiol, 2000. **38**(11): p. 3919-3925.
92. Cote, H.C., Brumme, Z.L., and Harrigan, P.R., *Human immunodeficiency virus type 1 protease cleavage site mutations associated with protease inhibitor cross-resistance selected by indinavir, ritonavir, and/or saquinavir.* J Virol, 2001. **75**(2): p. 589-594.
93. Doyon, L., Croteau, G., Thibeault, D., Poulin, F., Pilote, L., and Lamarre, D., *Second locus involved in human immunodeficiency virus type 1 resistance to protease inhibitors.* J Virol, 1996. **70**(6): p. 3763-3769.
94. Maguire, M.F., Guinea, R., Griffin, P., Macmanus, S., Elston, R.C., Wolfram, J., Richards, N., Hanlon, M.H., Porter, D.J., Wrin, T., Parkin, N., Tisdale, M., Furfine, E., Petropoulos, C., et al., *Changes in human immunodeficiency virus type 1 Gag at positions L449 and P453 are linked to I50V protease mutants in vivo and cause reduction of sensitivity to amprenavir and improved viral fitness in vitro.* J Virol, 2002. **76**(15): p. 7398-7406.
95. Kozisek, M., Saskova, K.G., Rezacova, P., Brynda, J., van Maarseveen, N.M., De Jong, D., Boucher, C.A., Kagan, R.M., Nijhuis, M., and Konvalinka, J., *Ninety-nine is not enough: molecular characterization of inhibitor-resistant human*

immunodeficiency virus type 1 protease mutants with insertions in the flap region. J Virol, 2008. **82**(12): p. 5869-5878.

96. Winters, M.A. and Merigan, T.C., *Insertions in the human immunodeficiency virus type 1 protease and reverse transcriptase genes: clinical impact and molecular mechanisms.* Antimicrob Agents Chemother, 2005. **49**(7): p. 2575-2582.
97. Saskova, K.G., Kozisek, M., Rezacova, P., Brynda, J., Yashina, T., Kagan, R.M., and Konvalinka, J., *Molecular characterization of clinical isolates of human immunodeficiency virus resistant to the protease inhibitor darunavir*. J Virol, 2009. **83**(17): p. 8810-8818.
98. Martinez-Cajas, J.L. and Wainberg, M.A., *Protease inhibitor resistance in HIV-infected patients: molecular and clinical perspectives.* Antiviral Res, 2007. **76**(3): p. 203-221.
99. Robinson, M.B., Blakely, R.D., Couto, R., and Coyle, J.T., *Hydrolysis of the brain dipeptide N-acetyl-L-aspartyl-L-glutamate. Identification and characterization of a novel N-acetylated alpha-linked acidic dipeptidase activity from rat brain.* J Biol Chem, 1987. **262**(30): p. 14498-14506.
100. Horoszewicz, J.S., Kawinski, E., and Murphy, G.P., *Monoclonal antibodies to a new antigenic marker in epithelial prostatic cells and serum of prostatic cancer patients.* Anticancer Res, 1987. **7**(5B): p. 927-935.
101. Halsted, C.H., *Jejunal brush-border folate hydrolase. A novel enzyme.* West J Med, 1991. **155**(6): p. 605-609.
102. Carter, R.E., Feldman, A.R., and Coyle, J.T., *Prostate-specific membrane antigen is a hydrolase with substrate and pharmacologic characteristics of a neuropeptidase.* Proc Natl Acad Sci U S A, 1996. **93**(2): p. 749-753.
103. Pinto, J.T., Suffoletto, B.P., Berzin, T.M., Qiao, C.H., Lin, S., Tong, W.P., May, F., Mukherjee, B., and Heston, W.D., *Prostate-specific membrane antigen: a novel folate hydrolase in human prostatic carcinoma cells.* Clin Cancer Res, 1996. **2**(9): p. 1445-1451.
104. Maraj, B.H., Leek, J.P., Karayi, M., Ali, M., Lench, N.J., and Markham, A.F., *Detailed genetic mapping around a putative prostate-specific membrane antigen locus on human chromosome 11p11.2.* Cytogenet Cell Genet, 1998. **81**(1): p. 3-9.
105. Watt, F., Martorana, A., Brookes, D.E., Ho, T., Kingsley, E., O'Keefe, D.S., Russell, P.J., Heston, W.D., and Molloy, P.L., *A tissue-specific enhancer of the prostate-specific membrane antigen gene, FOLH1*. Genomics, 2001. **73**(3): p. 243-254.

106. Bzdega, T., Turi, T., Wroblewska, B., She, D., Chung, H.S., Kim, H., and Neale, J.H., *Molecular cloning of a peptidase against N-acetylaspartylglutamate from a rat hippocampal cDNA library.* J Neurochem, 1997. **69**(6): p. 2270-2277.

107. Su, S.L., Huang, I.P., Fair, W.R., Powell, C.T., and Heston, W.D., *Alternatively spliced variants of prostate-specific membrane antigen RNA: ratio of expression as a potential measurement of progression.* Cancer Res, 1995. **55**(7): p. 1441-1443.

108. Hlouchova, K., Navratil, V., Tykvart, J., Sacha, P., and Konvalinka, J., *GCPII variants, paralogs and orthologs.* Curr Med Chem, 2012. **19**(9): p. 1316-1322.

109. Schulke, N., Varlamova, O.A., Donovan, G.P., Ma, D., Gardner, J.P., Morrissey, D.M., Arrigale, R.R., Zhan, C., Chodera, A.J., Surowitz, K.G., Maddon, P.J., Heston, W.D., and Olson, W.C., *The homodimer of prostate-specific membrane antigen is a functional target for cancer therapy.* Proc Natl Acad Sci U S A, 2003. **100**(22): p. 12590-12595.

110. Israeli, R.S., Powell, C.T., Corr, J.G., Fair, W.R., and Heston, W.D., *Expression of the prostate-specific membrane antigen.* Cancer Res, 1994. **54**(7): p. 1807-1811.

111. Israeli, R.S., Powell, C.T., Fair, W.R., and Heston, W.D., *Molecular cloning of a complementary DNA encoding a prostate-specific membrane antigen.* Cancer Res, 1993. **53**(2): p. 227-230.

112. Barinka, C., Sacha, P., Sklenar, J., Man, P., Bezouska, K., Slusher, B.S., and Konvalinka, J., *Identification of the N-glycosylation sites on glutamate carboxypeptidase II necessary for proteolytic activity.* Protein Sci, 2004. **13**(6): p. 1627-1635.

113. Rawlings, N.D. and Barrett, A.J., *Structure of membrane glutamate carboxypeptidase.* Biochim Biophys Acta, 1997. **1339**(2): p. 247-252.

114. Makarova, K.S. and Grishin, N.V., *The Zn-peptidase superfamily: functional convergence after evolutionary divergence.* J Mol Biol, 1999. **292**(1): p. 11-17.

115. Rajasekaran, S.A., Anilkumar, G., Oshima, E., Bowie, J.U., Liu, H., Heston, W., Bander, N.H., and Rajasekaran, A.K., *A novel cytoplasmic tail MXXXL motif mediates the internalization of prostate-specific membrane antigen.* Mol Biol Cell, 2003. **14**(12): p. 4835-4845.

116. Hlouchova, K., Barinka, C., Konvalinka, J., and Lubkowski, J., *Structural insight into the evolutionary and pharmacologic homology of glutamate carboxypeptidases II and III.* Febs J, 2009. **276**(16): p. 4448-4462.

117. Pangalos, M.N., Neefs, J.M., Somers, M., Verhasselt, P., Bekkers, M., van der Helm, L., Fraiponts, E., Ashton, D., and Gordon, R.D., *Isolation and expression of novel human glutamate carboxypeptidases with N-acetylated alpha-linked acidic dipeptidase and dipeptidyl peptidase IV activity.* J Biol Chem, 1999. **274**(13): p. 8470-8483.

118. Miyake, M., Kakimoto, Y., and Sorimachi, M., *A gas chromatographic method for the determination of N-acetyl-L-aspartic acid, N-acetyl-alpha-aspartylglutamic acid and beta-citryl-L-glutamic acid and their distributions in the brain and other organs of various species of animals.* J Neurochem, 1981. **36**(3): p. 804-810.

119. Bacich, D.J., Ramadan, E., O'Keefe, D.S., Bukhari, N., Wegorzewska, I., Ojeifo, O., Olszewski, R., Wrenn, C.C., Bzdega, T., Wroblewska, B., Heston, W.D., and Neale, J.H., *Deletion of the glutamate carboxypeptidase II gene in mice reveals a second enzyme activity that hydrolyzes N-acetylaspartylglutamate.* J Neurochem, 2002. **83**(1): p. 20-29.

120. Zhou, J., Neale, J.H., Pomper, M.G., and Kozikowski, A.P., *NAAG peptidase inhibitors and their potential for diagnosis and therapy.* Nat Rev Drug Discov, 2005. **4**(12): p. 1015-1026.

121. Williams, A.J., Lu, X.M., Slusher, B., and Tortella, F.C., *Electroencephalogram analysis and neuroprotective profile of the N-acetylated-alpha-linked acidic dipeptidase inhibitor, GPI5232, in normal and brain-injured rats.* J Pharmacol Exp Ther, 2001. **299**(1): p. 48-57.

122. Jackson, P.F., Cole, D.C., Slusher, B.S., Stetz, S.L., Ross, L.E., Donzanti, B.A., and Trainor, D.A., *Design, synthesis, and biological activity of a potent inhibitor of the neuropeptidase N-acetylated alpha-linked acidic dipeptidase.* J Med Chem, 1996. **39**(2): p. 619-622.

123. Speno, H.S., Luthi-Carter, R., Macias, W.L., Valentine, S.L., Joshi, A.R., and Coyle, J.T., *Site-directed mutagenesis of predicted active site residues in glutamate carboxypeptidase II.* Mol Pharmacol, 1999. **55**(1): p. 179-185.

124. Davis, M.I., Bennett, M.J., Thomas, L.M., and Bjorkman, P.J., *Crystal structure of prostate-specific membrane antigen, a tumor marker and peptidase.* Proc Natl Acad Sci U S A, 2005. **102**(17): p. 5981-5986.

125. Mesters, J.R., Barinka, C., Li, W., Tsukamoto, T., Majer, P., Slusher, B.S., Konvalinka, J., and Hilgenfeld, R., *Structure of glutamate carboxypeptidase II, a drug target in neuronal damage and prostate cancer.* EMBO J, 2006. **25**(6): p. 1375-1384.

126. Klusak, V., Barinka, C., Plechanovova, A., Mlcochova, P., Konvalinka, J., Rulisek, L., and Lubkowski, J., *Reaction mechanism of glutamate carboxypeptidase II revealed by mutagenesis, X-ray crystallography, and computational methods.* Biochemistry, 2009. **48**(19): p. 4126-4138.

127. Zhang, A.X., Murelli, R.P., Barinka, C., Michel, J., Cocleaza, A., Jorgensen, W.L., Lubkowski, J., and Spiegel, D.A., *A remote arene-binding site on prostate specific membrane antigen revealed by antibody-recruiting small molecules.* J Am Chem Soc, 2010. **132**(36): p. 12711-12716.

128. Pavlicek, J., Ptacek, J., and Barinka, C., *Glutamate carboxypeptidase II: an overview of structural studies and their importance for structure-based drug design and deciphering the reaction mechanism of the enzyme.* Curr Med Chem, 2012. **19**(9): p. 1300-1309.

129. Barinka, C., Rinnova, M., Sacha, P., Rojas, C., Majer, P., Slusher, B.S., and Konvalinka, J., *Substrate specificity, inhibition and enzymological analysis of recombinant human glutamate carboxypeptidase II.* J Neurochem, 2002. **80**(3): p. 477-487.

130. Hlouchova, K., Barinka, C., Klusak, V., Sacha, P., Mlcochova, P., Majer, P., Rulisek, L., and Konvalinka, J., *Biochemical characterization of human glutamate carboxypeptidase III.* J Neurochem, 2007. **101**(3): p. 682-696.

131. Barinka, C., Byun, Y., Dusich, C.L., Banerjee, S.R., Chen, Y., Castanares, M., Kozikowski, A.P., Mease, R.C., Pomper, M.G., and Lubkowski, J., *Interactions between human glutamate carboxypeptidase II and urea-based inhibitors: structural characterization.* J Med Chem, 2008. **51**(24): p. 7737-7743.

132. Ferraris, D.V., Shukla, K., and Tsukamoto, T., *Structure-activity relationships of glutamate carboxypeptidase II (GCPII) inhibitors.* Curr Med Chem, 2012. **19**(9): p. 1282-1294.

133. Stoermer, D., Liu, Q., Hall, M.R., Flanary, J.M., Thomas, A.G., Rojas, C., Slusher, B.S., and Tsukamoto, T., *Synthesis and biological evaluation of hydroxamate-Based inhibitors of glutamate carboxypeptidase II.* Bioorg Med Chem Lett, 2003. **13**(13): p. 2097-2100.

134. Blank, B.R., Alayoglu, P., Engen, W., Choi, J.K., Berkman, C.E., and Anderson, M.O., *N-substituted glutamyl sulfonamides as inhibitors of glutamate carboxypeptidase II (GCP2).* Chem Biol Drug Des, 2011. **77**(4): p. 241-247.

135. Krapcho, J., Turk, C., Cushman, D.W., Powell, J.R., DeForrest, J.M., Spitzmiller, E.R., Karanewsky, D.S., Duggan, M., Rovnyak, G., Schwartz, J., et al., *Angiotensin-converting enzyme inhibitors. Mercaptan, carboxyalkyl dipeptide, and phosphinic acid inhibitors incorporating 4-substituted prolines.* J Med Chem, 1988. **31**(6): p. 1148-1160.

136. Vitharana, D., E.;, F.J., D.;, S., Bonneville, G.W., Majer, P., and Tsukamoto, T., *Synthesis and biological evaluation of (R)- and (S)-2-(phosphonomethyl)pentanedioic acids as inhibitors of glutamate carboxypeptidase II.* Tetrahedron: Asymmetry, 2002. **13**(15): p. 1609-1614.

137. Jackson, P.F., Tays, K.L., Maclin, K.M., Ko, Y.S., Li, W., Vitharana, D., Tsukamoto, T., Stoermer, D., Lu, X.C., Wozniak, K., and Slusher, B.S., *Design and pharmacological activity of phosphinic acid based NAALADase inhibitors.* J Med Chem, 2001. **44**(24): p. 4170-4175.

138. Mesters, J.R., Henning, K., and Hilgenfeld, R., *Human glutamate carboxypeptidase II inhibition: structures of GCPII in complex with two potent inhibitors, quisqualate and 2-PMPA.* Acta Crystallogr D Biol Crystallogr, 2007. **63**(Pt 4): p. 508-513.

139. El-Zaria, M.E., Genady, A.R., Janzen, N., Petlura, C.I., Beckford Vera, D.R., and Valliant, J.F., *Preparation and evaluation of carborane-derived inhibitors of prostate specific membrane antigen (PSMA).* Dalton Trans, 2014. **43**(13): p. 4950-4961.

140. Shiosaki, K.L., C.W.; Leanna, M.R.; Morton, H.E.; Miller, T.R.; Witte, D.; Stashko, M.; Nadzan, A.M. , *Toward developing peptidomimetics: Successful replacement of backbone amide bonds in tetrapeptide-based CCK-A receptor agonists* bioorg Med Chem Lett, 1993. **3**: p. 855-860.

141. Kozikowski, A.P., Nan, F., Conti, P., Zhang, J., Ramadan, E., Bzdega, T., Wroblewska, B., Neale, J.H., Pshenichkin, S., and Wroblewski, J.T., *Design of remarkably simple, yet potent urea-based inhibitors of glutamate carboxypeptidase II (NAALADase).* J Med Chem, 2001. **44**(3): p. 298-301.

142. Majer, P., Jackson, P.F., Delahanty, G., Grella, B.S., Ko, Y.S., Li, W., Liu, Q., Maclin, K.M., Polakova, J., Shaffer, K.A., Stoermer, D., Vitharana, D., Wang, E.Y., Zakrzewski, A., et al., *Synthesis and biological evaluation of thiol-based inhibitors of glutamate carboxypeptidase II: discovery of an orally active GCP II inhibitor.* J Med Chem, 2003. **46**(10): p. 1989-1996.

143. Ghadge, G.D., Slusher, B.S., Bodner, A., Canto, M.D., Wozniak, K., Thomas, A.G., Rojas, C., Tsukamoto, T., Majer, P., Miller, R.J., Monti, A.L., and Roos, R.P.,

Glutamate carboxypeptidase II inhibition protects motor neurons from death in familial amyotrophic lateral sclerosis models. Proc Natl Acad Sci U S A, 2003. **100**(16): p. 9554-9559.

144. Zhang, W., Murakawa, Y., Wozniak, K.M., Slusher, B., and Sima, A.A., *The preventive and therapeutic effects of GCPII (NAALADase) inhibition on painful and sensory diabetic neuropathy.* J Neurol Sci, 2006. **247**(2): p. 217-223.
145. Takatsu, Y., Fujita, Y., Tsukamoto, T., Slusher, B.S., and Hashimoto, K., *Orally active glutamate carboxypeptidase II inhibitor 2-MPPA attenuates dizocilpine-induced prepulse inhibition deficits in mice.* Brain Res, 2011. **1371**: p. 82-86.
146. Majer, P., Hin, B., Stoermer, D., Adams, J., Xu, W., Duvall, B.R., Delahanty, G., Liu, Q., Stathis, M.J., Wozniak, K.M., Slusher, B.S., and Tsukamoto, T., *Structural optimization of thiol-based inhibitors of glutamate carboxypeptidase II by modification of the P1' side chain.* J Med Chem, 2006. **49**(10): p. 2876-2885.
147. O'Keefe, D.S., Bacich, D.J., and Heston, W.D., *Comparative analysis of prostate-specific membrane antigen (PSMA) versus a prostate-specific membrane antigen-like gene.* Prostate, 2004. **58**(2): p. 200-210.
148. Yao, V. and Bacich, D.J., *Prostate specific membrane antigen (PSMA) expression gives prostate cancer cells a growth advantage in a physiologically relevant folate environment in vitro.* Prostate, 2006. **66**(8): p. 867-875.
149. Yao, V., Berkman, C.E., Choi, J.K., O'Keefe, D.S., and Bacich, D.J., *Expression of prostate-specific membrane antigen (PSMA), increases cell folate uptake and proliferation and suggests a novel role for PSMA in the uptake of the non-polyglutamated folate, folic acid.* Prostate, 2010. **70**(3): p. 305-316.
150. Barwe, S.P., Maul, R.S., Christiansen, J.J., Anilkumar, G., Cooper, C.R., Kohn, D.B., and Rajasekaran, A.K., *Preferential association of prostate cancer cells expressing prostate specific membrane antigen to bone marrow matrix.* Int J Oncol, 2007. **30**(4): p. 899-904.
151. Ananias, H.J., van den Heuvel, M.C., Helfrich, W., and de Jong, I.J., *Expression of the gastrin-releasing peptide receptor, the prostate stem cell antigen and the prostate-specific membrane antigen in lymph node and bone metastases of prostate cancer.* Prostate, 2009. **69**(10): p. 1101-1108.
152. Conway, R.E., Petrovic, N., Li, Z., Heston, W., Wu, D., and Shapiro, L.H., *Prostate-specific membrane antigen regulates angiogenesis by modulating integrin signal transduction.* Mol Cell Biol, 2006. **26**(14): p. 5310-5324.

153. Foss, C.A., Mease, R.C., Cho, S.Y., Kim, H.J., and Pomper, M.G., *GCPII imaging and cancer.* Curr Med Chem, 2012. **19**(9): p. 1346-1359.
154. Goldenberg, D.M. and Sharkey, R.M., *Advances in cancer therapy with radiolabeled monoclonal antibodies.* Q J Nucl Med Mol Imaging, 2006. **50**(4): p. 248-264.
155. Troyer, J.K., Beckett, M.L., and Wright, G.L., Jr., *Location of prostate-specific membrane antigen in the LNCaP prostate carcinoma cell line.* Prostate, 1997. **30**(4): p. 232-242.
156. Mease, R.C., *Radionuclide based imaging of prostate cancer.* Curr Top Med Chem, 2010. **10**(16): p. 1600-1616.
157. Haseman, M.K., Rosenthal, S.A., and Polascik, T.J., *Capromab Pendetide imaging of prostate cancer.* Cancer Biother Radiopharm, 2000. **15**(2): p. 131-140.
158. Vallabhajosula, S., Kuji, I., Hamacher, K.A., Konishi, S., Kostakoglu, L., Kothari, P.A., Milowski, M.I., Nanus, D.M., Bander, N.H., and Goldsmith, S.J., *Pharmacokinetics and biodistribution of 111In- and 177Lu-labeled J591 antibody specific for prostate-specific membrane antigen: prediction of 90Y-J591 radiation dosimetry based on 111In or 177Lu?* J Nucl Med, 2005. **46**(4): p. 634-641.
159. Bander, N.H., Trabulsi, E.J., Kostakoglu, L., Yao, D., Vallabhajosula, S., Smith-Jones, P., Joyce, M.A., Milowsky, M., Nanus, D.M., and Goldsmith, S.J., *Targeting metastatic prostate cancer with radiolabeled monoclonal antibody J591 to the extracellular domain of prostate specific membrane antigen.* J Urol, 2003. **170**(5): p. 1717-1721.
160. Smith-Jones, P.M., Vallabhajosula, S., Navarro, V., Bastidas, D., Goldsmith, S.J., and Bander, N.H., *Radiolabeled monoclonal antibodies specific to the extracellular domain of prostate-specific membrane antigen: preclinical studies in nude mice bearing LNCaP human prostate tumor.* J Nucl Med, 2003. **44**(4): p. 610-617.
161. Bander, N.H., Milowsky, M.I., Nanus, D.M., Kostakoglu, L., Vallabhajosula, S., and Goldsmith, S.J., *Phase I trial of 177lutetium-labeled J591, a monoclonal antibody to prostate-specific membrane antigen, in patients with androgen-independent prostate cancer.* J Clin Oncol, 2005. **23**(21): p. 4591-4601.
162. Milowsky, M.I., Nanus, D.M., Kostakoglu, L., Vallabhajosula, S., Goldsmith, S.J., and Bander, N.H., *Phase I trial of yttrium-90-labeled anti-prostate-specific membrane antigen monoclonal antibody J591 for androgen-independent prostate cancer.* J Clin Oncol, 2004. **22**(13): p. 2522-2531.

163. Nakajima, T., Mitsunaga, M., Bander, N.H., Heston, W.D., Choyke, P.L., and Kobayashi, H., *Targeted, activatable, in vivo fluorescence imaging of prostate-specific membrane antigen (PSMA) positive tumors using the quenched humanized J591 antibody-indocyanine green (ICG) conjugate.* Bioconjug Chem, 2011. **22**(8): p. 1700-1705.

164. Cai, Z. and Anderson, C.J., *Chelators for copper radionuclides in positron emission tomography radiopharmaceuticals.* J Labelled Comp Radiopharm, 2014. **57**(4): p. 224-230.

165. Ermert, J. and Coenen, H.H., *Methods for (11) C- and (18) F-labelling of amino acids and derivatives for positron emission tomography imaging.* J Labelled Comp Radiopharm, 2013. **56**(3-4): p. 225-236.

166. Chen, Y., Foss, C.A., Byun, Y., Nimmagadda, S., Pullambhatla, M., Fox, J.J., Castanares, M., Lupold, S.E., Babich, J.W., Mease, R.C., and Pomper, M.G., *Radiohalogenated prostate-specific membrane antigen (PSMA)-based ureas as imaging agents for prostate cancer.* J Med Chem, 2008. **51**(24): p. 7933-7943.

167. Hillier, S.M., Maresca, K.P., Femia, F.J., Marquis, J.C., Foss, C.A., Nguyen, N., Zimmerman, C.N., Barrett, J.A., Eckelman, W.C., Pomper, M.G., Joyal, J.L., and Babich, J.W., *Preclinical evaluation of novel glutamate-urea-lysine analogues that target prostate-specific membrane antigen as molecular imaging pharmaceuticals for prostate cancer.* Cancer Res, 2009. **69**(17): p. 6932-6940.

168. Maresca, K.P., Hillier, S.M., Femia, F.J., Keith, D., Barone, C., Joyal, J.L., Zimmerman, C.N., Kozikowski, A.P., Barrett, J.A., Eckelman, W.C., and Babich, J.W., *A series of halogenated heterodimeric inhibitors of prostate specific membrane antigen (PSMA) as radiolabeled probes for targeting prostate cancer.* J Med Chem, 2009. **52**(2): p. 347-357.

169. Barrett, J., LaFrance, N., Coleman, R. E., Goldsmith, S., Stubbs, J., Petry, N., Vallabhajosula, S., Maresca, K., Femia, F., Babich, J., *Targeting metastatic prostate cancer [PCa] in patients with 123I-MIP1072 & 123I-MIP1095*

J NUCL MED MEETING ABSTRACTS 2009. **50** p. 522

170. Banerjee, S.R., Foss, C.A., Castanares, M., Mease, R.C., Byun, Y., Fox, J.J., Hilton, J., Lupold, S.E., Kozikowski, A.P., and Pomper, M.G., *Synthesis and evaluation of technetium-99m- and rhenium-labeled inhibitors of the prostate-specific membrane antigen (PSMA).* J Med Chem, 2008. **51**(15): p. 4504-4517.

171. Banerjee S.R., P.M., Byun Y., Green G., Fox J.J., Horti A.G., Mease R., Pomper M.G., *Ga-68- and In-111-labeled small molecule inhibitors of PSMA for prostate cancer imaging.* J Labelled Comp Radiopharm, 2009. **52(Supplement 1):S19**: p. (abstract).

172. Liu, H., Rajasekaran, A.K., Moy, P., Xia, Y., Kim, S., Navarro, V., Rahmati, R., and Bander, N.H., *Constitutive and antibody-induced internalization of prostate-specific membrane antigen.* Cancer Res, 1998. **58**(18): p. 4055-4060.

173. Ballangrud, A.M., Yang, W.H., Charlton, D.E., McDevitt, M.R., Hamacher, K.A., Panageas, K.S., Ma, D., Bander, N.H., Scheinberg, D.A., and Sgouros, G., *Response of LNCaP spheroids after treatment with an alpha-particle emitter (213Bi)-labeled anti-prostate-specific membrane antigen antibody (J591).* Cancer Res, 2001. **61**(5): p. 2008-2014.

174. Tagawa, S.T., Milowsky, M.I., Morris, M., Vallabhajosula, S., Christos, P., Akhtar, N.H., Osborne, J., Goldsmith, S.J., Larson, S., Taskar, N.P., Scher, H.I., Bander, N.H., and Nanus, D.M., *Phase II study of Lutetium-177-labeled anti-prostate-specific membrane antigen monoclonal antibody J591 for metastatic castration-resistant prostate cancer.* Clin Cancer Res, 2013. **19**(18): p. 5182-5191.

175. Li, Y., Tian, Z., Rizvi, S.M., Bander, N.H., and Allen, B.J., *In vitro and preclinical targeted alpha therapy of human prostate cancer with Bi-213 labeled J591 antibody against the prostate specific membrane antigen.* Prostate Cancer Prostatic Dis, 2002. **5**(1): p. 36-46.

176. Henry, M.D., Wen, S., Silva, M.D., Chandra, S., Milton, M., and Worland, P.J., *A prostate-specific membrane antigen-targeted monoclonal antibody-chemotherapeutic conjugate designed for the treatment of prostate cancer.* Cancer Res, 2004. **64**(21): p. 7995-8001.

177. Lupold, S.E., Hicke, B.J., Lin, Y., and Coffey, D.S., *Identification and characterization of nuclease-stabilized RNA molecules that bind human prostate cancer cells via the prostate-specific membrane antigen.* Cancer Res, 2002. **62**(14): p. 4029-4033.

178. Dhar, S., Gu, F.X., Langer, R., Farokhzad, O.C., and Lippard, S.J., *Targeted delivery of cisplatin to prostate cancer cells by aptamer functionalized Pt(IV) prodrug-PLGA-PEG nanoparticles.* Proc Natl Acad Sci U S A, 2008. **105**(45): p. 17356-17361.

179. Wolf, P., Alt, K., Wetterauer, D., Buhler, P., Gierschner, D., Katzenwadel, A., Wetterauer, U., and Elsasser-Beile, U., *Preclinical evaluation of a recombinant anti-*

prostate specific membrane antigen single-chain immunotoxin against prostate cancer. J Immunother, 2010. **33**(3): p. 262-271.

180. Wolf, P., Alt, K., Buhler, P., Katzenwadel, A., Wetterauer, U., Tacke, M., and Elsasser-Beile, U., *Anti-PSMA immunotoxin as novel treatment for prostate cancer? High and specific antitumor activity on human prostate xenograft tumors in SCID mice.* Prostate, 2008. **68**(2): p. 129-138.

181. Li, H., Hah, J.M., and Lawrence, D.S., *Light-mediated liberation of enzymatic activity: "small molecule" caged protein equivalents.* J Am Chem Soc, 2008. **130**(32): p. 10474-10475.